UNIVERSIDADE D
COIMBRA

Isabel Patrícia Dias Meireles

# Validating the role of the MAL/SRF pathways in promoting stem-like features downstream of the P-cadherin/actin cytoskeleton complex

**VOLUME 1**

**Dissertation of the Master's Degree in Biochemistry, supervised by Doctor Florence Janody, and Professor Doctor Paula Verissímo and presented to the Department of Life Sciences of the Faculty of Sciences and Technology of the University of Coimbra.**

October of 2021

Life sciences department

# Validating the role of the MAL/SRF pathways in promoting stem-like features downstream of the P-cadherin/actin cytoskeleton complex.

Isabel Patrícia Dias Meireles

Dissertation of the Master's Degree in Biochemistry, supervised by Doctor Florence Janody, and Professor Doctor Paula Verissímo and presented to the Department of Life Sciences of the Faculty of Sciences and Technology of the University of Coimbra.

October of 2021

This work was co-financed by the European Regional Development Fund (ERDF), through the Centro 2020 Regional Operational Programme under FEDER - Fundo Europeu de Desenvolvimento Regional through the COMPETE 2020 - Operational Programme for Competitiveness and Internationalisation and Portuguese national funds via FCT – Fundação para a Ciência e a Tecnologia, under CANCELSTEM project (POCI-01-0145-FEDER-016390).

“As we acquire knowledge,
things do not become more comprehensible,
but more mysterious”.

“Sometimes our light goes out, but is
Blown again into instant flame by an
encounter with another human being.”

Albert Schweitzer

# Acknowledgements

Throughout one of the most challenging and though times in my life, when the only one in the way was me, I need to express my gratitude to those who in one way or another supported me and contributed for the realization of this thesis. Without you the completion of this work would not be possible. These lines will never be enough to express you my gratitude.

Firstly I would like to thank to my supervisor, Drª Florence Janody. Thank you for accepting me in your laboratory, for all the guidance, support and encouragement, patience and for never given up on me. I learned a lot in the realization of this work.

To professor Drª Paula Veríssimo for being my co-supervisor.

To Patrícia and Sara who were crucial in this process, thank you for all the companionship, availability and knowledge they transmitted, all the concern.

To Drª Carla for all the availability to help.

It was a great pleasure and honour to work alongside the members of the Cytoskeletal Regulation & Cancer group.

To Paula and Maria who helped me in my struggles.

To my friends who lift me up in crucial times when I needed the most. In special Ana and Mariana for all the comfort and positive conversations.

And for last, those who are closest to my heart, without whom I would not be who I am today. All of this is as much for me as it is for you. To my mother, thank you for everything, for all the love, sacrifice and values. To my grandparents, in special to my grandmother in which I have the strongest and bravest role model I could ever have.

To all my deepest thank you.

# Table of contents

# List of figures

# List of tables

# Abbreviation list

α6β4- Integrin alpha 6 beta 4
αPS2- Integrin alpha-PS2
αPS4- Integrin alpha-PS4
ADH- Atypical ductal hyperplasia
AH- Atypical hyperplasia
AKT- Protein kinase B
ALDH1- Aldehyde dehydrogenase1
ALH- Atypical lobular hyperplasia
AP- anterior-postrior
ATP- *Adenosine triphosphate*
BCSC- Breast cancer steam cell
bs- Blistered
$Ca^{+}$- Calcium
CAM- Cell adhesion molecule
CBD- Catenin-binding domain
CDH1- Cadherin 1 or E-cadherin gene
CDH3 – Cadherin 3 or P-cadherin gene
CSC- Cancer steam cell
DCIS- Ductal carcinoma *in situ*
DV-dorsal-ventral
E-cadherin - Epithelial cadherin
ECM- *Extracellular matrix*
EMT- Epithelial mesenchymal transition
ER- Estrogen receptor
Gal80- Temperature-sensitive galactose/lactose metabolism regulatory protein
GFP- *Green fluorescent protein*
H3 -Histone 3
HER- Human epidermal growth factor
IgSF- Immunoglobulin superfamily
ITGB4- Integrin-β4

JMD- Juxtamembrane domain

KD- Knocked down

MESK2- Misexpression suppressor of KSR 2

MMP1- Matrix metalloprotease-1

MMP2- Matrix metalloprotease-2

MRTF- Myocardin-related *transcription factor*

N-cadherin – Neural cadherin

NPF- nucleating-promoting factor

Nub- Nubbin

P-cadherin - Placental-cadherin

PE- peripodial epithelium

PKB- Protein kinase B

PR- Progesterone receptor

Src- Tyrosine-protein kinase

SRF- Serum response factor

TNBC- Triple-negative breast cancer

UAS- Upstream Activating Sequences

WB – Western blot

# Abstract

Breast cancer is one of the most common neoplasms worldwide and the leading cause of cancer death amongst women. Tumorigenesis and progression to metastasis involves alterations in normal cells leading to increasing disorganization of the epithelium and disequilibrium of cellular proliferation, differentiation and migration. It is believed that breast cancer recurrence is caused by a specific tumorigenic cell subpopulation designated cancer stem cells (CSCs). These cells are defined by their ability to self-renew under non-differentiation conditions and to resist standard chemotherapeutic drugs and radiotherapy. The acquisition of CSC properties has been associated with alterations in cell adhesion molecules (CAMs). These proteins interact with the cytoskeleton functioning as signalling effector molecules involved in intracellular responses. Cadherins are a type of CAM with the essential role of mediate cell-cell adhesions. E-cadherin is a growth and invasion suppressor, its loss of function is associated with tumour invasion and metastasis formation. On the other hand, P-cadherin is overexpressed in triple negative breast carcinomas (TNBC), characterized by high histological grade and poor patient survival prognosis. It has been demonstrated that P-cadherin inhibit E-cadherin suppressive invasive function. Interestingly, P-cadherin expression promotes stem-like properties in breast cancer cells though SRC and α6β4 integrin, the mechanisms by which remain elusive. Cadherins intervene in the dynamic processes of actin cytoskeleton re-organization and signalling pathways. Based in previous observations from our group we hypothesize that MRTF/SRF pathway is involved in the acquisition of CSC properties. Taking that into account, we have generated a transgenic *Drosophila* model with conditional expression of human P-cadherin affecting wing disc primordium. We sought to validate this model to study P-cadherin effect in the acquisition of breast CSC features and identify signalling molecules and actin nucleators involved in the acquisition of the phenotype.

Using a *Drosophila* model, we demonstrated that P-cadherin restores cell–cell adhesion caused by the loss of E-cadherin in Drosophila epithelium similar to what occurs in breast cancer cells. P-cadherin has been shown to promote

AKT phosphorylation in TNBC cells, on contrary, results in fly epithelia suggest that it might not promote the acquisition of CSC properties. Interestingly, we also observed that knocking down the *Drosophila* integrin aPS2 or Src also suppresses the P-cadherin functional effects in the Drosophila wing. Taking together these findings indicate that the mechanisms by which P-cadherin affects the wing disc development are reminiscent to its functional effect in promoting breast CSC features, validating our model.

Observations appear to indicate that P-cadherin induces stem cell properties by controlling the MRTF-SRF pathway downstream. Knocking down *bs* or Drosophila MRTF supressed the P-cadherin phenotype, even though P-cadherin was not able to affect the expression of the predicted target genes of the pathway.

In addition, results indicate that knocking down the actin nucleators *arpc2* or *spire* suppressed the P-cadherin wing phenotype. However, knocking down bs or Drosophila MRTF did not further suppress the wing phenotype expressing P-cadherin and knocking down arpc2, indicating that bs and Drosophila MRTF are required downstream of arpc2 in the same pathway regulated by P-cadherin. Moreover, arpc2 and spire contribute to the regulation of P-cadherin activity by stabilizing its protein levels. Therefore, it is suggested that P-cadherin control the MRTF-SRF pathway promoting the conversion of actin monomers (G-actin) to actin filaments (F-actin).

Keywords: *Drosophila melanogaster,* Breast cancer, P-cadherin, Actin cytoskeleton, bs/MRTF pathway

# Introduction

# Introduction to cancer

## Anatomy of the mammary gland and epithelium organization

The adult female breast gland has the particularity of only complete its development and differentiation after birth. This feature relies on the dynamic alterations in response to hormonal changes during puberty, menstrual cycle, pregnancy, lactation and menopause (Vidi, P *et al.*, 2013). The mature mammary gland consists of 15-20 lobes each containing numerous lobules that are connected by branched ducts to the nipple (Fig. 1). Lobules consist of multiple acinus, the functional glandular unit, localized at the extremity of each ductal system, which primary function is to produce and secrete milk upon pregnancy. Supported within a network of fat tissue, the lobules and breast ducts are formed by a bilayered epithelium. An inner milk-producing luminal epithelial layer is formed by polarized cells, their apical domain face the lumen and the basolateral domain face an outer layer of myoepithelial cells, that contract to generate milk flow, resting on the basal membrane (Hinck, L & Näthke, I , 2014; Nisticò, P *et al*., 2014).

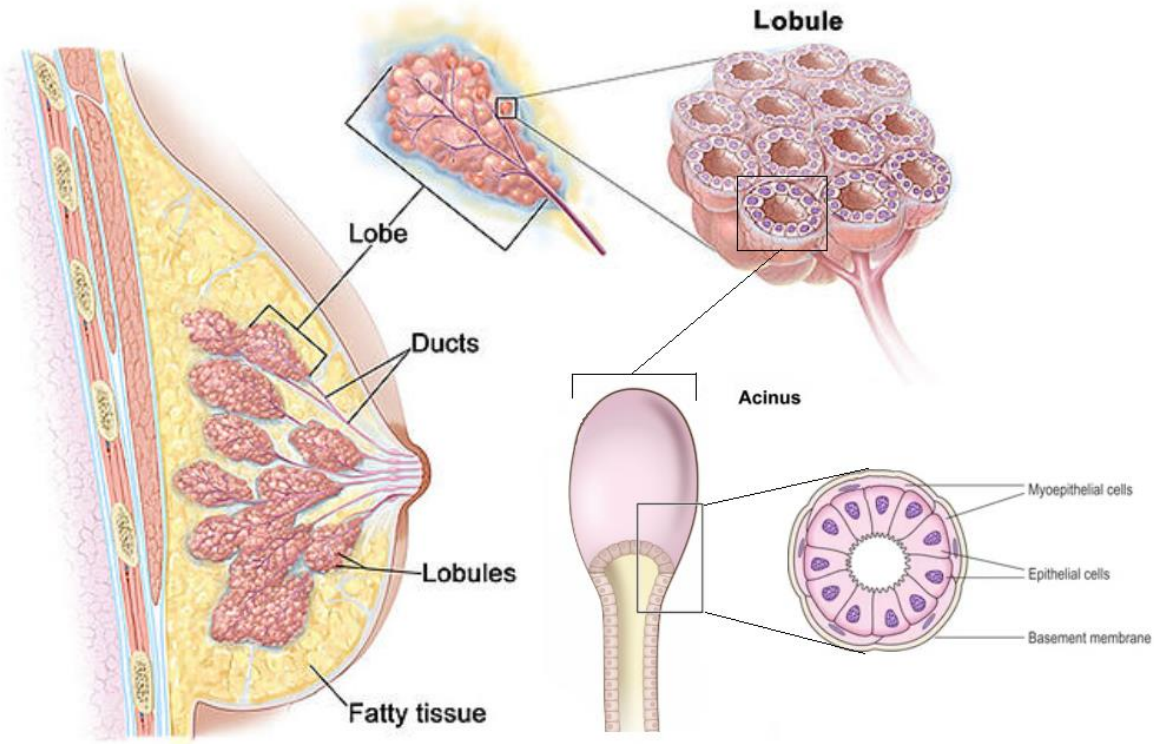

**Fig. 1- Schematic representation of the anatomy of the mammary gland, cross sections through a lobule and an acinus.** The mature mammary gland is formed by lobes each containing lobules consisting of multiple acinus that are connected by branched ducts to the nipple. The duct epithelium is formed by a luminal epithelial layer and an outer myoepithelial layer resting on the basal membrane. (Adapted from Terese Winslow LLC and Walker, R. A. 2009).

Morphogenesis and architecture of normal mammary ductal epithelium is ensured by cell-cell and cell-extracellular membrane contacts (Fig. 2). In the luminal epithelium lateral cell-cell adhesion is maintained through tight junctions, adherens junctions, desmosomes and gap junctions. Luminal and myoepithelial cells establish connections through desmosomes (Owens, M *et al*., 2013). Cell-cell adhesion in myoepithelium occurs though adherens junctions, desmosomes and gap junctions. Interaction of myoepithelial cells with the basement membrane is ensured by hemidesmosomes formed by laminin-332 and α6β4 integrin dimers (Vidi, P *et al*., 2013).

The major feature of luminal epithelia is the basoapical polarity axis. Tight junctions form a continuous band of actin around the cell, strictly defining polarity by separating cell membrane components and receptors between the apical and basolateral membrane domains. In luminal cells, adherens junctions are located subjacent to tight junctions. Cadherins are the most studied adherens junction proteins. In the mammary epithelium cadherin expression is cell type-specific, E-cadherin is expressed in luminal cells and P-cadherin is expressed in myoepithelial cells (Owens, M *et al*., 2013; Shamir, E & Ewald, E 2015). Desmosomes mainly providing mechanical strength intermediate by anchoring keratinous intermediate filaments to the plasma membrane (Owens, M *et al*., 2013).

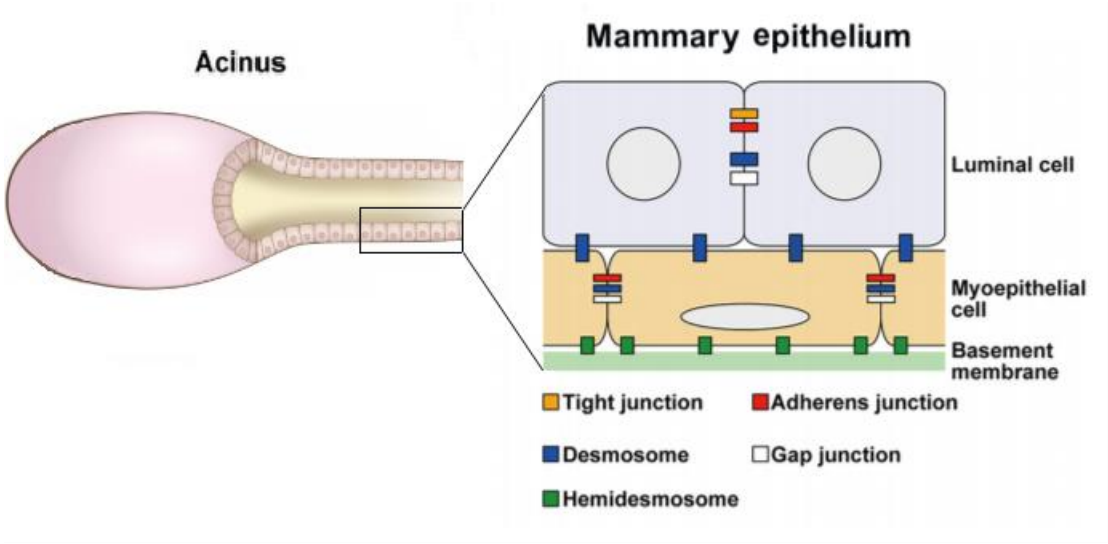


**Fig. 2- Types of cell adhesion complexes in mammary epithelium of a mammary duct.** (Adapted from Kitayama, M et al., 2016).

## Breast cancer burden

According to Globocan data from 2018 breast cancer is, amongst woman worldwide, the most commonly diagnosed type of cancer (11,6%) and leading cause of death (6,6%), with around 2 million cases diagnosed that year and more than 600 000 deaths (Bray *et al*., 2018).

## Breast cancer development and progression

Breast cancers can be classified as carcinomas or sarcomas, depending on the origin of affected cells. In breast tissue, cancers are principally classified as carcinomas, arising from the luminal epithelial cells of terminal ducts and milk-producing lobules and more rarely from the outer layer of basal cells. Carcinomas are characterized by alterations in normal cells and tissue architecture, their progression involves increasing disorganization of the epithelium. Sarcomas constitute less than 1% of primary cancers, arising from the stromal part of the breast including myofibroblasts and blood vessel cells (Feng, Y et al., 2018; Hinck, L & Näthke, I, 2014).

The malignancy progression implies sequential stages, starting with epithelial hyperproliferation and advancing to non-invasive or *in situ*, invasive, and metastatic carcinomas (Feng, Y *et al*., 2018; Place, A *et al.*, 2011). Clinical

data suggests that atypical hyperplasia (AH) of the breast, including atypical ductal hyperplasia (ADH) and atypical lobular hyperplasia (ALH) is a risk indicator associated with up to a 30% of preinvasive lesions with potential to progress to carcinoma (Donaldson, A *et al*., 2017; Kader, T *et al*., 2019). In hyperplasias and *in situ* carcinomas epithelial cells lose polarity and bilayered organization, neoplastic cells proliferation is confined to the ductal structures. The most critical step is progression from *in situ* to invasive ductal carcinoma, characterized by the breakdown of the myoepithelial cell layer and loss of the basement membrane. Ultimately, spread of tumor cells to distant sites originate metastatic disease (Nisticò, P *et al.*, 2014; Place, A *et al*., 2011).

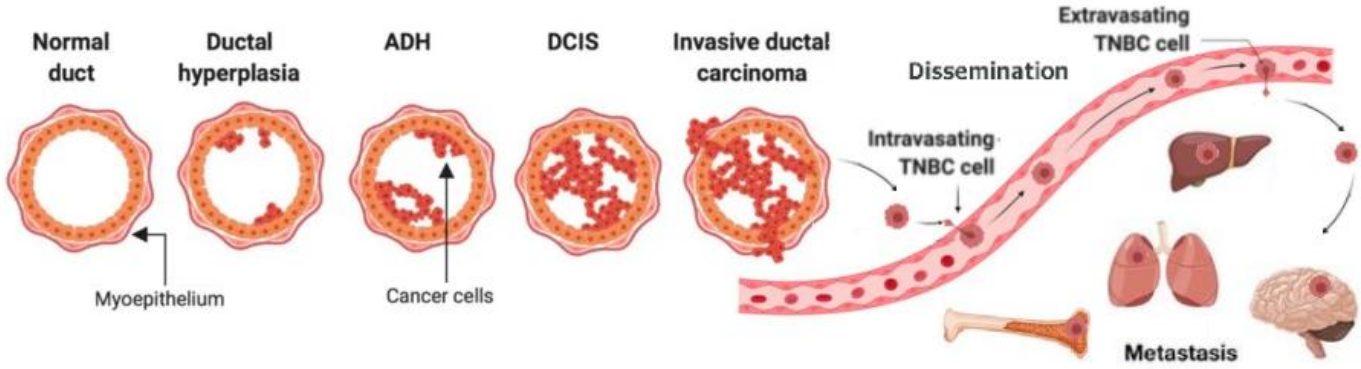


**Fig. 3- Stages of breast cancer progression**. A pre-invasive lesion develops in the mammary duct, it expands within the duct to ADH, progresses to DCIS, once escapes the duct is characterized as invasive ductal carcinoma. Invasive cells disseminate through blood vessels and metastasize upon reaching secondary sites (Adapted from Tower, H 2019).

Cancer is believed to arise from consecutive mutations leading to the acquisition of genetic and epigenetic alterations, a single breast tumor can comprises different cell types with distinct behaviors and responses to therapy. Breast cancer heterogeneity is reflected by staging systems and histopathologic classification. Breast cancer is classified according to their invasiveness relative to the primary tumor sites and pathological features (Feng, Y *et al*., 2018).

Histologically, breast cancer can be broadly classified into *in situ* carcinoma, that can be further sub-classified as either ductal (50%-75% of patients) or lobular (5%-15%of patients), or classified in invasive (infiltrating) carcinoma along with other rarer histologies counting for the remaining of

diagnoses (Malhtroa, M *et. al* 2010; Wake, A *et. al* 2019). Molecularly, four distinct subtypes of invasive cancer are defined according to the presence of three hormonal receptors estrogen receptor (ER), progesterone receptor (PR) and human epidermal growth factor (HER2). Luminal A categorized tumour that are ER and PR positive, while luminal B is associated with the expression of all receptors. Lastly, the triple-negative breast cancer (TNBC) subtype lacks all three receptors and are basal-like in 70% of cases (Turashvili, G *et. al* 2017). Accounting for 15% of all subtypes, TNBC is an extremely heterogeneous group. Yet, these cancers are associated with a high tumour grade and the presence of BRCA1 mutation. There is no available effective treatment for this type of cancer. (Dent, R et.al., 2007). Chemotherapy individually or in combination with surgery is a treatment option, though it lacks efficiency, the risk of recurrence in 5 years is very elevated (Hon *et al.* 2016; Prat, A 2025; Toft, *et al* D 2011, Weiman, V *et al.,* 2012).

## Cancer stem cells

Tumours comprise heterogeneous cell populations among which cancer stem cells (CSC) or tumour-initiating cells represent a minor subset. In breast cancer, CSC are designated breast cancer stem cells (BCSCs), they are considered responsible for cancer progression with high propensity to metastasize and prone to relapse, in virtue to their resistance to radiation, cytotoxic chemotherapy and molecular targeted therapy. These undifferentiated cells are capable of self-renewal, reconstituting the tumour giving rise to differentiated cells (Fig. 4) (Brooks, M *et. al,* 2015; Jordan, S *et. al* 2006). Over the years, research focused in identify, isolate and characterize BCSC validated some markers such as signal transducer CD24 (CD24), hyaluronan receptor (CD44) and aldehyde dehydrogenase1 (ALDH1). However, not all molecular signatures are expressed in all breast cancer subtypes, varying also according to histological grade (Da Cruz Paula & Lopes, 2017). To identify populations of CSC some of the used stemness markers are cell adhesion molecules, since

alterations in this proteins have been associated with the acquisition of CSC properties (Farahani, E *et al*., 2014).

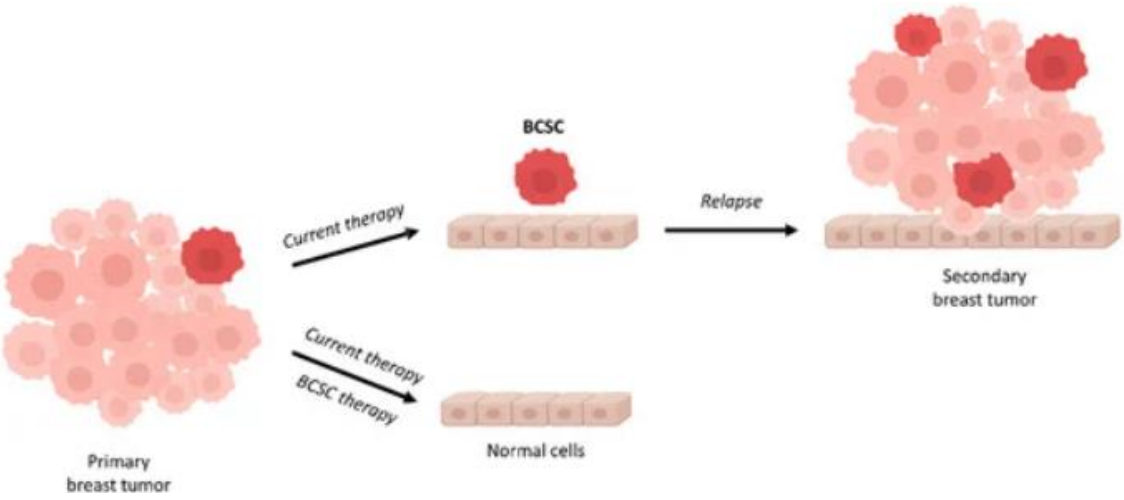


**Fig. 4 - Implication of cancer stem cells in tumour relapses.** BCSC population in the tumor is able to resist to conventional therapies and sustain slowly tumour growth conducting to relapse. (Adapted from Palomeras, S et al., 2018).

## Cell adhesion molecules in normal development and cancer

Cell adhesion molecules (CAMs) are majorly transmembrane receptor proteins expressed through the epithelium, endothelium and by specific immune cells (Janiszewska *et al*., 2020).

These proteins are of paramount importance in the maintenance of cells adhesion and cell anchoring, cytoskeletal organization and tissue structure, participation in morphogenesis, embryogenesis, organogenesis, immunological function, inflammation and wound healing (Makrilia *et al*., 2009).

CAMs also function as signalling effector molecules involved in intracellular responses, cell growth, survival, differentiation and transcriptional activity. The extracellular domain integrates extracellular cues from other cell adhesion molecules or the extracellular matrix with cell intrinsic signalling, interacting with the cytoskeleton, directly by its intracellular domain or via scaffolding proteins (Farahani *et al*., 2014; Janiszewska *et al*., 2020).

CAMs are divided in four principal groups: cadherins, integrins, selectins and immunoglobulin superfamily (IgSF) members. The classification of these proteins depends on the type of cellular junctions built by these proteins expressed on the cell surface. Cadherins essential role is mediate cell-cell

adhesions. Integrins mediate both adhesion between cells and interactions between the cell and its extracellular matrix (Janiszewska *et al*., 2020). Selectins are expressed by endothelial and bone-marrow-derived cells. Besides being involved in cell-cell adhesion, they also have signalling functions, responsible for leukocyte and platelets recruitment to sites of inflammation and migration of lymphocytes to peripheral lymph nodes (Borsig, 2019). Members of IgSF mediate cell-cell adhesions, are involved in immune responses and play a central role in neuronal development, establishing and maintaining neural connections and axon guidance (Juliano, 2002).

Alterations in the expression and function of CAMs have been implicated in various aspects contributing to cancer progression (Makrilia *et al*., 2009). Variability in cell adhesion result in plasticity of cell-cell junctions contributing to collective migration. Suppression of adhesion-molecule-mediated cell forces in cancer cells leads to its released into the lymphatic system or the blood stream. Upon invasion of tissues and organs, adhesive function may be restored, leading to the formation of new tumor colonies (Abduljauwad & Ahmed, 2019; Hanahan & Weinberg, 2011). Furthermore, one of the transformation steps of cells undergoing EMT is the weakening cell-cell adhesion in result of deregulations in the expression of specific cell-surface proteins, such as cadherins (Serrano-Gomez *et al*., 2016). Selectins and members of immunoglobulin superfamily are involved in the creation of a favourable environment for pre-metastatic niche and cancer progression (Borsig, 2019; Farahani *et al*., 2014).

## Integrins

Integrins are a family of cell adhesion receptors, comprising 24 heterodimeric transmembrane receptors generated from a combination of α and a β subunits, they are mediators of adhesion to several extracellular matrix components (Humphries *et al*., 2006).

Integrins take center-stage among receptors involved in the integration of signals form the external microenvironment and from the cell internal environment. Integrins often establish interaction with cadherin adhesion molecules in the activation of the same signalling pathways and prompting similar

cellular functions. In addition to oncogenic responses, mainly through communication with other transmembrane proteins, these interactions are called focal adhesions. The association of cadherins and integrins is implicated in cancer progression, controlling diverse aspects ranging from tumour initiation, assisting the malignant transformation of cells in the primary site, and initial invasion to metastatic reactivation of dormant disseminated tumour cells. (Nisticò, P *et al*., 2014; Vieira, A *et al*., 2014)

Some studies implicate certain integrins as positive regulators of tumorigenesis, the α6 integrins (α6β1 and α6β4) are the foremost receptors contributing to breast cancer progression. It was demonstrated that subunit integrin-β4 (ITGB4) can be considered as a marker to identify populations of CSC-enriched cells with a partial mesenchymal phenotype (Bieri et. al., 2017). In particular β1 and β4 integrin subunits are fundamental in directing polarity and breast tissue structure. Alterations in the basally localized integrin α6β4 leads to loss of polarity and to the formation of disorganized colonies in cultured breast epithelial cells (Nisticò *et al*., 2014). Integrin α6β4 is highly expressed in TNBC and responsible for driving aggressive traits by stimulating cell proliferation, resistance to apoptosis, angiogenesis, migration, invasion and metastasis. Findings indicate that integrin α6β4 regulates the expression of pro-invasive genes, enhance DNA repair and affect chemotherapy sensitivity of breast cancer cells (Chen, M *et al*., 2019). It was demonstrated in breast cancer cells that α6β4 integrin activates PI3K/Akt pathway to promote cell survival and invasion in p53 deficient cells (Bachelder, R *et.al* 1999). The serine/threonine kinase (AKT) or also known as protein kinase B (PKB) is a well described effector of PI3K/Akt/mTOR signalling pathway (Revati, S 2019). This pathway is frequently dysregulated in breast cancer, with at least one of the components altered in 70% of basal like breast cancer, and AKT upregulation counting in 24% of the cases (Knowles, E *et.al* 2009).

## Cadherins

Cadherins are transmembrane single-chain glycoproteins containing distinctive cadherin repeat sequences which mediate cell–cell adhesion through homotypic interactions in a calcium-dependent manner called adherens junctions (Patel, S. *et al.*, 2003). Cadherins are essential in preserve tissue integrity and barriers, tissue remodelling, maintain cell polarity, morphogenesis and homeostasis (Janiszewska, M *et al*., 2020).

This superfamily can be divided in classical cadherins (type I and II), desmosomal cadherins, protocadherins and atypical cadherins. Although cadherins expression is restricted to a distinct tissue distribution pattern are characterized, transient expression occurs during development in various other tissues. Designated accordingly to the tissue where it was firstly characterized, the classical cadherins are epithelial-cadherin (E-cadherin), placental-cadherin (P-cadherin) and neural-cadherin (N-cadherin) (Makrilia, N. *et al*., 2009; Patel, S. *et al.*, 2003).

The structure of classical cadherins is similar amongst themselves and well characterized (Fig. 5). Cadherins usually present a highly conserved cytoplasmic domain, a transmembrane domain, and an extracellular domain. Four ectodomains constituting the extracellular cadherin domain binds to $Ca^{2+}$ ions, responsible for the cadherins conformation facilitating its proper folding and turn the structure more rigid. Calcium connects these domains to a fifth ectodomain that comprises a N terminus containing a pre-domain that must be proteolytically removed to cadherin exert their adhesive capacity (Janiszewska, M *et al*., 2020; Patel, S. *et al*., 2003).

Adhesion junctions mediated by cadherins depends on its dynamic association with catenins. Cadherins interact though cytoplasmic domains to preferentially three subtypes of catenin proteins, α-catenins, β-catenins, and p120ctn family catenins. The cadherin cytoplasmatic domain can be divided in two subdomains: a juxtamembrane domain (JMD), wich is located proximal to the cell membrane binds to p120ctn and a catenin-binding domain (CBD) that binds to β-catenins. That connection has been referred as the cadherin-catenin complex and it binds to actin cytoskeleton. These complexes are connected

through β-catenins to a monomeric form of α-catenin, while a homodimeric forms of α-catenins do not bind to F-actin (Green, K *et al*., 2010; Kaszak, I *et al*., 2020).

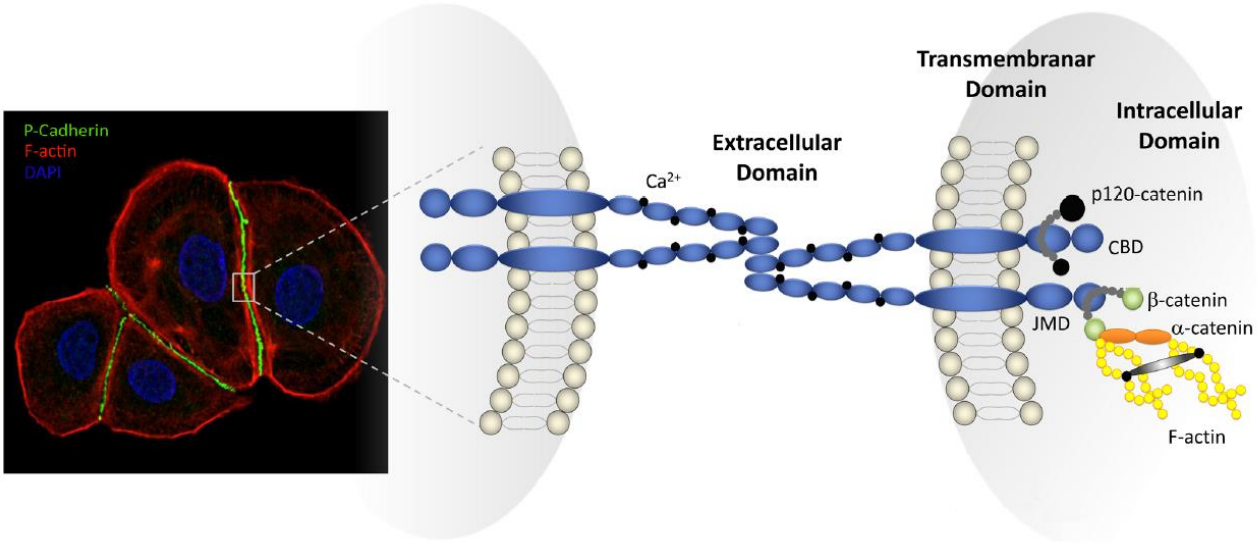


**Fig. 5- Schematic representation of the structure of an adhesive junction mediated by a classic cadherin (P-cadherin).** In the intercellular space, P-cadherin extracellular domains interact with P-cadherin extracellular domains of adjacent cells to mediate cell adhesion. The intracellular catenins bind to the cytoplasmic tail of P-cadherin. p120-catenin binds the cadherin tail at the juxtamembrane domain (JMD), whereas b-catenin binds to the distal catenin binding domain (CBD), a-catenin associates with b-catenin and is directly linked to the actin cytoskeleton (Adapted from Albergaria, A *et. al*, 2011).

## E-cadherin

E-cadherin is a type I cadherin with cell-cell adhesion function, binding cells via adherens junctions. With approximately 100kb and encoded by the gene *CDH1,* mapped in chromosome 16q22.1 comprising in total 16 exons (Wong, S *et al*., 2018). E-cadherin is the predominant cadherin expressed in epithelial tissues, is also present in luminal epithelial cells and myoepithelial/basal cells (Albergaria *et al*., 2011).

E-cadherin is one of the most studied tumour suppressor molecules. E-cadherin expression can be reliably used as a marker to differentiate invasive lobular carcinomas from invasive ductal carcinomas of the breast. Loss of E-cadherin function is observed in tumours with an infiltrative pattern of growth, in around 84% of lobular breast cancers and 38% diffuse gastric cancer. The molecular mechanisms impairing E-cadherin function comprise somatic CDH1 mutations, truncating mutation, loss of heterozygosity, promoter

hypermethylation and transcriptional inactivation (Alsaleem, M *et al*., 2019; Horne, H *et al*., 2018).

The loss or inactivation of the protein is associated with malignant cancer progression, invasion, metastasis, and decrease of survival in breast cancer patients (Paredes, J *et al*., 2012). The reactivation of endogenous E-cadherin or expression of exogenous E-cadherin lead to a partial suppression of tumorigenicity in carcinoma cells (Navarro *et al*., 1991).

Šlaus, N *et. al* described the mechanisms by which E-cadherin prevents cancer activation. In cells expressing high levels of the cell-cell protein β-catenin is sequestered at the membrane, avoiding its release and translocation to the nucleus and acting as an activator of Wnt signalling pathway (Pećina-Šlaus *et al*.,2003; Wong *et al*., 2018).

During EMT, cell-cell contacts are reduced due to downregulation of epithelial-specific cell–cell adhesion proteins of which E-cadherin is example.
As proved using human breast cancer cell lines, EMT induces loss of E-cadherin by methylation. Instead, occurs the overexpression of mesenchymal adhesion molecules (Dumont, N *et al*., 2008; Hollestelle, A *et al*., 2013). However, local advanced inflammatory breast cancer and aggressive highly metastatic breast cancers maintain E-cadherin normal expression. Remarkably those tumours present in simultaneous aberrant expression of P-cadherin strongly associated with worse patient survival (Ribeiro *et al*., 2010).

Ribeiro, *et al,* demonstrated that breast cancers cells expressing wild-type E-cadherin concomitant with aberrant expression of P-cadherin have increased capacity of invasion, motility and migration due to the formation of a soluble P-cadherin fragment. In normal context, cadherins form tight complexes with catenins functional linking them to the actin cytoskeleton. P-cadherin counteracts the normal invasive suppressor function of E-cadherin by interfering in the establishment that strong adhesion complex with intracellular catenins. Therefore, E-cadherin expression is not necessarily predictive of good prognosis in breast cancer, and it is also associated with increased cell survival and metastatic spread. Co-expression of those two proteins indicate worse patient survival than in cases in which only one of the cadherins is expressed, or there is no expression of any of them (Ribeiro *et al*., 2010; Ribeiro, *et al*., 2013).

In fact, in cases when P-cadherin was the only molecule expressed, it acts as an invasion suppressor, which suggests that P-cadherin inducible cellular invasion is dependent of E-cadherin endogenous and functional expression (Ribeiro *et al*., 2013; Vieira *et al.,* 2015). In the absence of E-cadherin expression, P-cadherin can interact with catenins, in a similar way to E-cadherin, and therefore being able to suppress invasion. Bazellieres, E et. al reported distinct roles regarding mechanotransduction for P- cadherin and E-cadherin. The first is regulates the levels of intercellular tension, whereas the latest sets the rate at which the intercellular tension builds up. In the absence of E-cadherin, P-cadherin takes the role of tension regulator and can trigger mechanotransduction preventing a decrease in intercellular tension (Bazellières *et al*., 2015).

## P- cadherin

P-cadherin is a type I cadherin with cell-cell adhesion function, binding cells via adherens junctions. Is encoded by *CDH3*, harbous 16 exons presenting high conservation between exon-intron boundaries, is maped in chromosome 16q22.1, in a region containing a cluster of several cadherin genes, only 32kb upstream of E-cadherin gene. Differing mainly in the extracellular portion, P-cadherin shares 66% of homology with E-cadherin. (Bussemarkers, M *et. al*, 1994; Hatta, M *et. al*, 1991).

P-cadherin is a key regulator of several cellular homeostatic processes involved in embryonic development of human foetal structures. It plays a crucial role in the maintenance of normal breast epithelial structural integrity, intervening in processes of cell differentiation, cell shape, cell polarity, growth and migration. Contributes to the undifferentiated state of a variety of adult tissues, such as epidermis, mesothelium, myoepithelial/basal layer of breast and prostate, ovary, cervix, endometrium, pancreas, lungs, organs of the digestive tract and urinary trac, hair follicle and corneal endothelium. In the mammary gland, P-cadherin expression is restricted to the stem cells that give rise to the basal myoepithelial cell layer, termed cap cells (Vieira, A *et. al*, 2012; Vieira, A *et. al*, 2015). The function of P-cadherin in the maintenance of normal breast epithelial architecture has been elucidated by ablation studies. Chanson, L *et. al* used an antibody to antagonize cell-cell interactions stablished with P-cadherin. *In vitro* self-

organizing assay showed that migration of mammary myoepithelial cells occurring during normal sorting of both layers was compromised *(Chanson, L et al*., 2011). Radice *et. al* demonstrated that normal mammopoiesis is disturbed by P-cadherin deletion, once *CDH3*-null female mice presented precocious mammary gland differentiation with alveolar differentiation, breast hyperplasia, as well as increased risk of develop dysplasia with age (Radice, G *et al.*, 1997).

Despite its importance P-cadherin is involved in malignant states specifically hereditary genetic syndromes and in cancer. Loss of P-cadherin expression or germline mutations causing P-cadherin functional inactivation by $Ca^{2+}$ binding disturbance or, synthesis of a truncated form can cause genetic diseases. (Basel-Vanagaite, L *et al*., 2011; Vieira, A *et al.,* 2015).

Regarding carcinogenesis, P-cadherin role depends on the molecular context and tumour cell model. P-cadherin has a tumour suppressive role in melanoma (Jacobs et al., 2011), hepatocarcinoma (Bauer, R *et al*., 2014), in gastric (Kim, M et al., 2010), and prostate carcinoma (Kümper & Ridley, 2010). Overexpression of P-cadherin in colorectal, pancreatic, gastric (Imai, S *et al*., 2018), cólon (Kumara, H *et al*., 2017), oral and oropharyngeal cancer (Lysne, D *et al*., 2014), ovarian (Ko & Naora, 2014) and non-small cell lung carcinoma (Imai, S *et al*., 2018) is associated with tumour progression and poor patient survival. In breast cancer, P-cadherin is overexpressed in 30% of all invasive carcinomas, is mainly found in the triple-negative and basal-like subgroup being associated with high histological grade and BRCA1 mutations (Paredes, J *et al*., 2005; Ribeiro, AS *et al*., 2013; Vieira, A *et al.,* 2015). Several studies have reported P-cadherin as a valuable independent indicator of poor prognosis in breast cancer patients, being associated with reduction of disease-free and overall survival, in addition to poorer locoregional and distant relapse-free interval (Paredes, J *et al*., 2005; Peralta, S *et al*., 1999; Turashvili, G *et al*., 2011). P-cadherin has been associated with well stablished markers for poor prognosis like Ki-67, EGFR, CK5, CK14, vimentin, p53 and HER-2 (Vieira, A *et al.,* 2015). Peralta, P *et. al* demonstrated that P-cadherin is negatively associated with the expression of hormonal receptors (ER and PR). It the report it was also shown independent association with tumour size and lymph node metastasis (Peralta, S

*et al*., 1999). P-cadherin has shown to present high sensitivity in distinguish the basal phenotype of breast carcinomas (Sousa, B *et al*., 2010).

The mechanisms linked to the tumour promoting effects resulting in an increase of aggressive behaviour have been broadly characterized. Intracellular signalling is mediated by P-cadherin interaction with βctn and p120ctn molecules, responsible for the stabilization of the adherens junction complex at the cell surface enabling physical interaction with the actin cytoskeleton. P-cadherin disruption of E-cadherin interaction with both p120ctn and βctn interferes with the tumour suppressive function of E-cadherin promoting cancer cell invasion (Vieira, A *et al.,* 2015). Ribeiro, AS. *et. al* demonstrated that the overexpression of P-cadherin results in increased cell motility, migration and invasion capacity through matrigel. It was proved that P-cadherin induces alterations in cell polarity, leading edge morphology, formation and increase of cytoplasmatic area of membrane protrusions, which typically portrays cells with motile behaviour. In addition, P-cadherin favours the production of pro-invasive factors, such as metalloproteases to the extracellular matrix, specifically MMP-1 and MMP-2, which leads to ectodomain cleavage, producing a soluble fragment with pro-invasive activity (Ribeiro, AS *et al*., 2013). Mechanisms leading to metastatic dissemination of cancer cells mediated by P-cadherin comprise cadherin switching and alterations in mechanotransduction, epithelial to mesenchymal transition and stem cell signalling (Vieira, A *et al.,* 2015).

Vieira, A 2012 showed that P-cadherin mediates stem cell properties being associated with the expression of stem markers like CD44, CD49f, and aldehyde dehydrogenase 1 (ALDH1) in the basal subtype of breast cancer. P-cadherin favours the endurance of aggressive cancer cells, often exhibiting stem-like properties and responsible for resistance to standard cancer therapies, by conferring protection to x-ray induced cell death, and potentiating metastasis and tumour relapses. Depletion of P-cadherin caused a reduction in the expression of CD49f and CD44v6 isoform of CD44 stem cell markers. Furthermore, silencing of P-cadherin in those cell population showed decrease in self-renewal capacity *in vitro*, reduction in the ability to grow colonies in 3D matrigel cultures and lower tumorigenicity in nude mice. The data states that this protein could be an important mediator of stem cell properties in cancer cells (Vieira, A *et al.,* 2012).

The overexpression of P-cadherin in several cancer, including breast contracts with the lower levels expressed in normal tissues appears to suit this protein for cancer immunotherapy. Novel targeted therapeutic agents may be developed targeting disruption of P-cadherin signalling (Imai, K *et al*., 2008; Zhang, C *et al*., 2010). A human monoclonal antibody against P-cadherin (PF-03732010, Pfizer) has highly selectivity and specificity in antimetastatic activity in several cancer models, including breast cancer, alongside with gastric, lung, prostate and colon carcinomas. The antibody degrades β-catenin, antagonizing P-cadherin–regulated cell-cell adhesion and signalling pathways implicated, resulting in antimetastaticand antiproliferative activity. P-cadherin suppression resulted in suppression of cytoplasmatic vimentin, reflecting a diminishing in the metastatic activity and apoptosis. In spite of the efficacy in the animal models and absence of adverse side effects no beneficial effect was observed in humans (Zhang, C *et al*., 2010).

P-cadherin overexpression in breast cancer cells is significantly associated with SRC activation suggesting upstream signaling regulated by P-cadherin (Ribeiro, AS. *et al*., 2010; Vieira, A & Paredes, J, 2015). P-cad has also been shown to promote stemness activity through Src (Vieira, A. *et al*., 2014). Vieira, *et al* shown the need for P-cadherin in the adhesion of breast cancer cells to specific ECM receptors. The expression of α6β4 integrin, a receptor for laminin was found to depend on P-cadherin expression. The α6β4 integrin heterodimer was proved to be implicated in maintenance of stem cell properties and cell invasion, though an association with metastatic dissemination was not stablished (Vieira, A et. al., 2014). Notably, Vieira et al reported that signalling through α6β4 integrin occurs in a P-cadherin dependent way to increase AKT activation levels (Vieira, A *et.al.,* 2014).

# The actin cytoskeleton

## Dynamic of actin cytoskeleton

Cells can perform alterations at a biological level in response to biochemical and biomechanical cues (Azadi, S *et. al*., 2019; Werner, S *et al*.,

2019). Those changes rely in the cytoskeleton, a dense mesh-like array of actin anchored to cell membranes. Cytoskeleton is in the core of cellular mechanical support and resistance to stress, morphogenesis, migration, intracellular vesicular traffic, uptake of extracellular material, cell division, muscle contraction and cell-cell adhesion (Pizarro-Cerdá, J *et al*., 2017). Structures involved in the formation of adherens junctions, such as cadhenins, intervene in the dynamic processes of actin cytoskeleton re-organization and signaling pathways. WNT/β-catenin signaling pathway regulates the self-renewal and migration of BCSCs, promotes metastization and tumor growth in breast cancer (Pai,S *et al*., 2017). Moreover, RhoA GTPase activity in the migratory behaviour is regulated by p120-catenin (Epifano, C *et al*., 2014).

## Actin filament nucleation

Monomers of globular actin (G-actin) form dimers and trimers in a process called actin nucleation, then self-assemble into two proto filament polymers (F-actin) coiled together in a helical form with an overall molecular polarity. There is a constant flux of ATP-actin monomers added to the barbed end, while ADP-actin monomers are removed at the pointed end (Rauhala *et al.*, 2013). This cyclical process designed tread-milling, is the root of cytoskeletal dynamic assembly process (Brayford, S *et al.*, 2015).

Polimerization of actin filaments is enhanced by the activity of cellular actin nucleators responsible for accelerating polymerization of actin monomers (Pizarro-Cerdá, J *et al.*, 2017). There are three major classes of actin nucleators that function by distinct mechanisms: the Arp2/3 complex (working alongside with nucleating-promoting factors - NPFs) such as WASH, WHAMM and JMY), formins and tandem-monomer-binding nucleators (Sitar, T *et al*., 2011).

### The Arp2/3 complex

The evolutionarily conserved Arp2/3 protein complex (Fig. 6) was the first nucleating factor identified in eukaryotic cells, as known so far, this is the only molecular machine that generates branched actin networks. The Arp2/3 complex consists of 7 subunits: The two proteins structurally similar to actin, namely

actin-related proteins ARP2 and ARP3, and five additional proteins, ARPC1, ARPC2, ARPC3, ARPC4, and ARPC5 with a total mass of approximately 250kDa. This multiprotein complex revels an inactive conformation, where Arp2 and Arp3 are maintained far apart by the other five subunits, their activation involves bringing together Arp2 and Arp3. The complex activity is tightly regulated by the phosphorylation of its subunits and nucleation-promoting factors (NPFs) such as N-WASP or WAVE by recruiting ATP-bound actin monomers to stimulate and activating conformational change. Upon it's activation, at the actin branching site, ACTR2 and ACTR3 are folded to form the first subunits of the daughter filament, while a dimer formed by ARPC2 and ARPC4 bounds to the side of pre-existing actin filaments (mother filaments) and initiate the elongation forming a lateral branch (daughter filament) at 70º. The process is described as autocatalytic since actin filaments are both substrates (mother) and products (daughter) of the branching reaction generating filaments at an exponential rate (Molinie, N *et al.* 2018).

ARPC2 subunit holds the central structural position required for maintaining the structural integrity (Rauhala, H *et al*., 2013). Supposedly ArpC3 and Arp3 bridge to increases the efficiency of nucleation, while ARPC1 takes only a minor role and Arpc5 tethers Arp2 to the rest of the complex. The recently formed filaments can serve as substrates to further drive the reaction into generate an exponential increase of actin filaments (Molinie, N *et al.* 2018; Pizarro-Cerdá, J *et al*., 2017; Wagner, A *et al*., 2013).

Moreover, Arp2/3 complex is tightly regulated to orchestrate actin-related functions such as migration, membrane trafficking, cell division, formation of focal adhesions, endocytosis, phagocytosis and infection (Choi, J *et al*., 2019).

Particularly, among these ARPC2, plays a fundamental role in actin filaments nucleation, and Golgi apparatus polarization. Arpc2 plays a crucial role in actin assembly to form lamellipodial protrusions, inducing cell shape change and locomotion (Cheng, Z *et al*., 2019; Pizarro-Cerdá, J *et al*., 2017).

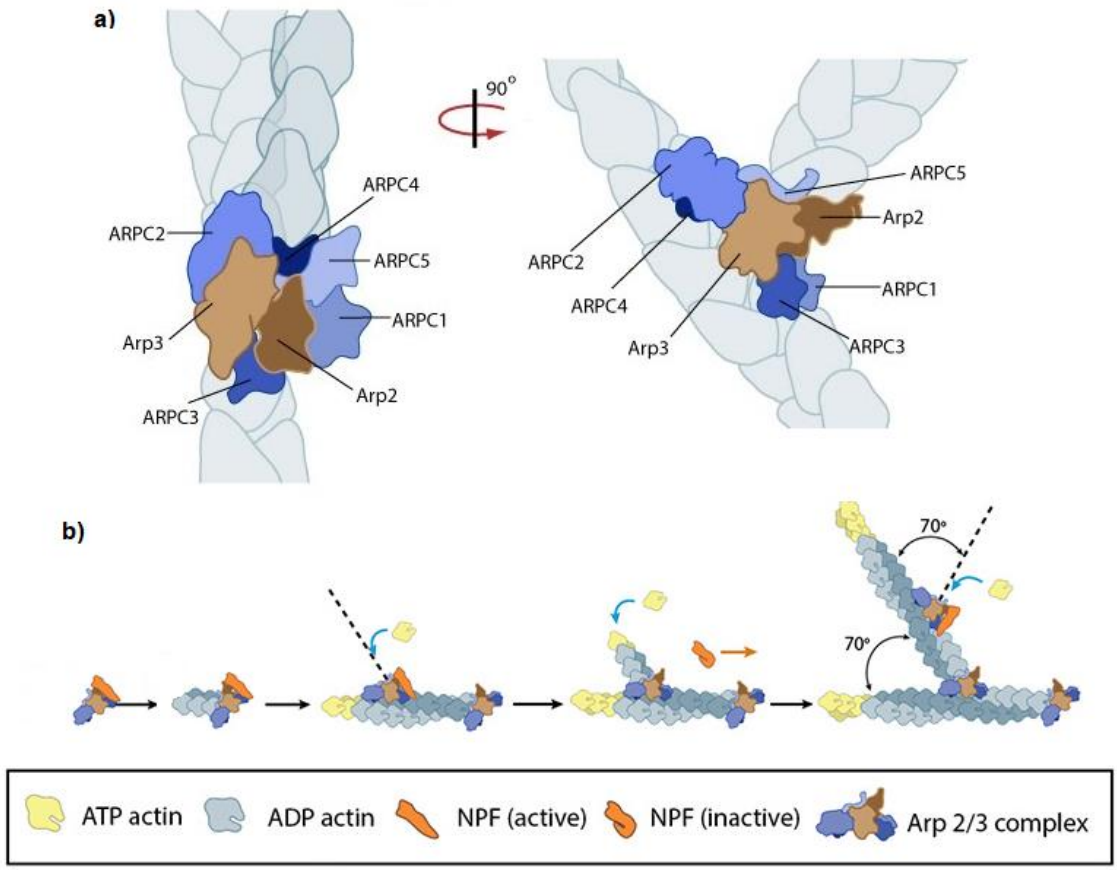


**Fig. 6- The Arp 2/3 complex**. a) Components of the Arp2/3 complex (ARP2, ARP3, ARPC1, ARPC2, ARPC3, ARPC4, and ARPC5). b) Actin nucleation process by Arp 2/3 complex. NPFs activates the Arp2/3 complex. The Arp2/3 complex binds to a pre-existing (mother) filament and nucleates ATP-binder actin monomers forming a new branched actin filament serving as substrate of a new branching reaction. The branched filaments are formed at a angle of 70° relative to the barbed ends of the existing filaments. (Adapted from MBINFO National University of Singapure, 2018)

## Spire

Spire is a nucleator-promoting factor, is comprised in the tandem-monomer-binding nucleators category. Contains four consecutive WH2 domains (formed by 17–27 amino acid long actin-binding motifs) and a β-thymosin domain at the amino-terminal portion (Sitar *et al*., 2011).

The actin nucleation process taken upon spire is not fully understand but some similar mechanisms have been proposed along the years. More recently it was suggested that each of WH2 domains mediates the gathering of actin monomers into nucleation process. Two molecules of Spire are bonded together by one formin dimer, each spire molecule binds four actin molecules, that then can form a complete filament seed creating a nucleating complex. When the actin

complex is bound to formin homology 1 domain within the complex, spire dissociates from the pointed end of the growing filament allowing promotion of elongation (Pfender *et al*., 2011; Quinlan *et al*., 2005; Sitar *et al*., 2011).

It was also assigned to spire a role in membrane traffic processes. It had been described that spire is upregulated in cancer and transformed cells, it accumulates at invadosomes sites and in cytoplasmic vesicles trafficking towards them. (Firat-Karalar & Welch, 2011; Lagal *et al*., 2014).

## The actin cytoskeleton in cancer

Cancer is one of the many diseases arising from cytoskeleton dysregulation. Several studies indicate that cancer cells and non-malignant cells possess different mechanical and physical properties (Azadi, S *et. al*., 2019). Alteration in cell stiffness are associated with different cytoskeleton structures and may indicate cellular malignancy state. In normal cells actin stress fibres are present in the apical region contribution to stiffness, while in the tumorigenic cells they only exist in the basal region not providing significant contribution to rigidity (Calzado-Martín, A et al., 2016). In breast cancer cells tumour with increased metastatic potential were reportedly correlated with less organized cytoskeleton, with lower expression levels of actin, and less viscosity (Hu, J et al., 2018).

Rauhala et. al, analysed the particular contribution of ARP2/3 complex subunits in migration capacity of pancreatic cancer cells, the most prominent effect of cell migration decrease was observed with silencing ARPC4. Chang, Z et. al has reported that Arpc2 is overexpressed in breast cancer cells, promoting cell proliferation, invasion and metastasis by triggering EMT though activation of TGF-β pathway. In the same study, clinical data shown highly association with tumour stage and grading, lymph node metastasis and reduction of overall survival in patients suffering from breast cancer. It was also reported by Zhang *et. al* that ARPC2 may intervene in gastric cancer cell proliferation and migration, as well as increased aggressive behaviour. Arpc2 also modulate gene expression in gastric cancer, cancer-promoting genes were upregulated whereas tumour suppress genes were downregulated ( Cheng, Z *et al*., 2019; Rauhala, H *et al*., 2013; Cheng, Z *et al*., 2019). In a study conducted by Choi, J 2019 *et. al* the team

performed an expression profiling of ARPC2 knock down colon cancer cells and end up selecting pimozide as a migrastic drug and ARPC2 functional modulator. The results indicated inhibition of cell migration and invasion by disrupting the structure of the lamellipodial actin network at the leading edge of the cells in a variety of cancer cell lines (Choi, J *et al*., 2019). Taken together those results provide valuable information that the Arp2/3 complex might be a good therapeutic target for the discovery of migrastatic drugs. Pimozide, a clinically used antipsychotic drug, was demonstrated to be an inhibitor of ARPC2 with antitumor and antimetastatic activity (Choi, J *et al*., 2019).

## SRF/MRTF signalling pathway

Cytoskeletal dynamics of assembly, activity and turnover of actin-based structures is regulated by Rho GTPases and their multiple effectors (Medjkane, S. *et al.*, 2009). Rho family GTPases and their multiple effectors regulate myocardin related transcription factors (MRTFs), from which MRTF-A (MKL1, MAL) and MRTF-B (MKL2) are members. MRTF activity is controlled by actin monomer availability fluctuation. to MRTF remains inactive when is binded to G-actin, upon dissociation MRTF can translocate to the nucleus and activate MRTF-SRF complex (Fig. 7) (Seifert, A & Posern, G 2017). Control the activity of serum response factor (SRF), a highly conserved nuclear transcription factor ubiquitously expressed (Gau & Roy, 2018). Functional studies suggest that MRTF acts exclusively through SRF, in contrast SRF can also bind other transcriptional coactivators, mainly members of TCF (ternary complex factor) family. The recruitment of cofactors occurs in a gene-specific manner (Esnault, C. *et al*., 2014; Gineitis,D *et al*. 2001). Genes regulated by MRTF encode components of the cytoskeleton involved in mechanotransduction, cell-cell and cell-matrix contacts and signaling proteins (Seifert, A & Posern, G 2017). SRF transcriptionally regulates several actin cytoskeleton-associated genes, including actin, growth-promoting, muscle-specific, and contractility-related genes among other genes involved in transcription regulation, cell growth, cell adhesion and cell migration (Esnault, C. *et al*., 2014; Medjkane, S. *et al.*, 2009; Rajakylä, E *et al*., 2014).

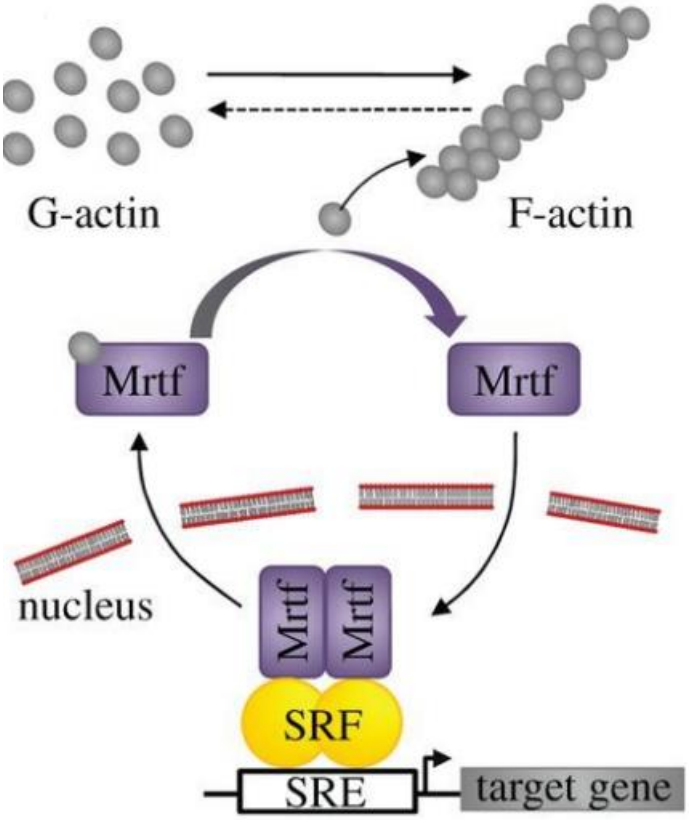


**Fig. 7 - MRTF/SRF signaling pathway.** F-actin assembly leads to decrease of G-actin, relieving inhibition of Mrtf, which translocates to the nucleus and complexes with SRF to drive transcription of genes. (Adapted from Jonchère, V *et al*., 2017)

Breast cancer cells expressing high levels of αV- and β1-integrins activate MRTF-A and SRF, which in turn upregulates expression of target genes associated with migration and invasion (Hermann, M *et al*., 2016). Medjkane had shown that depletion of MRTFs or SRF in breast cancer cells reduced cell adhesion, spreading, invasion and motility, also impairs metastatic colonization (Medjkane, S. *et al.*, 2009). Using human breast carcinoma cells, it was confirmed that MRTF–SRF and YAP–TEAD pathways are mutually dependent, interacting indirectly through their ability to control cytoskeletal dynamics (Foster, C *et al*., 2017). Moreover, MRTF family proteins interact with YAP to potentiate its transcriptional activity, the recruitment of a transcriptional coactivator enhance the expression of target genes required *in vivo* for the metastasis of breast cancer cells (Kim, T *et al*., 2017).

## Drosophila as a cancer study model

Over the years Drosophila Melanogaster has proved to be an important investigation tool enabling important discoveries in the cancer field. Identification of human cancer oncogenes members of conserved signalling cascades such as EGFR, Ras, Myc, Notch, YAP, MAPK, Wnt, Hedgehog, Dpp, and in addition tumor suppressor genes such as PTEN, P53, NF1, APC, and Rb were firstly characterized in Drosophila (Pan, *et al*., 2010; Vidal, M *et al*. 2006). The activation of these cancer pathways in imaginal disc epithelia leads to benign tissue hyperplasia but due to its short lifespan acquisition of mutations leading to cancer development is precluded. Throughout their life cycle cell divisions occur at a much lower number in *Drosophila* than in a human who needs to sustain tissues over longer periods of time (Beira, J *et al*., 2016; Tipping, M *et al*., 2014). On contrary, discovered neoplastic tumour suppressor genes such as lethal giant larvae (lgl), discs large (dlg) and scribble (scrib) lead to tumour formation in flies when mutated (Mirzoyan, Z *et al*., 2019). The establishment of linkage between cancer-related genes into complex signalling pathways allowed the discovering of Hippo signalling pathway (Pan, *et al*., 2010). Knowledge on regulation of cell polarity, cell-cell cooperation and cell competition elucidates mechanisms underlying tumour growth and metastasis (Gonzales *et al*., 2013; Mirzoyan, Z *et al*., 2019; Vidal, M *et al*. 2006).

Even though indispensable in the study of cancer, in cell culture models many aspects of intact epithelia are absent or altered. The study of the hole organism is crucial to comprehend the cancer process. Is becoming increasingly clear that to understand the disease complexity the importance of cell function, cell-cell, and tissue interaction play important must be taken account. Tumour formation, overgrowth and metastasis are the product of a combination of aberrant signalling pathways, mutations, and epigenetic alterations. Understanding how those elements establish functional interactions calls for the use of flexible genetic models (Hanahan & Weinberg, 2011; Vidal, M *et al*., 2006).

Drosophila melanogaster, the fruit fly genome is in overall 60% homologous to that of humans, the identity raises up to 80% concerning the conserved functional domains of proteins. Approximately 75% of human disease-

related genes have functional orthologues in flies. Besides, there is a substantial conserved function of cellular regulatory systems and signalling pathways between human and fly. The Hippo signalling pathway is a key regulator of tissue size during Drosophila development, is responsible for coordinate limit tissue growth by suppressing cell proliferation and by promoting apoptosis to achieve normal tissue size, is highly conserved in mammals. Hippo pathway deregulation has been implicated in a wide variety of human cancers (Wang, Y *et al*., 2018). The core of the pathway is a kinase cascade in which Hippo (Hpo) forming a complex with Salvador scaffold protein (Sav) and Mob as Tumor Suppressor adaptor protein (Mats) phosphorylates and activates the serine/threonine Warts (Wts). A downstream effector of this pathway is Yorkie (Yki), a transcriptional co-activator (Meng, Z *et al*., 2016; Taha, Z *et al*., 2018). The activation of Hippo pathway inhibits Yki oncogene activity preventing its translocation to the nucleus and interaction with transcription factor Scalloped (SD) leading to the activation of target genes responsible for regulating cell growth, proliferation, and survival (Snigdha, k *et al*., 2019).

In case of cancer-related genes perturbation Drosophila melanogaster can display phenotypes that parallel classic human cancer hallmarks, for example sustained proliferation and growth, prolonged survival, metastization to sites distant from their origin, evasion of apoptotic signals, genome instability, and metabolic reprogramming (Beira, J *et al*., 2016; Tipping, M *et al*., 2014). The availability of powerful genetic tools for screenings and recombination techniques applied to the amenability for genetic manipulation and tractability of flies enables fast screens to discover and characterize molecular mechanisms by which human mutations cause disease phenotype (Ugur, B *et al*., 2016). All of these features alongside with a brief generation time and low maintenance costs sets the stage for Drosophila as a robust system with great potentials in addressing complex problematics in cancer biology, allowing their modulation into a model organism like Drosophila, capable of mimicking tumour's biology in the context of intact epithelia (Mirzoyan, Z *et al*., 2019; Ugur, B *et al*., 2016).

Drosophila generation time is quite brief, 11-12 days at 25ºC (Fig. 8) and produces a considerable number of progeny, enabling a rapid building and expansion of new strains for various assays. The development of this

holometabolous insect occurs through three stages: embryo, larva, and pupa. At 25°C the larva stage lasts about four days: first and second larva instar takes about 24h and the third larval instar stage is twice as long, 48 h. At the end of it the larvae wander along the walls of the vial in reach for an appropriate place for pupariation, occurring around 120 h after egg laying (Sonoshita, M *et al*., 2016).

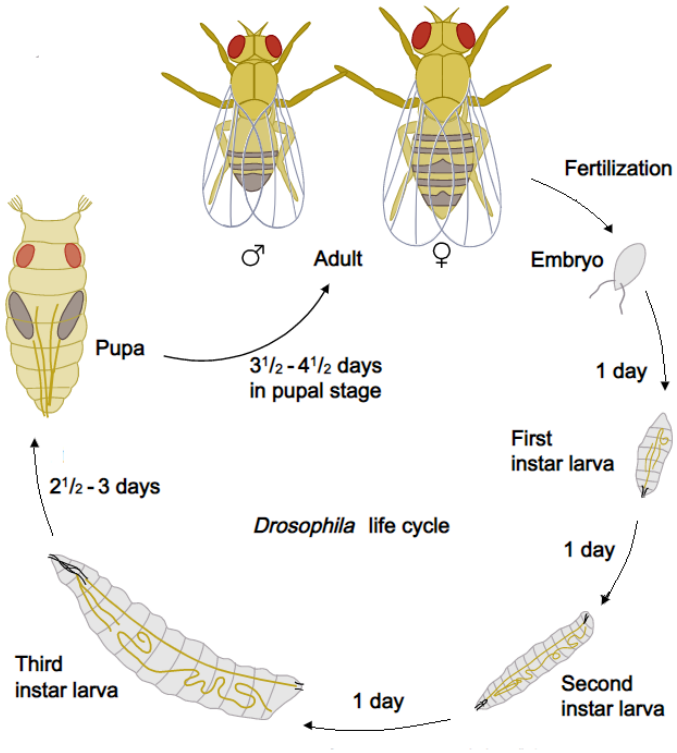


**Fig. 8- *Drosophila* life cycle takes approximately 10-12 days at 25ºC.** *Drosophila* develops in through three stages: embryo, larva, and pupa**.** (Adapted from McNamara, H by McGraw-Hill Companies)

## *Drosophila* imaginal discs

In *Drosophila*, a cluster of epithelial cells from the embryo known as imaginal discs are defined during embryogenesis and matures during larval stages giving rise to the major adult body parts such as eyes, wings, legs, or genitalia. In total there are 19 of this autonomously developing precursor structures in the larva. In the first instar larvae stage discs contain about 20-70 cells, during second and third instar stages cells divide exponentially with cell number doubling about every 10 h at the latest instar stage (Beira, J *et al*., 2016). Imaginal discs (Fig. 9) are formed by two contiguous epithelia with a

characteristic apico-basolateral architecture in a bag-like shape, a columnar shape layer (the disc proper-DP) and a squamous layer (the peripodial epithelium -PE) consisting in the outer layer (Fristom, D *et al*., 1975). At the end of first instar the formation of the anterior-posterior (AP) and dorsal-ventral (DV) define compartmented boundaries. By the end of third instar wing discs present three cell lineages which will become the future notum, hinge and wing destined to form the adult fly wing and mesonotum (Ulrike, N, 2013). Imaginal discs are fully formed prior to pupariation containing between 10.000 to 50. 000 cells (Beira, J *et al*., 2016).

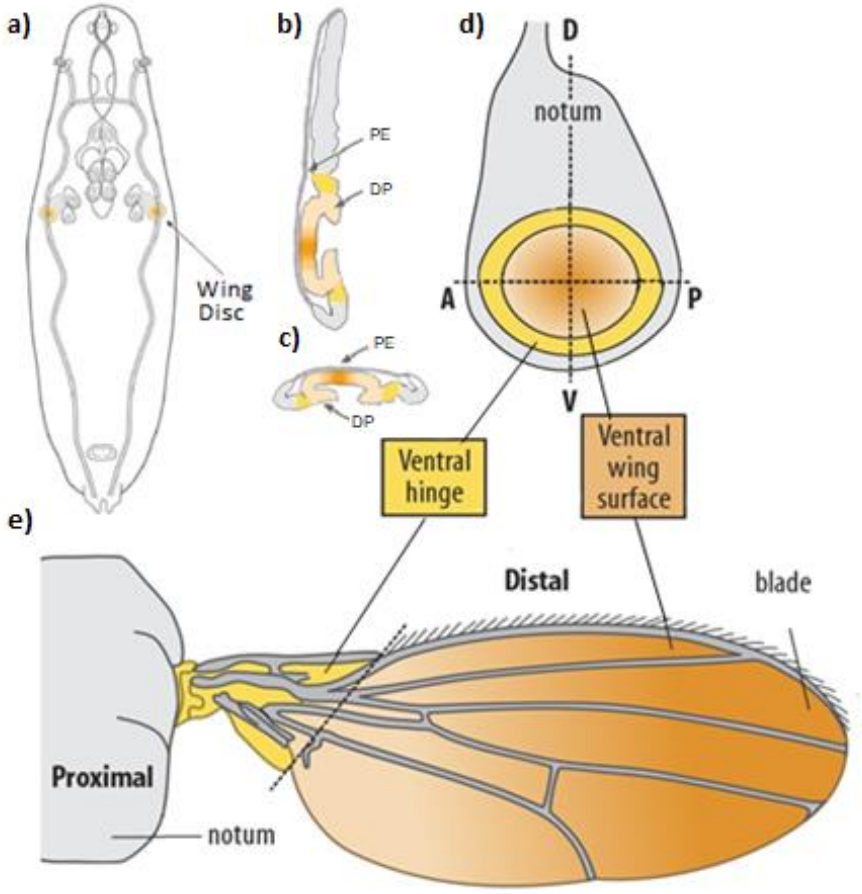


**Fig. 9- The wing imaginal disc location in larva, representation of the epithelial layers, patterning and structure development in the adult *Drosophila*.** a) schematic representation of a third instar larvae and localization of imaginal disc. b) and c) longitudinal and transversal sections of the wing disc showing the disk proper (DP) and Peripodial epithelium (PE). d) frontal view of the wing disc showing the ventral wing surface, the ventral hinge and the notum and their development in the formation of an e) adult dorsal mesothorax highlighting. (Adapted from Staveley, B in http://www.mun.ca/)

Due to the possibility of genetic content manipulation without consequence on the survival of the larva, wing discs can provide an advantageous tool to carry

out genetic screens for the study of fundamental aspects of biology. The existence of wing specific drivers allows gene manipulation with spatial and temporal precision. It is possible to overexpress or knocked down genes in particular segments or boundaries of the wing while maintaining wild type cells in the neighbouring (Mirzoyan, Z *et al*., 2019; Sonoshita, M *et al*., 2016; Tipping, M *et al*., 2014). Major morphologically and biochemically shared similarities between disc cells and human epithelial cells highlight the relevance of the application of discoveries in biomedical research (Beira, J *et al*., 2016; Mirzoyan, Z *et al*., 2019).

## Human P-cad expression in *Drosophila* imaginal disc affects wing development

Preliminary data from genetic interactions made by our group to identify possible regulators involved downstream of P-cad had shown a phenotypic interaction with the *DSRF*/*DMRTF* signalling pathway. Observations indicate that P-cad expression in the *Drosophila* wing disc epithelium affects its normal development compared to control wings expressing *GFP* (Fig. 10 compare b with a). Knocking down *DMRTF* or *DSRF* in adult wings expressing *GFP* (Fig. 10 c and e) rescued their total area ($p<0.0001$) (Fig. 10 g), though no significant effect was observed in their anterior-posterior length (Fig. 10 h) compared to adult wings expressing *GFP* (Fig. 10 a). Knocking down *DMRTF* or *DSRF* in adult wings expressing *P-cad* (Fig. 10 d and f) rescued their total area and their anterior-posterior length defect ($p<0.0001$) (Fig. 10 g and h) compared to adult wings expressing *P-cad* and *mCherry* (Fig. 10 b). These observations indicate that *DMRTF* and *DSRF* are required to induce *P-cad* phenotype.

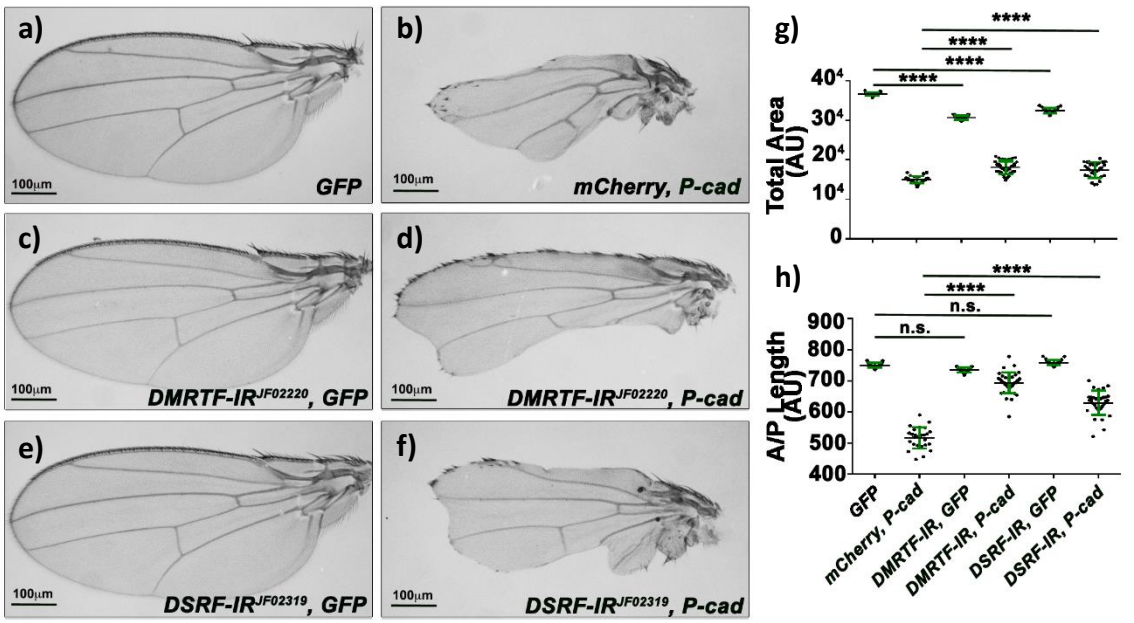


***Fig. 10*- Knocking down *D-MRTF* or *DSRF* rescues adult wing phenotype induced by *P-cad* expression** a) to f) Adult wings from a)*GFP* (control) or b) *nub> mCherry, P-cad* or c) *nub>D-MRTF*-IR, GFP or d) *nub> D-MRTF*-IR, *P-cad* or e) *nub>DSRF*-IR, GFP or f) *nub> DSRF*-IR, *P-cad*. Measurements of wing g) total area and h) anterior-posterior length. Statistical significance was calculated using one-way ANOVA; * indicates statistical significance towards control **** $p<0.0001$, n.s. indicates non-significant

Moreover, preliminary data from genetic interactions made to identify enhancers or suppressors involved in the P-cad induced phenotype had shown a phenotypic interaction with *arpc2* and *spire*. Observations indicate that knocking down *arpc2* or *spire* in adult wings expressing *GFP* (Fig. 11 c and e) did not show any differences in the anterior-posterior length and total area (Fig. 11 g and h), compared to control adult wings expressing *GFP* (Fig. 11 a). Adult wings expressing *P-cad, arpc2*-IR (Fig. 11 d) rescued their total area ($p<0.0001$) (Fig. 11 g) and their anterior-posterior length ($p<0.0001$) (Fig. 11 h), compared to wings expressing *P-cad* alone (Fig. 11 b). Similarly, adult wings expressing *P-cad, spire*-IR (Fig. 11 f) rescued their total area ($p<0.0001$) (Fig. 11 g) and their anterior-posterior length ($p<0.0001$) (Fig. 11 h), compared to wings expressing *P-cad* alone (Fig. 11 b).

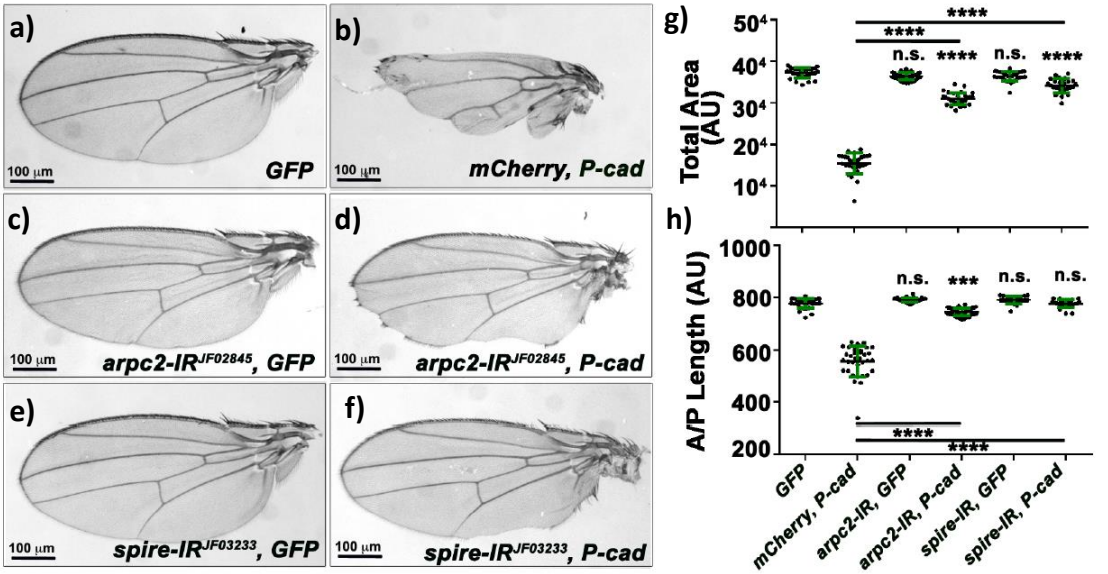


**Fig. 11- Knocking down *arpc2* or *spire* rescues adult wing phenotype induced by *P-cad* expression** a) to f) Adult wings from a)*GFP* (control) or b) *nub> mCherry, P-cad* or c) *nub> arpc2*-IR, GFP or d) *nub> arpc2*-IR, *P-cad* or e) *nub> spire*-IR, GFP or f) *nub> spire*-IR, *P-cad*. Measurements of wing g) total area and h) anterior-posterior length. Statistical significance was calculated using one-way ANOVA; * indicates statistical significance towards control *** $p<0.001$, **** $p<0.0001$, n.s. indicates non-significant

# Hypothesis and aims

It has been known that cell adhesion molecules are involved in the acquisition of stem cell-like properties. P-cadherin in particular is responsible for promote of cancer stem cell properties in breast cancer cells. Nevertheless, the mechanisms by which signals are transmitted to the nucleus to induce a CSC-like phenotype remains elusive. Based in previous observations from our group we hypothesize that MRTF/SRF (bs/D-MRTF in Drosophila) pathway is involved in the acquisition of CSC properties.

The goal of my research project is to test this hypothesis, so we sought to:

1) Validate *Drosophila melanogaster* as a model to study P-cadherin in the acquisition of breast CSC features. Determining if Drosophila ortholog of P-cad effectors known in breast cancer were required to affect wing development downstream of P-cad.

2) Identify signalling molecules and actin nucleators involved in the P-cadherin-induced CSC features. Analysing if target genes of bs/D-MRTF pathway are upregulated by *P-cad* expression and analysing the requirement of *arpc2* and *spire* in the overactivation of the bs/D-MRTF signalling pathway acting downstream of P-cadherin.

# Materials and methods

## The Gal 4-UAS system

The Gal4-UAS system (Fig. 12) is a genetic bipartite tool native to yeast later adapted to Drosophila melanogaster. This system physically separates in two distinct transgenic lines its two components, the target gene from its transcriptional activator. One transgenic line carries a transgenic driver, Gal4, able to recognize an Upstream Activation Sequence (UAS) and a second line carrying an UAS sequence coupled to an intrinsic promoter and a cloning site for the insertion of an interest gene. Crossing those two lines it will result in expression of the target gene in the progeny. Gal4 dictates the expression of the target gene, in the absence of Gal4 the UAS construct is silent. The use of GAL4 system allows generation of multiple driver lines carrying a wide range of regulatory elements controlled GAL4 expression (Caygill & Brand, 2016; Elliott DA, *et al.*, 2008).

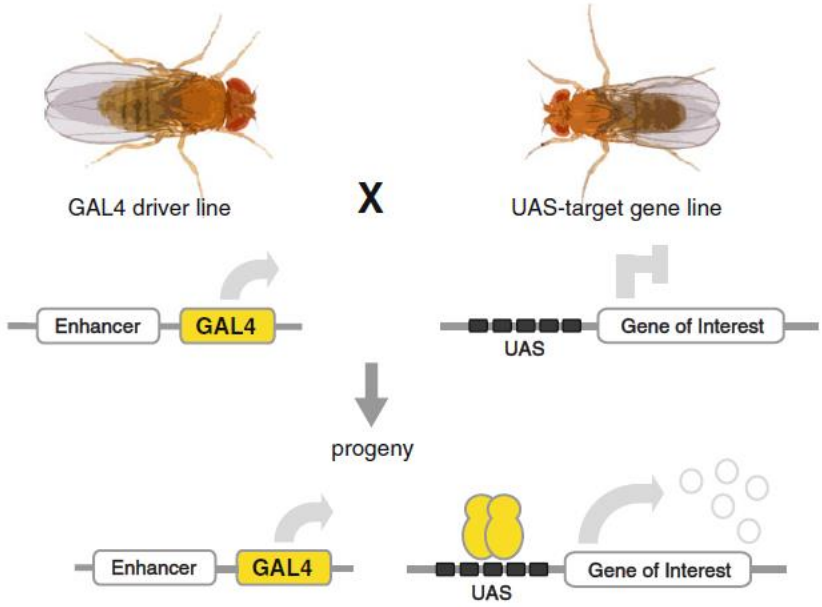


**Fig. 12- Schematic representation of the GAL4-UAS system for transgene expression.** The transcriptional activator Gal4 and the target gene are separated in two transgenic lines. In the absence of Gal4 the UAS construct is silent. Crossing the two lines results in targeted gene expression in the progeny (Caygill & Brand, 2016).

## The Gal 80 system

Gal4 activity can be antagonized by physical interaction with Gal80 protein. A dimer of Gal80 can bind to the GAL4 dimer preventing the activation of

transcription, even though Gal4 can still bind to a UAS sequence. Under the control of the *tubulin 1*α promoter Gal80 can be expressed ubiquitously and repressing Gal4 activity. The temperature sensitive GAL80 ($GAL80^{ts}$) (Fig. ***13***) offers a flexible tool of temporal control of the GAL4 system. $GAL80^{ts}$ is incapable of bind to Gal4 at temperatures above 25ºC, the permissive temperature for repression is 18ºC. The advantage coming from Gal4 and Gal80 interaction is the refine of different expression pattern of GAL4-dependent transgenes by limiting their expression in defined temporal windows (Caygill & Brand, 2016; Elliott DA, *et al.*, 2008).

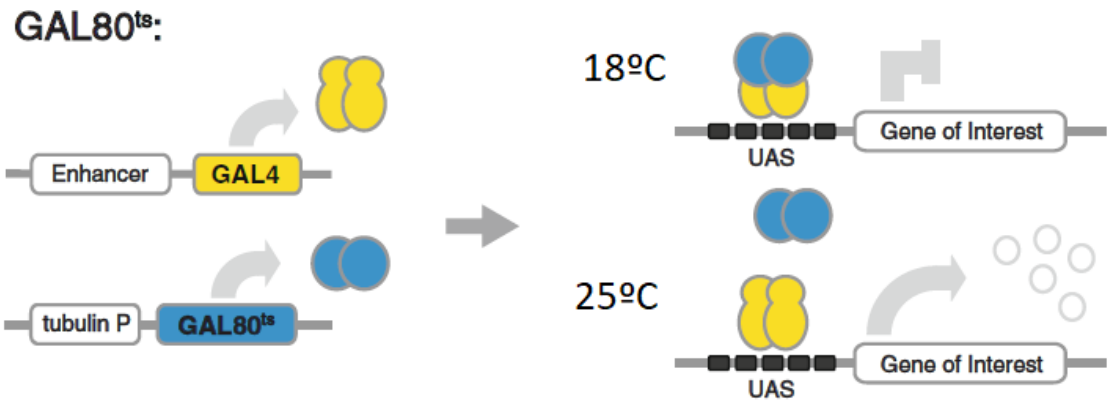


**Fig. 13- Schematic representation of the GAL4-UAS system by temperature sensitive GAL80 ($GAL80^{ts}$).** The physical interaction between $GAL80^{ts}$ inhibits GAL4 activity at the permissive temperature of 18 °C, at 25ºC $GAL80^{ts}$ is incapable of bind to Gal4 allowing the expression of GAL4-dependent transgenes (Caygill & Brand, 2016).

## Fly husbandry and maintenance

The fly stocks and crosses used in this work were maintained at 25ºC, accordingly to standard conditions. Flies were maintained in a 25mm diameter plastic vial containing a yeast-glucose-agar based medium.

## Fly strains and crosses

To address the scientific enquiries several *Drosophila* crosses were performed at a 3:1 female to male ratio. Fly stocks obtained from the Bloomington Drosophila Stock Centre have associated the stock numbers.

- Genetic interactions between *P-cad* and *DE-cad*:

*nub*-Gal4, UAS-*mCD8::GFP* X wild type oregon
*nub*-Gal4, UAS-*P-cad*/Cyo X UAS-*mCherry*
*nub*-Gal4, UAS-*mCD8::GFP* X UAS-*DE-cad*-IR$^{32904}$
*nub*-Gal4, UAS-*P-cad*/Cyo X UAS-*DE-cad*-IR$^{32904}$

- Genetic interactions between *P-cad* and *DAKT1*:

*nub*-Gal4, UAS-*mCD8::GFP* X wild type oregon
*nub*-Gal4, UAS-*P-cad*/Cyo X UAS-*mCherry*
*nub*-Gal4, UAS-*mCD8::GFP* X UAS-*DAKT1*-IR$^{33615}$
*nub*-Gal4, UAS-*P-cad*/Cyo X UAS-*DAKT1*-IR$^{33615}$

Stocks generation
*tub*-Gal80$^{ts}$, TM2/ TM6β X IF/Cyo; UAS-*DAkt1*-IR$^{33615}$/TM6β
↓
*tub*-Gal80$^{ts}$/Cyo; UAS-*DAkt1*-IR$^{33615}$/TM6β (Stock)

*tub*-Gal80$^{ts}$, TM2/ TM6β X IF/Cyo; UAS-*mCherry*
↓
*tub*-Gal80$^{ts}$/Cyo; UAS-*mCherry*/TM6β (Stock)

*nub*-Gal4, UAS-*mCD8::GFP* X wild type oregon
*nub*-Gal4, UAS-*mCD8::GFP* X tub-Gal80$^{ts}$/Cyo; UAS-*DAkt1*-IR$^{33615}$/TM6β
*nub*-Gal4, UAS-*P-cad*/Cyo Tb X tub-Gal80$^{ts}$/Cyo; UAS-*mCherry*/TM6β
*nub*-Gal4, UAS-*P-cad*/Cyo Tb X tub-Gal80$^{ts}$/Cyo; UAS-*DAkt1*-IR$^{33615}$/TM6β

- Genetic interactions between *P-cad* and integrin *αPS4*:

*nub*-Gal4, UAS-*mCD8::GFP* X wild type oregon
*nub*-Gal4, UAS-*P-cad*/Cyo Tb X UAS-*mCherry*
*nub*-Gal4, UAS-*mCD8::GFP* X UAS-*αPS4*-IR$^{44534}$

*nub*-Gal4, UAS-*P-cad*/Cyo X UAS-*αPS4*-IR$^{44534}$

- Genetic interactions between *P-cad* and *arpc2* or *spire*:

*nub*-Gal4 UAS-*mCD8::GFP* X wild type oregon
*nub*-Gal4, UAS-*P-cad*/Cyo Tb X UAS-*mCherry*
*nub*-Gal4, UAS-*P-cad*/Cyo Tb X UAS-*arpc2*-IR$^{28011}$
*nub*-Gal4, UAS-*P-cad*/Cyo Tb X UAS-*spire*-IR$^{30516}$

- Genetic interactions between *P-cad* and *bs* or *D-MRTF*:

*nub*-Gal4, UAS-*mCD8::GFP* X wild type oregon
*nub*-Gal4, UAS-*P-cad*/Cyo Tb X UAS-*mCherry*
*nub*-Gal4, UAS-*P-cad*/Cyo Tb X UAS-*bs*-IR$^{26755}$
*nub*-Gal4, UAS-*P-cad*/Cyo Tb X UAS-*D-MRTF*-IR$^{31930}$

- Genetic interactions between *P-cad*, *arpc2* and *bs* or *D-MRTF:*

*nub*-Gal4, UAS-*mCD8::GFP* X Wild type
*nub*-Gal4, UAS-*P-cad*/Cyo X UAS-*CD2::RFP*; UAS-*mCherry*
*nub*-Gal4, UAS-*P-cad*/Cyo; UAS-*arpc2*-IR$^{28011}$ X UAS-*mCherry*
*nub*-Gal4, UAS-*GFP*; UAS-*mCherry* X UAS-*D-MRTF*-IR$^{31930}$
*nub*-Gal4, UAS-*P-cad*/Cyo; UAS-*arpc2*-IR$^{28011}$ X UAS-*D-MRTF*-IR$^{31930}$
*nub*-Gal4, UAS-*GFP*; UAS-*mCherry* X UAS-*bs*-IR$^{26755}$
*nub*-Gal4, UAS-*P-cad*/Cyo; UAS-*arpc2*-IR$^{28011}$ X UAS-*bs* -IR$^{26755}$

## Western Blot

To prepare western blot extracts, third instar wing imaginal discs were dissected in phosphate buffer (0.5M Na2HPO4; 0.5M NaH2PO4, at a 72:28 ratio in 4 volumes of $H_2O$). The wing discs were placed in a solution of 10 µL of 5X Laemmli buffer; 7 µL of 7X protease inhibitors; 5 µL of 10X phosphatase inhibitors

and 28 µL of phosphate buffer. The extracts were boiled at 100ºC for 5 min and centrifuged at maximum speed (16 000 rpm). Samples were loaded in a SDS polyacrylamide gel electrophoresis (PAGE) (compositions at **Erro! A origem da referência não foi encontrada.** 1.5 mm thickness embedded in 1X running buffer (25 mM Tris, 190 mM glycin, 0.1 % (w/v) SDS). Proteins were fractioned for approximately 90 min at 90V. Proteins were then transferred to a PVDF membrane, previously activated in methanol for 5 min, in 1X transfer buffer (48 mM Tris, 39 mM glycine, 20% methanol, 1.3 mM SDS). Transfer was performed in a box of ice for 2h30min at 300A. Ending that time, membranes to detect P-cadherin were blocked with 5% non-fat milk in 1X TBS supplemented with 0.1% tween-20 (TBS-T) solution and membranes to detect the H3 or Lamin loading proteins were blocked with 3%BSA in 1X TBS-T solution for 1h at room temperature and incubated overnight at 4ºC with primary antibody diluted in TBS-T. The following day membranes were rinsed 4x7 min in TBS-T. Afterwards, membranes were incubated for 1h at room temperature with secondary antibody diluted in solutions of 3 % non-fat milk or 1% BSA in TBS-T. Once more, membranes were rinsed 4x7 min in in TBS-T and for 15 min in 1X TBS. Chemiluminescent detection was performed using Immobilon Western Chemiluminescent HRP Substrate (WBKLS0100, Millipore) and revealed in Bio-Rad ChemiDoc XR equipment (Bio-Rad, UK). Bands intensity were obtained and quantified using the Image Lab Software (Bio-Rad, UK). Intensity value of samples was normalized with loading band intensity value.

Antibodies

Primary: mouse anti-P-cadherin 1:500 (610228, BD TransLab), secondary: anti-mouse HRP 1:2500 (Jackson ImmunoResearch)

Primary: rabbit anti-H3 1:3000 (9715, Cell Signalling), secondary: anti-rabbit HRP 1:5000 (Jackson ImmunoResearch)

Primary: mouse anti-lamin 1:5000 (ADL 67.10), secondary: anti-mouse HRP 1:5000 (Jackson ImmunoResearch).

**Table 1- Composition of polyacrylamide gels used in Western Blot**

| | Stacking 5% | Resolving 7% | Resolving 12% |
|---|---|---|---|
| Acrylamide (30%) | 0,4 mL | 2.39 mL | 3.20 mL |
| $H_2O$ MiliQ | 1,7 mL | 4.95 mL | 2.62 mL |
| Tris 1X pH8.8 | | 2.5 mL | 2.0 mL |
| Tris 1.5X pH6.8 | 0,3 mL | | |
| 10% SDS | 25 µL | 100 µL | 80 µL |
| 105 APS | 25 µL | 100 µL | 80 µL |
| TEMED | 2.5 µL | 10 µL | 8 µL |

## RNA isolation

RNA isolation from 30 wing discs was performed using NZY Total RNA Isolation Kit by Nzytech. It was added 350 µL of buffer NR and 20 mM of DTT (ditiotreitol) to the wing disc pellet, the sample was lised by mixing with micropipet. The lysate was transferred into an NZYSpin homogenization column (purple ring) placed in a 2 mL collection tube and centrifuged for 1 min at 11 000*g*. The flow-through was transferred into a new 1.5 mL microcentifuge tube where 350 µL of 70% ethanol was added and then mixed with micropipet. The lysate was transferred to an NZYSpin Binding column (blue ring) and centrifuged at 11 000x*g* for 30 s. The flow-through was discard and the column was placed back into the collection tube. After, 350 µL of Buffer NI was pipeted against the column wall and a centrifugation at 11 000x*g* for 30 s was made. The flow-through was discard and the column was placed back into the collection tube. From the previously prepared digestion mix (10µL of DNase I + 90µL of digestion buffer) 95 µL were added directly into the centre of the silica membrane of the column (blue ring). Lysate was incubated at room temperature for 15 min. Ending that time 200 µL of Buffer NWR1 was added and a centrifugation of 1 min at 11 000x*g* was performed. The flow-through was discarded and the column was placed back in the same collection tube. Afterwards, it was added 600 µL of Buffer NWR2

(ensuring that the ethanol was previously added) and it was made a centrifuge at 11 000x*g* for 1 min. Once more the flow-through was discard and the column was placed back in the collection tube. It was repeated the wash with 250 µL of Buffer NWR2. It was also performed a centrifugation at 11 000x*g* for 1 min and repeated again to dry the column membrane, the flow-through was discarded. NZYSpin Binding Column was placed in a clean 1.5 mL RNase-free microcentifuge tube and 30µL of RNase-free water directly to the column membrane. Finally, it was made a centrifugation at 11 000x*g* for 1min to elute the RNA. For long term conservation RNAs were stored at -80°C.

## RNAi quantification and purity

To determine RNA concentration and purity, each sample was analysed using Nanodrop 1000 Spectrophotometer (Thermo Scientific, Wilmington, DE, USA). RNA concentration was measured at absorbance at 260nm, the absorbance ratios A260/A280 and A260/A230 indicated sample purity.

## cDNA synthesis

RNA extracted from the samples was reversely transcribed, the entire experiment was made on ice. A mixture of 1µL of random hexamer primers at 50ng/µL and 1µL of dNTPs at 10Mm was added to a determined volume of RNA with a concentration of 500ng diluted in RNase free water to reach 16µL of total volume. The mixture was placed in the thermal cycler at 65ºC for 5 min. Ending that time the mixture was placed on ice for 1 min. Then, a mix of 1µL of M-MuLV reverse transcriptase, 2µL of 10X Reaction buffer and 1µL of Nzy ribonuclease inhibitor was added to each sample and adjusted to a total volume of 20 µL. The samples were placed in thermal cycler using the following incubation steps: 25ºC for 10 minutes, 37ºC for 50 minutes and 70ºC for 15 minutes. The synthetized cDNAs were stored at -4ºC.

## cDNA amplification and integrity evaluation

PCR was carried out to confirm cDNA sample integrity. It was prepared a mix containing 2 µL of 5X Go 2Taq Flexi buffer; 1 µL of $MgCl_2$ at 25 mM; 0.2 µL of DNTP's at 10 mM; 0.05 µL of Go Taq Flex G2; 0.3 µL of reverse and forward primers; 1 µL of cDNA at a concentration of 10ng/ µL and 5.15 µL of Rnase free water. The samples were placed in thermocycler using the following cycling steps: 95ºC for 2 minutes, 95ºC, 60ºC and 72ºC at 1 min repeated 30 times and 72ºC for 5 minutes. The amplified cDNA was stored at -4ºC. PCR amplification product was subsequently subject to electrophoresis in a 2% (W/V) agarose gel in 1X TAE buffer at 90V for 30 minutes. It was prepared a marker sample to compare the products size constituted by 10 µL of RGS Low Range with 1 µL of 6X gel red loading dye, samples were prepared using 5 µL of the PCR product and 1 µL of 6X gel red loading dye. The agarose gel was analysed in Bio-Rad ChemiDoc (Biorad, UK) and in the software ImageLab (Bio-Rad, USA).

## Primer reconstitution

The primer vials were centrifuged at 1000 rpm for 10 seconds to dislodge the power form the walls. Primers were reconstituted according to manufactures instructions. The indicated volume of RNase free water was added to the lyophilized powder to create a stock with a concentration of 100 µM. Primers were incubated at 37ºC for 30 min in 300 rpm agitation. Primers were then diluted to a work concentration of 10µM. Primers stock as well as working dilutions were stored at -4ºC.

## qPCR

Firstly, qPCR was performed to assess primers efficiency using serial dilutions of cDNA in each reaction (25 ng/µL; 5 ng/µL; 1 ng/µL; 0.2 ng/µL and 0.04 ng/µL). This way it was possible to create a standard curve with five CT value points. The slop of the curve was determined to calculate primer efficiency

accordingly to the formula: $E = \left(10^{\frac{1}{n}} - 1\right) \times 100$. Efficiency values of each primer are shown in **Erro! A origem da referência não foi encontrada.**

To perform qPCR for each sample it was prepared a mix containing 5 µL of 2X iTAQ SyBR Green; 0.3 µL of reverse and forward primers; 3.4 µL of RNase free water and 1 µL of cDNA at a concentration of 10 ng/µL. The reactions were carried out in a Real time CFX 96 qPCR (Bio-Rad, CA, USA) equipment. Amplification started with denaturation at 95ºC for 3 minutes, followed by 40 cycles of a 2 steps cycle: first of all, a denaturation step of 20 seconds at 95ºC, an annealing step for 30 seconds at 60ºC, it followed a step of 55ºC for 10 seconds, and after an increment of 1ºC to 95ºC. The relative expression was calculated using RpL32 as a reference gene in the application of method 2-ΔΔCt, proposed by Pfaffl (Pfaffl, M 2001).

**Table 2- Primers sequences and efficiency**

| Primer | Sequence | Efficiency |
|---|---|---|
| PS2 | F: CTCGATGTTCGGATTCAGCAT<br>R: CGGGAGGTGTCGAATTTGGG | 84,45% |
| PS4 | F: GTTGGCCCTTCAATCCGAAAT<br>R: GCCACCATAATACTTTTCTCCCG | 87,79% |
| MESK2 | F: CCCACTTTGCCAGAGGATTAC<br>R: CAATCACCGACTTTAGGCCAA | 83,71% |
| RpL32 | F: GGCAGTATCCATTGAGTTTCC<br>R: AAGTGTGCGGCTCGTATT | 108,73% |

## Drosophila wings quantification

Pictures were captured in a Nikon Digital Sight ds-v1 camera coupled in a Nikon SMZ 1500 stereomicroscope and processed in NIS-Elements F 2.20. All measurement parameters length (Fig. 14**Erro! A origem da referência não foi encontrada.** a), area (Fig. 14 b) and circularity (Fig. 14 c) were manually drawn and quantified in FIJI (NIH) software.

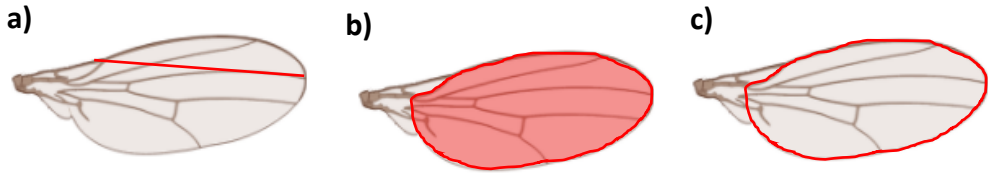


**Fig. 14-Drosophila melanogaster wing measured parameters.** For each wing, the a) length, b) total area and c) circularity were measured as represented by the red sections.

## Statistical analyses

Graphical representation of data was plotted, typically mean ± SD, in Graphpad Prism 7. Statistical analyses were also performed using the same program, exact p values, and statistical tests used are reported in figure legends. For statistical comparison between groups one-way ANOVA tests were used in wing measured parameters analyses. Student's unpaired t test was used in Western Blot analyses and qRT-PCR analyses. *Bartlett's test* was utilized to evaluate variance homogeneity and Brown-Forsythe test was utilized to evaluate the equality of group variances.

# Results

# 1- Drosophila E-cadherin act as effector of human P-cad for wing disc development but *Drosophila* AKT1 does not

Expressing P-cadherin (P-cad) in the *Drosophila* wing disc epithelium affects wing development (Fig. **10** b). To demonstrate that this phenotype constitutes a good model to identify P-cad effectors that are relevant to its functional effect in cancer, we tested if the Drosophila ortholog of some of the P-cad effectors already known were also required to affect wing development downstream of P-cad. Among those, E-cadherin (E-cad) is required downstream of P-cad to increase tumorigenicity (Ribeiro, AS *et al*., 2013). Moreover, it has been reported that P-cad promotes Akt phosphorylation in breast cancer cells (Vieira, A *et al.*, 2014). To test the requirement of E-cad and Akt downstream of P-cad, we analysed the effect of knocking down Drosophila *E-cad* (*DE-cad*) or *Akt* (*D-Akt1*) on the P-cad adult wing phenotype. If the effect of *P-cad* in the fly wing also requires *DE-cad* or *D-Akt1*, reducing *DE-cad* or *D-Akt1* levels should suppress the P-cad adult wing phenotype.

For all crosses we used the *nubbin*-Gal4 *(nub*-Gal4) driver to direct the expression of UAS-*P-cad* and of UAS-RNA interference construct targeting *DE-cad* (*DE-cad*-IR) or against *D-Akt1* (*D-Akt1*-IR) to degradation in the most proximal domain of the wing disc epithelium (pouch) starting at 2$^{nd}$ instar larval stage. As a wild type control, we crossed a transgenic line carying *nub*-Gal4 and *GFP* under the control of UAS binding sites (UAS-*GFP*) with a wild type strain. To evaluate the effect of knocking down *DE-cad* or *D-Akt1*, the *nub*-Gal4, UAS-*GFP* line was crossed with a line carrying UAS-*DE-Cad*-IR or UAS-*DAkt*-IR. To access the effect of expressing P-cad alone, a transgenic fly line expressing *P-cad* under the control of *nub*-Gal4 was crossed with a strain carrying UAS-mCherry. To test the consequences of knocking down *DE-cad* or *D-Akt1* on the *P-cad* wing phenotype, the *nub*-Gal4, UAS-*P-cad* line was crossed with UAS-*DE-cad*-IR or UAS-*DAkt*-IR lines. UAS-*GFP* or UAS-*mCherry* were used to normalize the number of UAS constructs between each cross. To evaluate the phenotypic effect resulting from these crosses, the wings of female progeny were collected

and evaluated through the measurement of three parameters: their anterior-posterior length, their total area and their circularity.

Drosophila wings expressing *P-cad* and *mCherry* (Fig. 15 b) revealed an impairment in wing development compared to control wings (Fig. 15 a). In wings expressing *GFP* and knocked down for *DE-cad*, the phenotype was so severe that only the vestigial structures of the wing were present (Fig. 15 c). Expressing *P-cad* in these wings restored wing development (Fig. 15 b). Conversely, the reduction in *DE-cad* rescued some aspect of the *P-cad* phenotype. Wings expressing *P-cad* and knocked down for *DE-cad* showed larger area ($p<0.01$) (Fig. 15 f) and were more circular ($p<0.0001$) (Fig. 15 g), compared to *P-cad*, *mCherry* wings (Fig. 15 b). However, knocking down *DE-cad* in *P-cad* expressing wings did not rescue the anterior-posterior length defect, compared to *P-cad*, mCherry wings. Instead, a reduction in *DE-Cad* levels further reduced the anterior-posterior length of *P-cad*-expressing wings ($p<0.05$) (Fig. 15 e).

Overall, these observations indicate that *P-cad* expression rescues the phenotype induced by *DE-cad* knocked down. Conversely knocking down *DE-cad* also rescues the small wing phenotype induced by *P-cad.* Therefore, we can conclude that *P-cad* requires *DE-cad* to affect wing development.

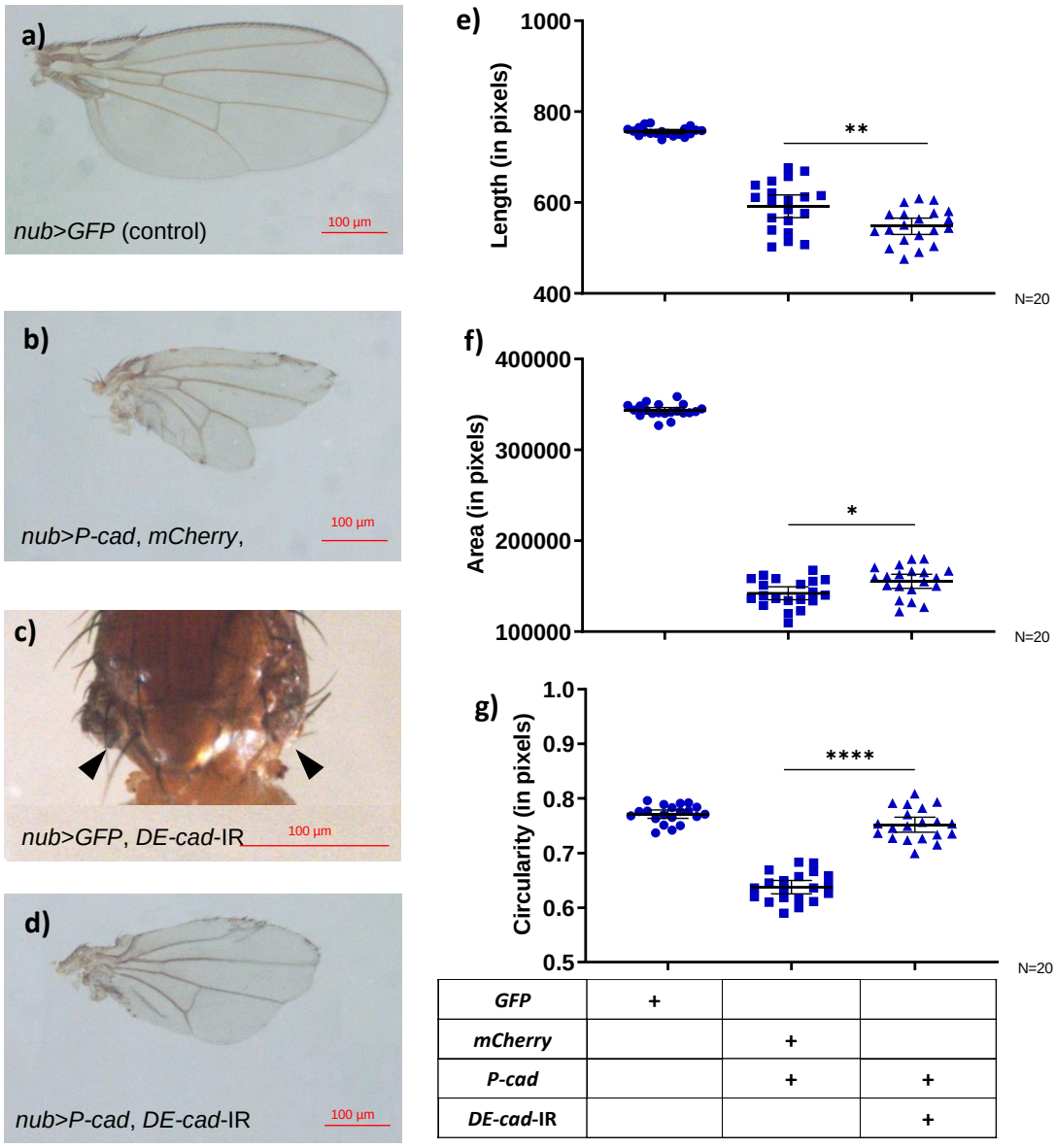


**Fig. 15 - Knocking down *DE-cad* rescues the adult wing phenotype induced by *P-cad* expression, *P-cad* expression rescues the adult wing phenotype induced by *DE-cad* knocked down.** a) to d) Adult wings from a) *nub*> *GFP* (control) or b) *nub*> *P-cad*, mCherry or c) *nub*> *GFP*, *DE-cad*-IR or d) *nub*> *P-cad*, *DE-cad*-IR. e) to g) measurements of wing e) anterior-posterior length, f) total area and g) circularity. Arrows indicate vestigial wing structures. Plots are quantifications of 20 adult wings from female flies, horizontal bars represent mean value, error bars indicate standard deviation. Statistical significance was calculated using one-way ANOVA; * indicates statistical significance towards control * p<0.01, **p<0.05, **** p<0.0001

To determine if *D-AKT1* is required downstream of *P-cad* to affect wing development, we tested the effect of knocking down *D-Akt1* in *P-cad*-expressing wings using the same strategy that the one described to test the role of *E-cad*. In a first set of experiments, all crosses were maintained at 25ºC in order to allow nub-Gal4 to function as driver at 2$^{nd}$ instar larvae (Fig. 16).

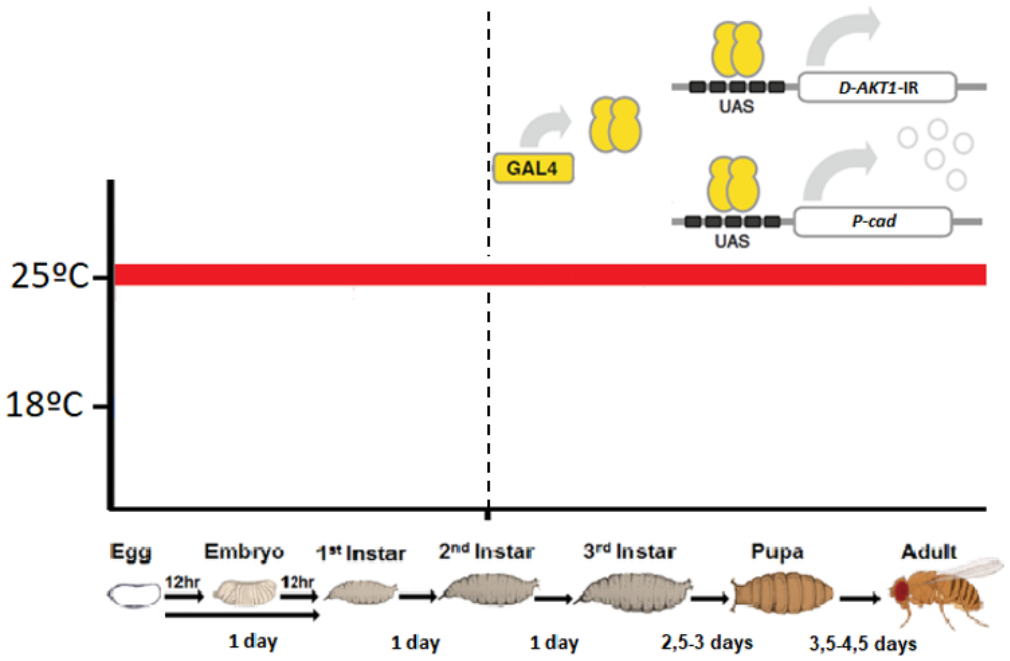


**Fig. 16- Schematic of the experimental setting to express UAS-*P-cad* and UAS-*AKT1-IR* at 2nd instar larvae.** Crosses were maintained at 25ºC allowing *nub*-Gal4 to function as driver in 2nd instar larvae. In those temperature conditions *P-cad* is expressed and *D-AKT1* is knocked down.

In crosses expressing *D-Akt1*-IR and GFP (Fig. 17 c) or *P-cad* (Fig. 17 d), under *nub*-Gal4 control, the number of progeny was very low. Sometime only one or frequently no fly arised from these crosses. The few adults expressing *D-Akt1*-IR and *GFP* showed very defective and wrinkled wings (Fig. 17 c) compared to adult wings expressing P-cad and mCherry (Fig. 17 b). Knocking down *D-Akt1* does not rescue the size defect of *P-cad* expressing wings. Instead, *D-Akt1* depletion resulted in even more severe wing defects that only displayed vestigial structures (Fig. 17 d), compared to adult wings expressing P-cad and mCherry (Fig. 17 b). Overall, these observations suggest that *D-AKT1* is required for wing development. A possible explanation for the reduction in progeny number may be the fly inability to emerge from the pupae because *D-Akt1* knocked down could affect the wing hinge. As the reduction of *D-Akt1* levels enhanced the defects of *P-cad*-expressing wings (Fig. 17 b), these results also suggest that *P-cad* does not require *D-Akt1* to affect wing development.

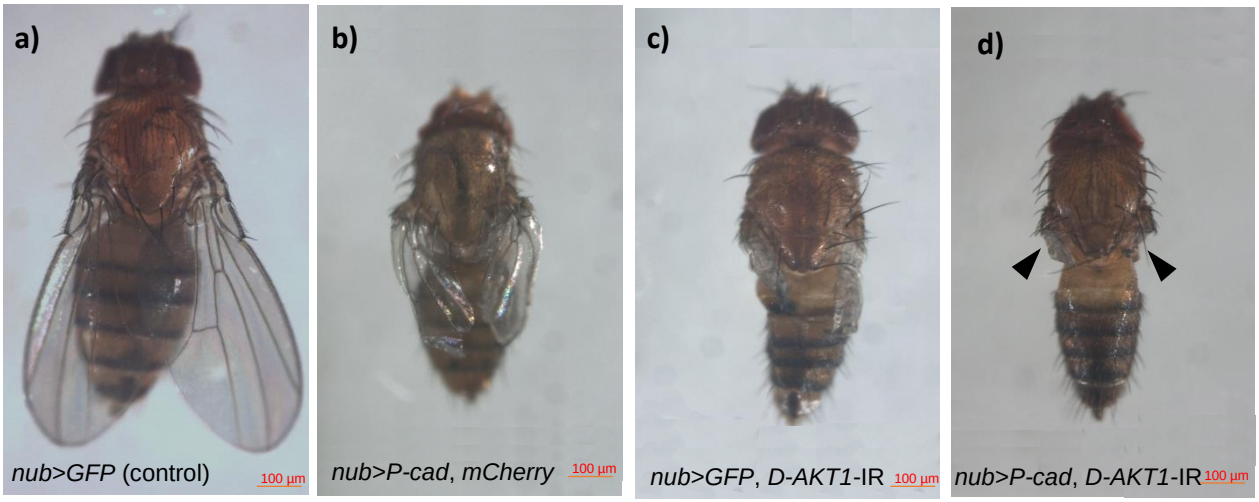


**Fig. 17- Knocking down *D-Akt1* does not rescue the adult wing phenotype induced by *P-cad* expression.** a) to d) Adult wings from female flies from a) *nub> GFP* (control) or b) *nub> P-cad*, *mCherry* or c) *nub> GFP*, *D-AKT1*-IR or d) *nub> P-cad*, *D-AKT1*-IR. Arrows indicate vestigial wing structures.

Yet, since knocking down D-*AKT1* at 2nd instar larvae in the distal wing disc epithelium using the nub-Gal4 driver led to a limited number of progeny, we used the Gal80$^{ts}$ system to delay the timing of *D-AKT1* Knocked down (Fig. 18). The crosses were maintained at 18ºC for 7 days in order to allow *tub*-Gal80$^{ts}$ to function as a repressor of Gal4 activity until the beginning of 3rd instar larvae. Crosses were then placed at 25ºC to induce Gal4 activity. The control wings were obtained by crossing a transgenic line carrying *nub*-Gal4 and UAS-*GFP* with a wild type fly stock. To knock down *D-Akt1* at 3rd instar larval stage a transgenic line carrying *nub*-Gal4, UAS-*GFP* and tub Gal 80$^{ts}$ was crossed with a transgenic line bearing UAS-*D-Akt1*-IR. To obtain wings expressing UAS-*P-cad* alone or with UAS-*D-Akt1*-IR at 3rd instar larval stage, *nub*-Gal4, UAS-*P-cad* flies were crossed with a tub-Gal80$^{ts}$; UAS-mCherry or tub-Gal80$^{ts}$; UAS-*D-Akt1*-IR strains respectively.

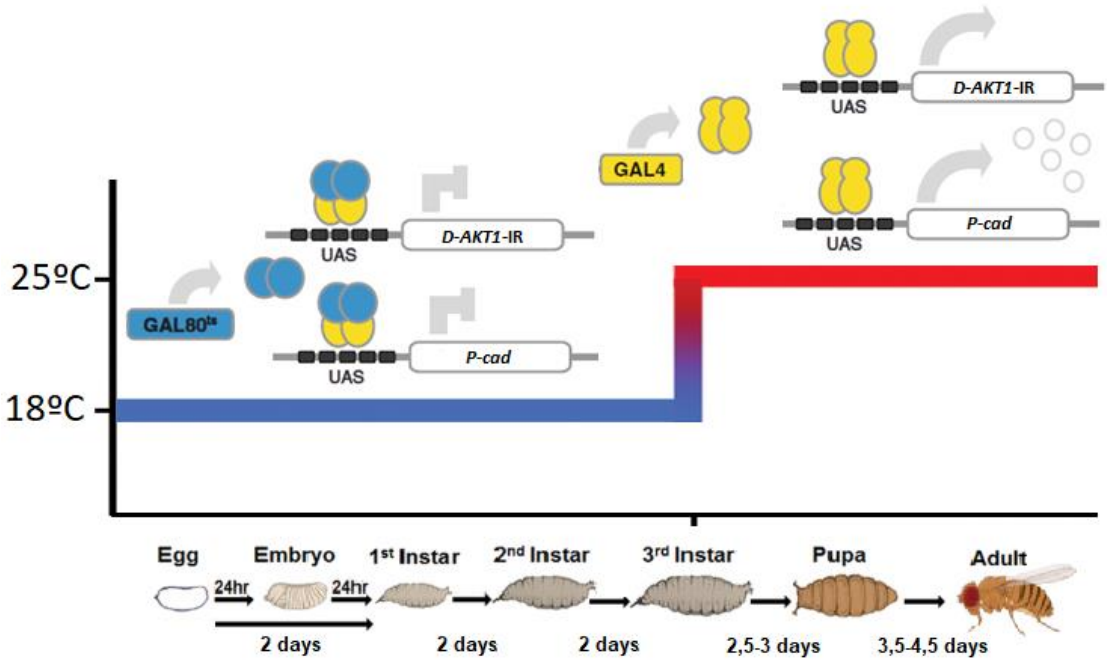


**Fig. 18- Schematic of the experimental setting to express UAS-*P-cad* and UAS-*AKT1-IR* at 3rd instar larvae using Gal80ts.** Crosses were maintained at 18ºC for 7 days in order to allow tub Gal80ts to function as a repressor of Gal4 activity. In those temperature conditions *P-cad* and *D-AKT1* are not expressed. After 7 days, corresponding to 3rd instar larval stage crosses were placed at 25ºC to induce Gal4 activity. In those temperature conditions *P-cad* is expressed and *D-AKT1* is knocked down.

Results demonstrate that expressing *P-cad* (Fig. 19 b) at 3rd instar larvae stage did not seem to ameliorate the wing phenotype compared to wings expressing *P-cad* at 2nd instar larvae stage (Fig. 17 b). Similarly, knocking down *D-Akt1* in the absence of P-cad at 3rd instar larval stage did not appear to weaken the wing phenotype (Fig. 19 c), compared to those knocked down for *D-Akt1* at 2nd instar larval stage (Fig. 17 c). However, wings in which *D-AKT1* and *P-cad* were expressed at 3rd instar larval stage appeared similar to those expressing *P-cad* only (Fig. 19 compare d with b). These results suggest that P-cad expression at 3rd instar larval stage supresses the phenotype resulting from the reduction of *D-AKT1*.

Taken together the results appear to indicate that *P-cad* does not require *D-AKT1* to affect wing development. However, *P-cad* expression rescues the phenotype induced by *D-AKT1* knocked down.

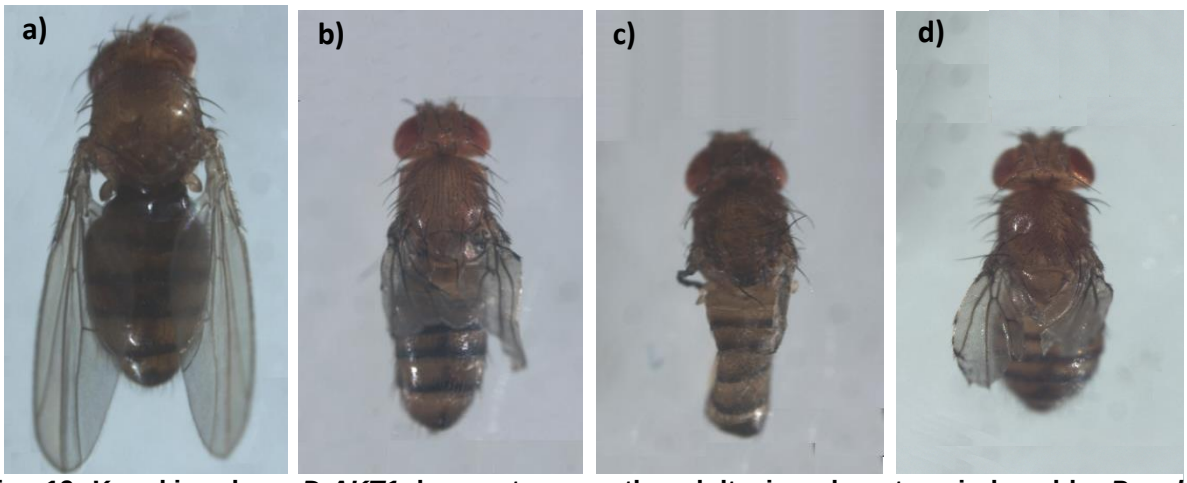


**Fig. 19- Knocking down *D-AKT1* does not rescue the adult wing phenotype induced by *P-cad* expression, *P-cad* expression rescues the adult wing phenotype induced by *D-AKT1* knocked down.** a) to d) Adult wings from female flies from a) *nub> GFP* (control) or b) *nub> P-cad*, *mCherry*; tub Gal80$^{ts}$ or c) *nub> GFP*, tub Gal80$^{ts}$ *D-AKT1*-IR or d) *nub> P-cad*, tub Gal80$^{ts}$ D-*AKT1*-IR. Arrows indicate vestigial wing structures.

## 2- The bs/MRTF pathway is not required to stabilize P-cad

Initial screens had already advocated a phenotypic interaction between P-cad and the *bs*/*D-MRTF* signalling pathway (Fig. 10). Two different hypotheses can explain the rescue of the *P-cad* expressing wing phenotype by the reduction of *bs* or *D-MRTF* function. The *bs*/*D-MRTF* pathway could act upstream of *P-cad*, stabilizing *P-cad* or controlling its sub-cellular localization. Alternatively, the *bs*/*D-MRTF* pathway could act downstream of *P-cad*, being overactivated by *P-cad* to affect wing development. To determine which type of regulation occurs, we tested the effect of knocking down *bs* or *D-MRTF* on *P-cad* levels by Western blot in wing imaginal discs. A cross between the transgenic line *nub*-Gal4, UAS-*GFP* and a wild type fly strain was used as a negative control. The *P-cad* conditional expression levels were determined by crossing the transgenic line expressing *nub*-Gal4, UAS-*P-cad* with three other lines carrying either UAS-*mCherry* or UAS-*bs*-IR or UAS-*D-MRTF*-IR.

By western blot, the anti-P-cad antibody revealed two bands of close molecular weight that are absent in *nub>GFP* wing disc extracts that did not

express P-cad. To evaluate total P-cad levels, the intensity levels of both bands were quantified (Fig. 20 a and Supplementary figure 1). In one of the experiments, the levels of H3 used as loading control were too uneven between samples so the replicate was excluded from quantification. Results did not show significant differences in *P-cad* expression levels in wing discs expressing *mCherry* compared to those expressing *P-cad* when either *bs* or *D-MRTF* was reduced by knocked down (Fig. 20 b). These results indicate that knocking down *bs* or *D-MRTF* does not affect *P-cad* expression levels.

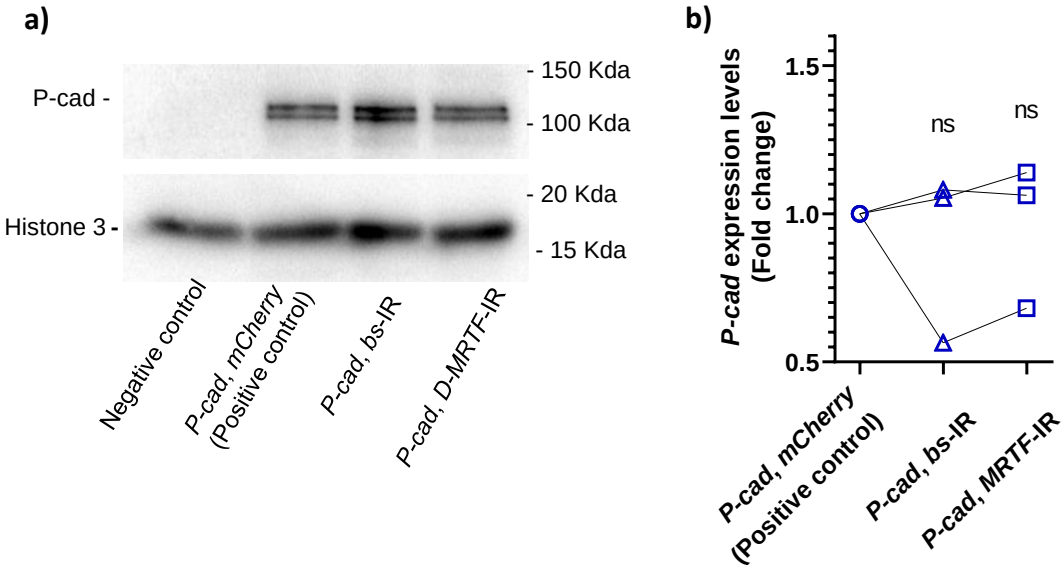


**Fig. 20- Knocking down bs or *D-MRTF* does not affect *P-cad* levels.** Western blots on Drosophila wing disc extracts from *nub> GFP* (negative control); *nub> P-cad*, *mCherry* (positive control); *nub> P-cad*, *bs*-IR or nub> *P-cad*, D-*MRTF*-IR. a) Upper membrane was blotted with anti-P-cad antibody, which reveals two bands at a molecular weight of ≈120 Kda. The lower membrane was blotted with anti-Histone 3 (H3) antibody used as loading control, which reveals one band at a molecular weight of ≈17 Kda. b) Quantifications are from four biological replicates. The intensity of the two P-cad bands were first normalized to H3 levels used as loading control and then to the intensity levels of P-cad in *nub>P-cad, mCherry* wing disc extracts to evaluate for fold change. Error bars indicate standard deviation. Statistical significance was calculated using one-way ANOVA. ns indicates non-significant.

To verify that the wing discs extracts used to perform the western blots were knocked down for *bs* or *D-MRTF*, adult wings from each cross were mounted. We could confirm that knocking down *bs* suppressed the small wing phenotype induced by *P-cad* (Fig. 21 compare c with b), as their anterior-posterior length ($p<0.0001$) (Fig. 21 e) and total area ($p<0.0001$) (Fig. 21 f) were significantly increased, compared to adult wings expressing *P-cad* and *mCherry* under *nub*-Gal4 control. However, adult wings expressing *P-cad* and knocked

down for *bs* (Fig. 21 c) showed no differences in circularity (p= 0.8803) (Fig. 21 g) compared to adult wing expressing *P-cad* and mCherry (Fig. 21 b). Similar results were observed for wings expressing *P-cad* and *D-MRTF*-IR (Fig. 21 compare d with b), which showed a significant rescue in anterior-posterior length and total area compared to *nub>P-cad*, *mCherry*-expressing wings (p<0.0001) (Fig. 21 e and f). Nevertheless, knocking down *D-MRTF* (Fig. 21 d) significantly reduced wing circularity (p<0.01) (Fig. 21 g), since these wings appear to be more elongated, compared to wing phenotype expressing *P-cad* alone (Fig. 21 b). As we could recapitulate the genetic observations previously observed between *P-cad* and *bs* or *D-MRTF* with the crosses used to prepare protein extracts, we can conclude that bs or *D-MRTF* are unlikely stabilizing *P-cad*.

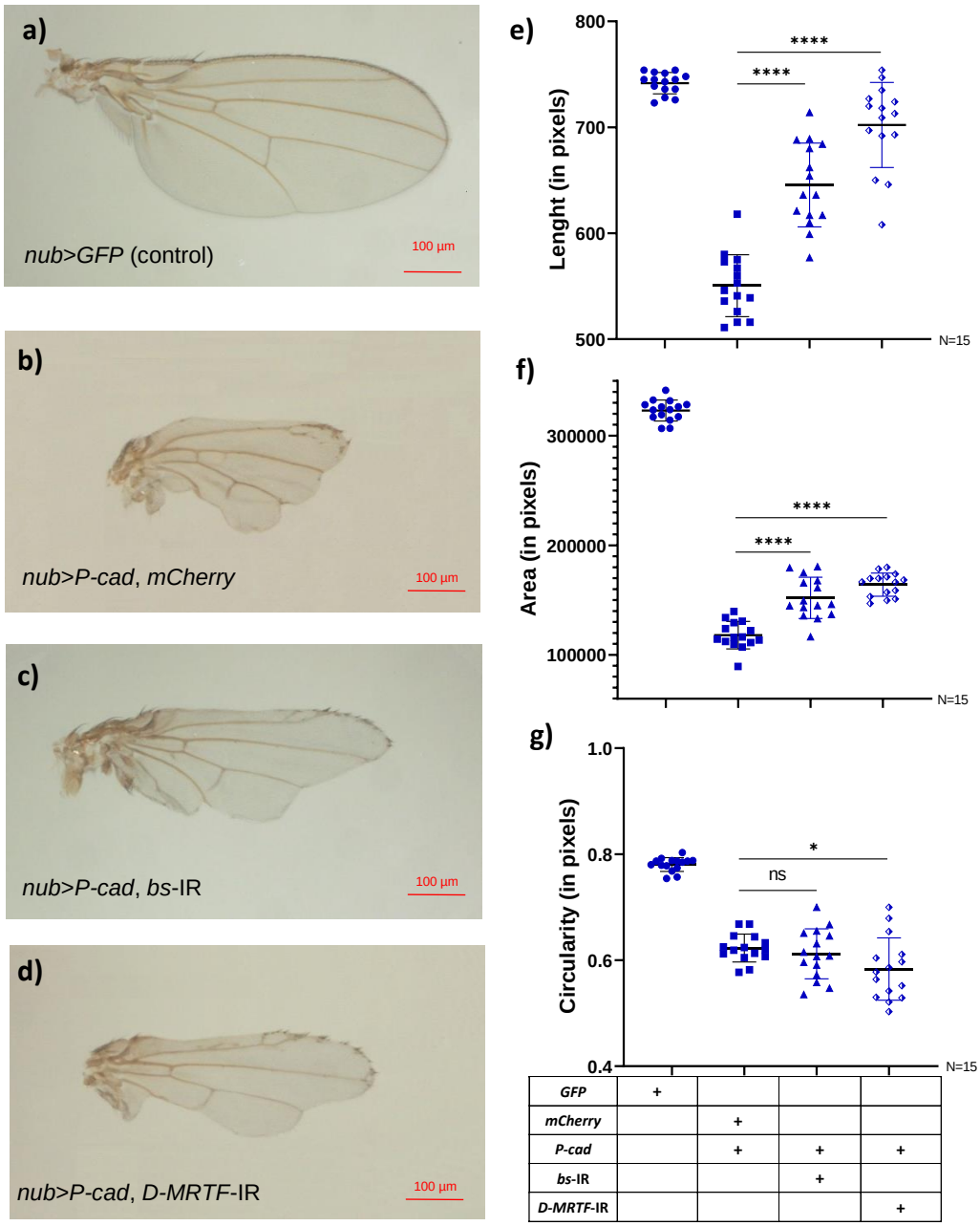


**Fig. 21- Knocking down bs or *D-MRTF* rescues adult wing phenotype induced by *P-cad* expression**. a) to d) Adult wings from a) *nub>GFP* (control) or b) *nub>P-cad*, *mCherry* or c) *nub>P-cad*, *bs*-IR or d) *nub>P-cad*, *D-MRTF*-IR. e) to g) measurements of wing e) anterior-posterior length, f) total area and g) circularity. Plots are quantifications of 15 adult wings from female flies, horizontal bars represent mean value, error bars indicate standard deviation. Statistical significance was calculated using one-way ANOVA; * p<0.01, **** p<0.0001, ns indicates non-significant.

## 3- P-cadherin does not regulate the expression of bs/MRTF signalling pathway target genes

Altogether these observations support the hypothesis by which *P-cad* affects wing development through activation of the *bs/D-MRTF* signalling pathway. Therefore, next we went to look for possible target genes of *bs/D-MRTF* pathway to confirm the *P-cad* expression is able to upregulate these targets. We crossed information from literature on target genes of the pathway identified in wings discs expressing *D-MRTF* (Jonchère, V *et al*., 2017) with genes deregulated by microarray in the Src inducible mammary epithelial cell line MCF10A-ER-Src, which transiently upregulates P-cad (Iliopoulos, D *et al*., 2009). From the five common target genes, we selected *MESK2* (*NDRG1* orthologue in human) alongside with two *Drosophila* integrins *αPS2* and *αPS4* (Fig. 22) as P-cad upregulates *α*6 integrin in established cancer cell lines (Vieira, A *et al*., 2014).

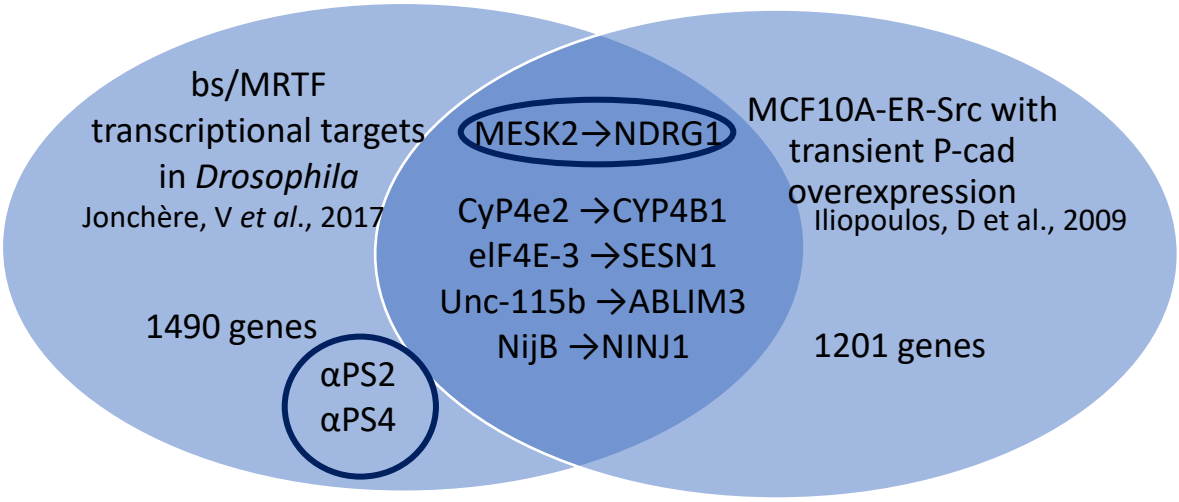


**Fig. 22- Data crossing for the selection of bs/MRTF pathway target genes in Drosophila to analyse its affection by P-cad.** Diagram shows overlap between target genes of the bs/MRTF pathway and genes deregulated in the Src inducible mammary epithelial cell line MCF10A-ER-Src with transient P-cad overexpression identified five common genes, only MESK2 was selected. In addition, two integrins, αPS2 and αPS4 were also selected.

To test if the expression of the selected genes was regulated by *P-cad* expression we quantified by qPCR the mRNA levels of *MESK2*, *αPS2* and *αPS4*

on wing disc extracts expressing *P-cad* and *mCherry* under *nub*-Gal4 control, compared to control wing disc extract expressing *GFP* under *nub*-Gal4. The analyses of mRNA expression levels of the three chosen target genes did not show significant differences in discs expressing *P-cad*, compared to control discs (Fig. 23 a, b and c). The results indicate that *P-cad* expression does not appear to affect *MESK2*, *αPS2* and *αPS4* expression.

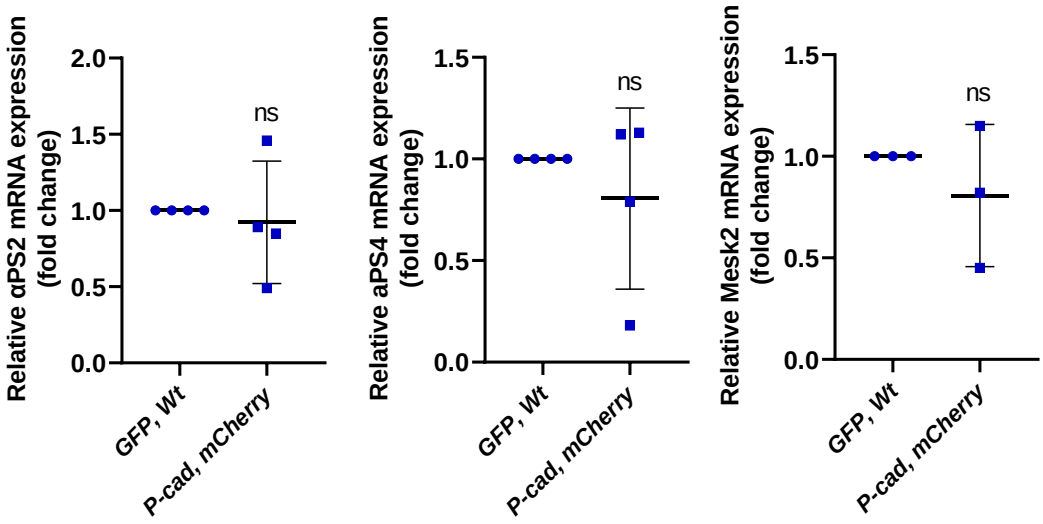


**Fig. 23- *P-cad* expression does not affect the mRNA expression levels of selected bs/MRTF pathway target genes**. a) *αPS2*, b) *αPS4* and c) *MESK2* mRNA levels in *nub>GFP* (control) or *nub> P-cad*, *mCherry* wing imaginal discs. Statistical significance was determined by Student's unpaired t test. ns indicates non-significant

Although *P-cad* did not affect *MESK2* and *αPS2* expression, knocking down either one of these *bs/D-MRTF* target genes is able to suppress the P-cad wing phenotype (F. Janody, unpublished data). We therefore tested if knocking down *αPS4* could also rescue the P-cad wing phenotype. As in previous experiments, a cross between the transgenic line *nub*-Gal4, UAS-*GFP* and a wild type fly strain was used as control for wild type adult wings. The *nub*-Gal4, UAS-*GFP* was also crossed with flies carrying a UAS-*αPS4*-IR transgene. The transgenic fly line expressing *nub*-Gal4, UAS-*P-cad* was crossed with the UAS-*mCherry* or UAS-*αPS4*-IR strains. Once again, adult wings resulting from these crosses were compared by measuring their anterior-posterior length, total area and circularity. It was verified that adult wings expressing GFP and knocked down for *αPS4* (Fig. 24 c) were bigger in their anterior-posterior length, total area and

circularity ($p<0.0001$) (Fig. 24 e, f and g), compared to adult wings expressing *P-cad* and *mCherry* under *nub*-Gal4 control (Fig. 24 b). However, wings expressing *P-cad* and knocked down for *αPS4* were smaller in anterior-posterior length ($p<0.01$) (Fig. 24 d and e) and total area ($p<0.0001$) (Fig. 24 d and f), compared to wings expressing *P-cad* and *mCherry* (Fig. 24 b, e and f). Moreover, wings expressing *P-cad* and knocked down for *αPS4* did not show any differences in circularity ($p=0,5964$) (Fig. 24 d and g) compared to wings expressing *P-cad* and *mCherry* (Fig. 24 b and g). Therefore, those results indicate that *αPS4* is not required for *P-cad* to affect wing development. In contrast, *αPS4* prevents P-cad functional effects in the Drosophila wing.

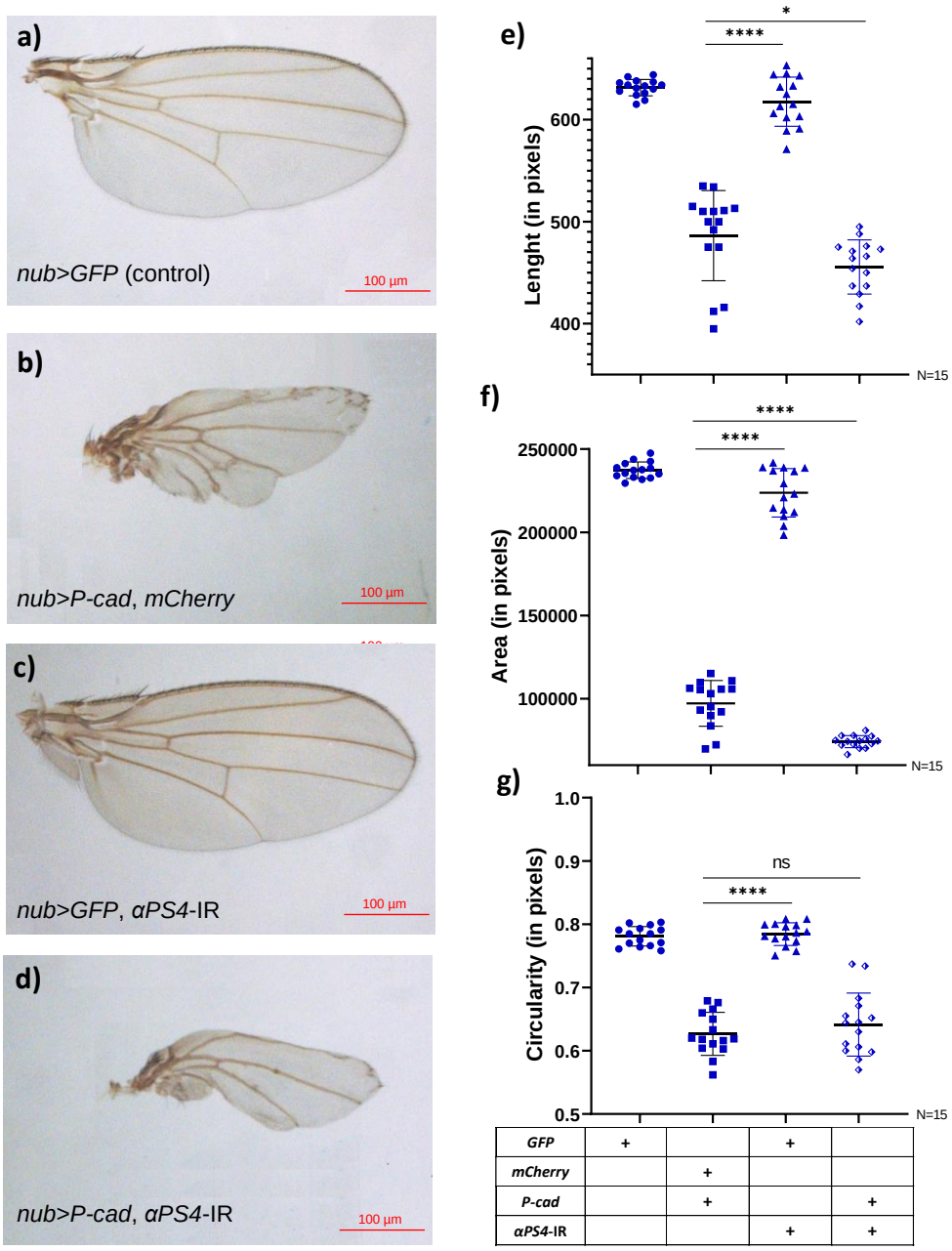


**Fig. 24- Knocking down *αPS4* does not rescue the adult wing phenotype induced by *P-cad* expression.** a) to d) Adult wings from a) *nub> GFP* (control) or b) *nub> P-cad*, *mCherry* or c) *nub> GFP*, *αPS4*-IR or d) nub> *P-cad*, *αPS4*-IR. e) to g) measurements of wing e) anterior-posterior length, f) total area and g) circularity. Plots are quantifications of 15 adult wings from female flies, horizontal bars represent mean value, error bars indicate standard deviation. Statistical significance was calculated using one-way ANOVA; * indicates statistical significance towards control * p<0.01, **** p<0.0001, ns indicates non-significant.

Overall, these observations suggest that *P-cad* affects wing development at least through activation of the *bs/D-MRTF* pathway. However, this does not

seem to involve the upregulation of the three bs/D-MRTF target genes *MESK2*, *αPS2* and *αPS4*.

## 4- The two actin nucleators Arpc2 and Spire affect P-cad stability

In great availability of actin monomers (G-actin) D-MRTF/MRTF-A are sequestrated in the cytoplasm, preventing its translocation to the nucleus and transcriptional activity through bs/SRF (Weissbach, J *et al*., 2016; Sokolova, M *et al*., 2016). The conversion of actin monomers to actin filaments (F-actin) is strongly favoured by the activity of actin nucleators (Pizarro-Cerdá *et al.*, 2017). Our preliminary data showed that knocking down the two actin nucleators *arpc2* or *spire* suppressed the P-cad wing phenotype (Fig. 11). Therefore, P-cad could enhance bs/D-MRTF activity by promoting F-actin assembly. However, we cannot exclude that Arpc2 or Spire controls P-cad levels or localization. To discard the possible regulation of *P-cad* levels by Arpc2 or Spire, we analysed by western blot P-cad levels in wing imaginal discs knocked down for arpc2 or spire. Serving as negative control, we used protein extracts from cross between the *nub*-Gal4, UAS-*GFP* transgenic line and a wild type fly strain. *P-cad* levels were determined by crossing the *nub*-Gal4, UAS-*P-cad* transgenic line with fly lines carrying either UAS-*mCherry* or UAS-*arpc2*-IR or UAS-*spire*-IR. Quantification of the two bands revealed by the anti-P-cad antibody (Fig. 25 a) showed that knocking down *arpc2* (**$p<0.05$) or spire (*** $p<0.001$) significantly reduced *P-cad* levels (Fig. 25 a, b and Supplementary figure 2).

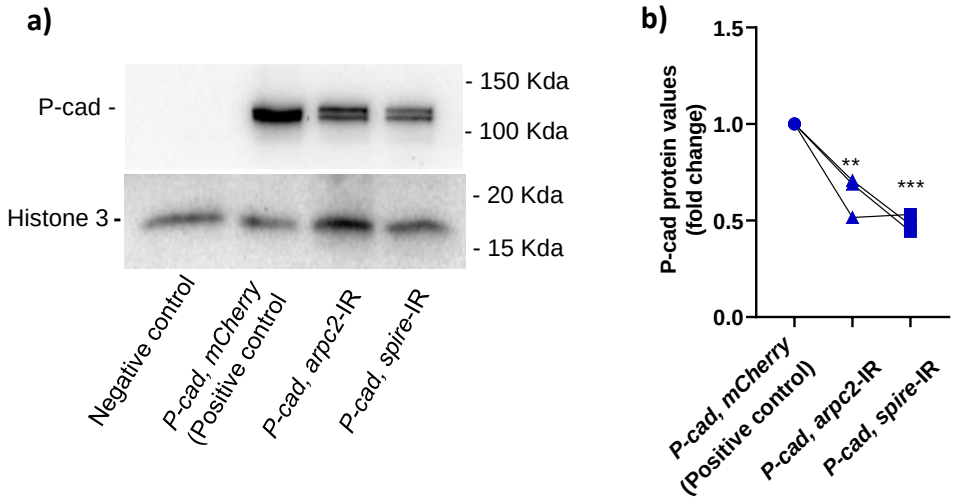


**Fig. 25- Knocking down *arpc2* or *spire* reduces *P-cad* expression levels**. Western blots on Drosophila wing disc extracts from *nub>GFP* (negative control) or *nub> P-cad*, *mCherry* (positive control) or *nub>P-cad*, *arpc2*-IR or *nub>P-cad*, *spire*-IR. a) Upper panel shows membrane blotted with an anti-P-cad antibody, which reveals two bands of P-cad at a molecular weight of ≈120 Kda. Lower membrane was blotted with an anti-Histone 3 (H3) antibody, which reveals a band at a molecular weight of ≈17 Kda. b) Quantifications are from three biological replicates. The levels of the two P-cad bands were first normalized to the loading control H3 and then to the intensity levels of P-cad in *nub>P-cad*, *mCherry* wing disc extracts to evaluate for fold change. Error bars indicate standard deviation. Statistical significance was calculated using one-way ANOVA. * indicates statistical significance towards control **p<0.05, *** p<0.001

By western blot, the P-cad band with high molecular weight could correspond to the unprocessed form of the protein, while the lower band is likely the processed form glycosylated, which localizes to the cellular membrane (J. Paredes, personal communication). A possible explanation for the reduction of P-cad protein levels induced by *arpc2* or *spire* knocked down is that P-cad fails to be targeted to the membrane. So, we performed additional western blot using gels at 7% in order to separate the two bands and to evaluate the effect of *arpc2* or *spire* knocked down on the stability of each band. The same crosses that those made in the previous section, were performed to prepare protein extracts. The results show in two of the replicates that reducing *arpc2* or *spire* reduces *P-cad* levels of both bands, compared to those expressing *P-cad* and *mCherry*, in accordance with the previous western blot (Fig. 26 a, b and Supplementary figure 3 compare to Fig. 25 a, b and Supplementary figure 2). However what appears to be an outside replicate shows an increase of *P-cad* levels in the upper band in the extracts expressing *P-cad* and knocked down for *arpc2* or *spire,* compared to those expressing *P-cad* and *mCherry* (Fig. 26 a, b and Supplementary figure 3). One of the replicates present higher values of *P-cad* expression levels in

extracts knocked down for *arpc2* or *spire* than in the other two replicates. This explains why the statistical significance is lost or reduced when *arpc2* or spire, respectively is knocked down (from *** p<0.001 to * p<0.01), and lost for the lower band compared with the results from the previous experiment (Fig. 26 b and Supplementary figure 3). The origin of this outlier replicate could be an error in extract preparation. Therefore, it would be necessary to perform another experiment to proper conclude. Because, even though the results appear to indicate that *arpc2* does not contribute for *P-cad* stabilization and *spire* contributes to the stabilization of *P-cad* upper band we can not overlook that in two replicates we verified that knocking down *arpc2* or spire reduced *P-cad* levels.

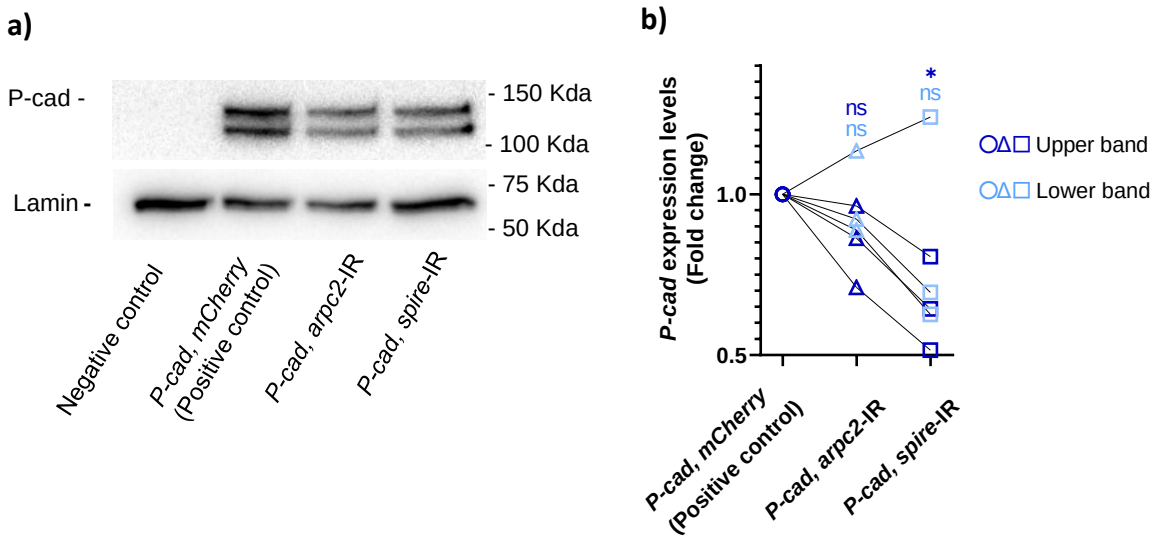


**Fig. 26- Knocking down *arpc2* or *spire* does not alter *P-cad* unprocessed or processed form expression levels.** Western blots on Drosophila wing disc extracts from *nub>GFP* (negative control) or *nub>P-cad*, *mCherry* (positive control) or *nub>P-cad, arpc2*-IR or *nub>P-cad*, *spire*-IR. a) Upper panel shows membrane blotted with an anti-P-cad antibody, which reveals two bands of P-cad at a molecular weight of ≈120 Kda. Lower membrane was blotted with an anti-Lamin antibody, which reveals a band at a molecular weight of ≈74 Kda. b) Quantifications are from three biological replicates. The levels of the two P-cad bands were first normalized to the loading control Lamin and then to the intensity levels of P-cad in *nub>P-cad*, *mCherry* wing disc extracts to evaluate for fold change. Error bars indicate standard deviation. Statistical significance was calculated using one-way ANOVA. * p<0.01, n.s. indicates non-significant

To verify that the wing disc extracts used to perform the western blots (Fig. 25 andFig. ***26***) were knocked down for arpc2 or spire, adult wings from each cross were mounted. We could confirm that knocking down arpc2 suppressed the small wing phenotype induced by P-cad (Fig. 27, compare c with b), as their

anterior-posterior length ($p<0.0001$) (Fig. 27 e) and total area ($p<0.0001$) (Fig. 27 f) were significantly increased, compared to adult wings expressing P-cad and mCherry under nub-Gal4 control. Moreover, wings expressing P-cad and knocked down for arpc2 showed no differences in circularity ($p= 0,9923$) (Fig. 27 c and g) compared to wings expressing P-cad and mCherry (Fig. 27 b and g). Similar results were observed for wings expressing P-cad and spire-IR, (Fig. 27 compare d with b), which showed a significant increase in anterior-posterior length, total area ($p<0.0001$) (Fig. 27 e, f) and circularity ($p<0.001$) (Fig. 27 g), compared to nub>P-cad, mCherry-expressing wings ($p<0.0001$) (Fig. 27 e, f). Overall, these results indicate that arpc2 and spire contribute to the regulation of *P-cad* activity by stabilizing its protein levels.

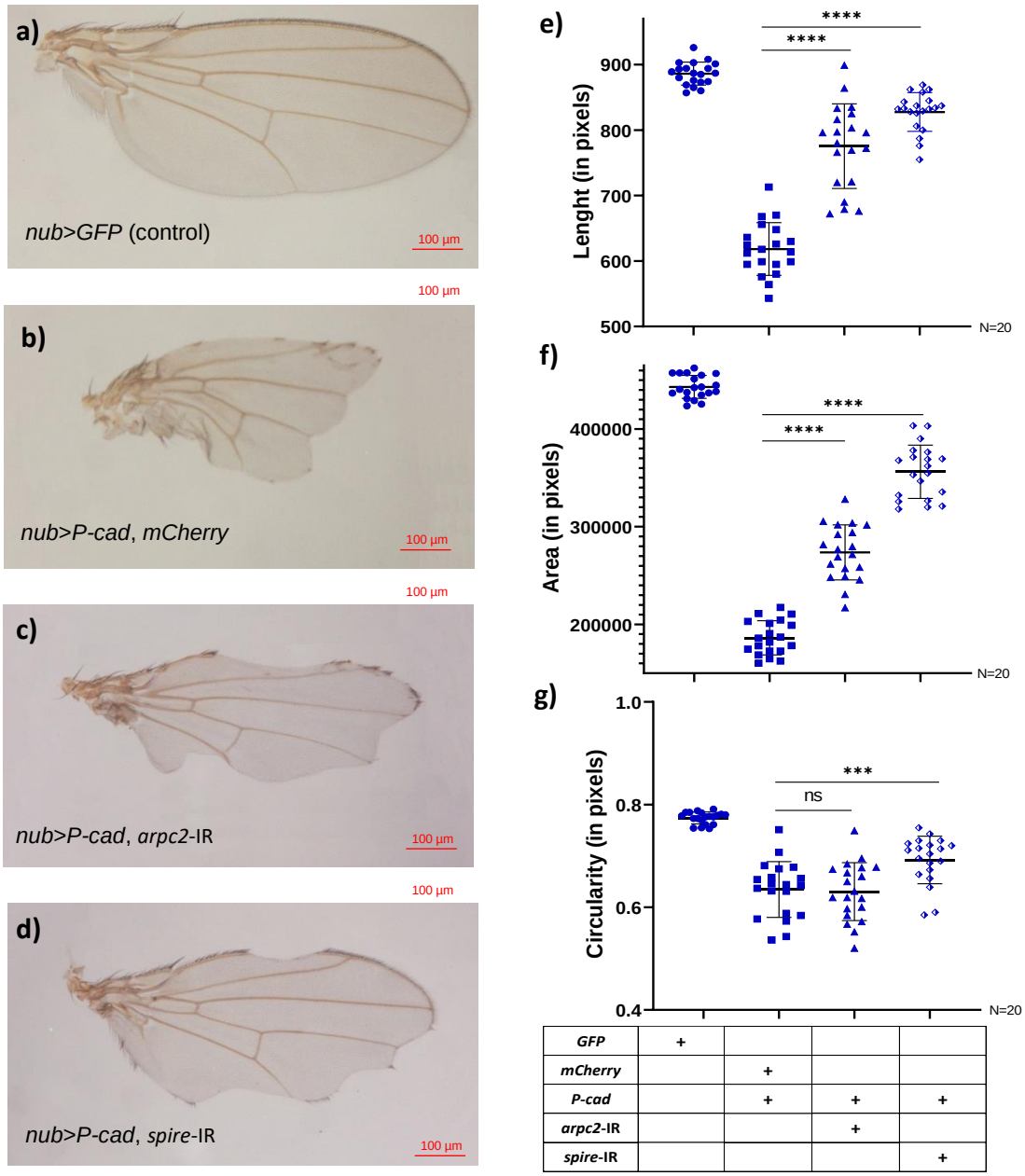


**Fig. 27- Knocking down *arpc2* or *spire* rescues the adult wing phenotype induced by *P-cad* expression.** a) to d) Adult wings from a) *nub>GFP* (control) or b) *nub>P-cad*, *mCherry* or c) *nub> P-cad*, *arpc2*-IR or d) *nub> P-cad*, *spire*-IR. e) to g) measurements of wing e) anterior-posterior length, f) total area and g) circularity. Plots are quantifications of 20 adult wings from female flies, horizontal bars represent mean value, error bars indicate standard deviation. Statistical significance was calculated using one-way ANOVA; * indicates statistical significance towards control *** p<0.001, **** p<0.0001, ns indicates non-significant.

## 5- Arpc2 and bs or D-MRTF act in the same pathway downstream of P-cad

Although *arpc2* and *spire* stabilizes *P-cad* (Fig. 25Fig. ***26*** andFig. ***27***), this does not exclude the possibility that they are also required downstream of *P-cad* to enhance the bs/D-MRTF signalling pathway. To test the possibility that *arpc2*, *bs* and *MRTF* act in the same pathway we tested if *bs* or *D-MRTF* synergizes with *arpc2* to affect wing development downstream of *P-cad* using genetic interactions between *P-cad*, *arpc2* and *bs* or *D-MRTF*. If knocking down *bs* or *D-MRTF* further suppresses the *nub>P-cad, arpc2-IR* phenotype, this would indicate that *bs* or *D-MRTF* regulation occurs downstream arpc2. In contrast, if knocking down *bs* or *DMRTF* does not affect the *nub>P-cad*, *arpc2*-IR phenotype, this would indicate that *bs* or *D-MRTF* regulation occurs upstream of arpc2. However, we cannot exclude the possibility that *arpc2* could be inducing a wing phenotype by other mechanism occurring in parallel but independent from the bs/D-MRTF signalling pathway. If knocking down *bs* or *D-MRTF MRTF* further suppresses the *nub>P-cad, arpc2-IR* phenotype, this would indicate that *arpc2* acts in parallel to the bs/D-MRTF signalling pathway. On the contrary, if knocking down *bs* or *D-MRTF MRTF* does not affect the *nub>P-cad, arpc2-IR* phenotype this would indicate that *arpc2* acts within the bs/D-MRTF signalling pathway.

Results confirmed that knocking down *arpc2* restored the anterior-posterior length and total area ($p<0.0001$) (Fig. 28 h and i), but did not restored circularity ($p<0.05$) (Fig. 28 j), of adult wings expressing *P-cad* and *mCherry* under *nub*-Gal4 control (Fig. 28 h, i and j), compared to wings expressing *P-cad*, *RFP* and *mCherry* under *nub*-Gal4 control (Fig. 28 b). This comes in contradiction to what it was previously observed, wings expressing *P-cad* and knocked down for *arpc2* showed no differences in circularity ($p= 0,9923$) (Fig. 28 c and g) compared to wings expressing *P-cad* and *mCherry* (Fig. 28 b and g). Yet adult wings expressing *P-cad* and *mCherry* under *nub*-Gal4 control were still significantly reduced in anterior-posterior length, total area and circularity, compared to normal wings expressing GFP (Fig. 28 a).

Adult wings expressing *P-cad, arpc2*-IR, and *bs*-IR under *nub*-Gal4 control (Fig. 28 e) were not longer ($p >0.05$) (Fig. 28 h) or significantly bigger ($p= 0,8231$)

(Fig. 28 i) than wings expressing *P-cad, mCherry* and *arpc2*-IR under *nub*-Gal4 control (Fig. 28 c). However, expressing *bs*-IR suppressed the circularity defect ($p<0.0001$) (Fig. 28 j) of *P-cad, mCherry* and *arpc2*-IR expressing wings (Fig. 28 compare c with e).

Adult wings expressing *P-cad, arpc2*-IR, and *MRTF*-IR under *nub*-Gal4 control (Fig. 28 g) were not significantly longer ($p> 0.9999$) (Fig. 28 h) or bigger ($p= 0.3670$) (Fig. 28 i) than wings expressing *P-cad, mCherry* and *arpc2*-IR under *nub*-Gal4 control (Fig. 28 c). However, adult wings expressing *MRTF*-IR suppressed the circularity defect ($p<0.05$) (Fig. 28 j) of *P-cad, mCherry* and *arpc2*-IR expressing wings (Fig. 28 , compare c with g).

Since the phenotype of adult wings knocked down for *bs* or *D-MRTF* do not present significant differences from adult wings expressing *P-cad, mCherry* and *arpc2*-IR, indicates that the possibility of the wing phenotype being the result of a cumulative effect induced by *arpc2*-IR acting in an independent way of the bs/D-MRTF signalling pathway is very unlikely.

Overall, these observations suggest that *bs* and *D-MRTF* are required downstream of *arpc2* in the same pathway regulated by *P-cad* to affect wing development.

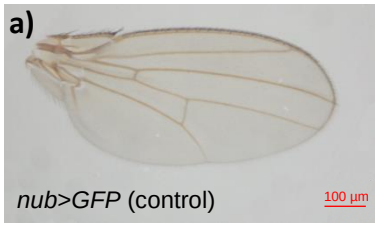





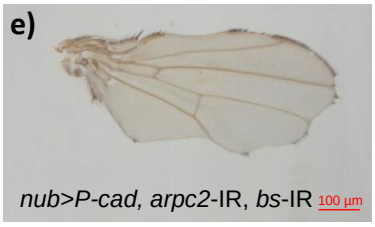


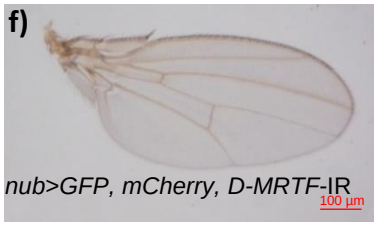



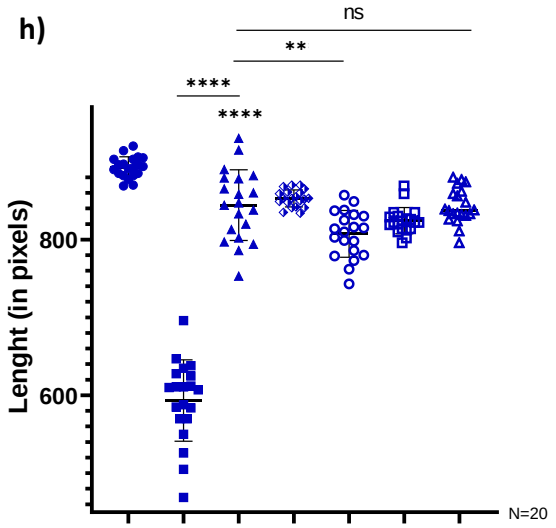


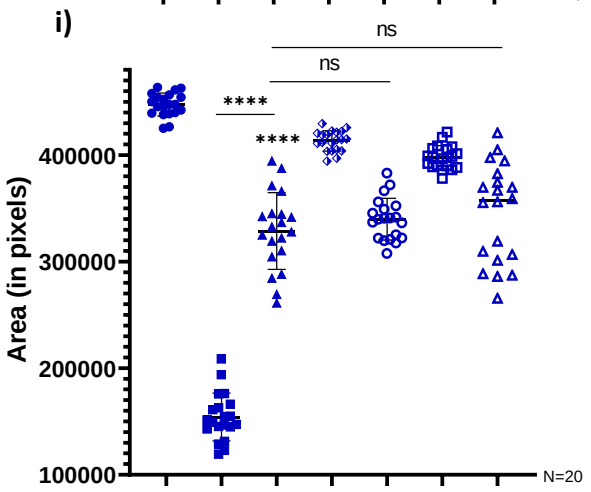


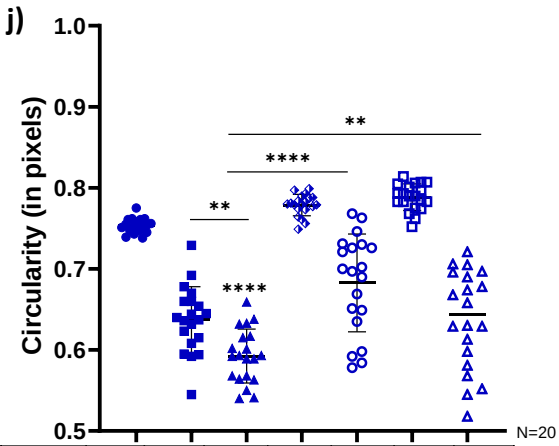


| | | | | | | | |
|---|---|---|---|---|---|---|---|
| *GFP* | + | | | + | | + | |
| *mCherry* | | + | + | + | | + | |
| *P-cad* | | + | + | | + | | + |
| *arpc2*-IR | | | + | | + | | + |
| *bs*-IR | | | | + | + | | |
| *MRTF*-IR | | | | | | + | + |

**Fig. 28- *P-cad* requires *bs* and *D-MRTF* downstream of *arpc2* to affect wing development** a) to g) Adult wings from a) *nub> GFP* (control) or b) *nub> P-cad, RFP, mCherry* or c) *nub>P-cad* , *mCherry*, *arpc2*-IR or d) *nub>GFP, mCherry*, *bs*-IR or e) *nub> P-cad, arpc2*-IR, *bs*-IR or f) *nub>GFP, mCherry*, *D-MRTF*-IR or g) *nub> P-cad arpc2*-IR *D-MRTF*-IR. h to j) Measurements of wings h) anterior-posterior length, i) total area and j) circularity. Plots are quantifications of 20 adult wings from female flies, horizontal bars represent mean value, error bars indicate standard deviation. Statistical significance w was calculated using one-way ANOVA; * indicates statistical significance towards control **p<0.05, **** p<0.0001, ns indicates non-significant.

# Discussion

In breast cancer, P-cad is overexpressed being established as an indicator of poor patient prognosis (Paredes, J *et. al*, 2005). It has also been associated with increased aggressive behaviour and *in vivo* tumorigenicity, as well as a promoter of cancer stem cell properties (Ribeiro, AS *et. al*, 2013; Vieira, A *et. al*, 2014). To uncover the signalling pathways mediated by P-cad that induce stem-like features, we used a transgenic *Drosophila melanogaster* model with conditional expression of human P-cad. We provide evidence that the consequences of expressing human P-cad in the wing disc primordium are reminiscent to those of overexpressing P-cad in breast cancer cells. In addition, based on our observations suggesting that P-cad affects wing differentiation by overactivating the bs/MRTF signalling pathway, we propose that the SRF/MRTF-A signalling pathway could be a critical regulator of stemness activity downstream of P-cad.

## 1- Drosophila melanogaster constitutes a suitable model to elucidate the role of P-cad in carcinogenesis

Our data indicates that knocking down *DE-cad* resulted in the suppression of the small wing phenotype induced by *P-cad* expression (Fig. 15 c). These results indicate that *P-cad* requires *DE-cad* to affect the wing development. Consistent with these observations, studies performed in triple-negative breast cancer cells shown that P-cad signals though E-cad to promote cell invasion and migration *in vitro* and tumour growth *in vivo* (Ribeiro, AS *et. al*, 2013). Conversely, our results also demonstrate that P-cad expression rescues the vestigial wing phenotype induced by *DE-cad* knocked down. Ribeiro *et. al*, observed in human breast cancer cells that in the absence of E-cad expression, P-cad promoted the relocation of beta-catenin to the cell membrane, rescuing the formation of adherens junctions and cell–cell adhesion (Ribeiro, AS *et. al*, 2013). Thus, like in breast cancer cell P-cad also restore cell–cell adhesion caused by the loss of *DE-cad* in Drosophila epithelium.

We found that knocking down *D-AKT1* had a severe impact in wing development, suggesting that D-AKT1 is required for normal wing development. Consistent with our observations, alterations of the insulin signalling at the AKT

level results in retardation of organ and organism size in *Drosophila (Gaou, X et. al*, *2001;* Hietakangas, V *et. al*, 2009*).* AKT has also a critical role in the regulation of cell proliferation, cell growth and apoptosis, metabolism, reproduction and longevity (Hietakangas, V *et. al*, 2009; Ruiz, P *et. al*, 2019; Puseenam, A *et. al*, 2009). Knocking down *D-AKT1* in wings expressing *P-cad* did not ameliorate the phenotype. Instead, it resulted in even more severe defects, illustrated by flies presenting only vestigial wing structures, suggesting that D-Akt1 controls wing disc differentiation in parallel to P-cad. The lower number of progeny, possibly explained by the severity of the phenotype, which could incapacitate the pupae from hatching, led us to delay the timing of *D-AKT1* knocked down and *P-cad* expression. Results show that adult wings expressing *P-cad* and knocked down to *D-AKT1* at 3$^{rd}$ instar larval stage presented a phenotype similar to wings expressing *P-cad* only, suggesting that P-cad rescues wing growth downstream of the loss of D-Akt1. This observation is inconsistent with those obtained when D-Akt1-IR was co-expressed with P-cad at 2$^{nd}$ instar larval stage (Fig. 17 d). Therefore, the possibility that the fly genotype was wrong must be considered. In TNBC cells, P-cad has been shown to promote AKT phosphorylation (Vieira, A *et. al*, 2014). Our results in fly epithelia suggest that in TNBC, AKT phosphorylation by P-cad might not promote the acquisition of CSC properties. Yet, we cannot exclude that AKT has distinct effects downstream of P-cad in the wing disc epithelium and in TNBC cells.

P-cad has also been shown to promote stemness activity through the integrins $\alpha 6\beta 4$ and Src (Vieira, A. *et al*., 2014). Accordingly, knocking down the Drosophila integrin $\alpha$PS2 or Src (Src64B) also suppresses the P-cad adult wing phenotype (S. Silva and F. Janody, data not shown). Overall, these findings indicate that the mechanisms by which P-cad affects the wing disc development are reminiscent to P-cad-functional effect in promoting breast CSC features. Therefore, Drosophila melanogaster can be considered a suitable model to study the role of P-cad in carcinogenesis.

## 2- P-cad could promote steam-like features through the SRF/MRTF signalling pathway

Diverse observations are consistent with a model by which P-cad induces stem cell activity by controlling the MRTF-SRF pathway (Fig. 29). First, knocking down *bs* or *D-MRTF* supressed the phenotype of adult wings expressing *P-cad* (Fig. 21 c and d). As bs and D-MRTF do not seem to regulate P-cad stability (Fig. 20) or localization (F. Janody, data not shown), bs-D-MRTF may act downstream of P-cad to affect wing development. Second, P-cad expression was positively associated with the expression of SRF/MRTF target genes (Chen-Ying, L *et. al.*, 2016). Third, overexpression of MRTF-A in breast epithelium promotes Epithelium-to-Mesenchymal transition (EMT) (Seifert, A *et. al.*, 2017), a key process associated with the acquisition of breast CSC properties, as breast CSCs and mammary epithelial that have undergone EMT express similar markers (Chaffer, C *et. al.*, 2013; Mani, S *et. al.*, 2008). Fourth, TAZ, a known inducer of breast CSC, metastatic ability, chemoresistance and tumorigenic potential, is a target gene of MRTF/SRF in breast cancer (Bartucci, M *et. al.*, 2013; Liu, C *et. al.*, 2015).

However, P-cad was not able to affect the expression of predicted bs/D-MRTF target genes *MESK2*, *αPS2* and *αPS4* expression (Fig. 23). Yet, *MESK2* and *αPS2*, but not *αPS4,* are required to mediate the P-cad adult wing phenotype (Fig. 24 and F. Janody, personal communication). Still, in P-cad-expressing cells, SRF-MRTF may control the expression of specific sets of target genes in cooperation with other transcription factors to affect wing differentiation or promote breast CSC features. Accordingly, SRF-MRTF-A has been shown to synergize with YAP-TEAD. Each pathway indirectly potentiates the activity of the other since their genomic targets are mutually dependent, even if the gene expression is only directly regulated by one pathway. (Foster, C *et. al.*, 2017).

## 3- P-cad may enhance SRF/MRTF signalling by controlling F-actin dynamics

Our observations are also consistent with a model by which the overactivation of MRTF-SRF by P-cad occurs though actin regulation (Fig. 29). Consistent with this hypothesis, we found that knocking down the actin nucleators *arpc2* or *spire* suppressed the P-cad wing phenotype (Fig. 27). Moreover, knocking down *bs* or *D-MRTF* did not further suppress the phenotype of adult wings co-expressing *P-cad* and *arpc2-IR*, indicating that *arpc2* and *bs* or *D-MRTF* acts in the same pathway downstream of *P-cad* (Fig. 28).

Furthermore, inducing the actin expression rescues the defects induced by MRTF deficiency in both Drosophila and human breast cancer cells. (Esnault, C *et al.*, 2014; Pizarro-Cerdá, J *et al.*, 2017). Additionally, P-cad promotes F-actin assembly in breast cancer cells. The regulatory role of P-cad in cell invasion and migration requires the re-organization of the actin cytoskeleton to form cell membrane protrusions, structures characteristic of moving cells (Ribeiro, AS *et. al*, 2010).

Finally, stem cell differentiation requires actin reorganization. Cytoskeleton rearranges in an induced response to specific physical cues such as chemokines, growth factors or alterations in the stiffness of a substrate, to deliberately determine the fate of stem cells. (Ambriz, X *et. al*, 2018; Boraas, L *et. al*, 2018; Charpentier, M *et. al*, 2014).

The MRTF-SRF transcription axis regulates major cytoskeletal genes, including actin itself, however, in this case a feedback loop that would ensure that the actin levels continue to support the actin dynamics is unlikely to occur.

P-cad is unlikely to control the actin-SRF/MRTF signalling pathway through E-cad, as knocking down *E-cad* in *P-cad* expressing wings restored the anterior-posterior boundary (Fig. 15), while reducing *bs* or *D-MRTF* levels improved significantly wing length (Fig. ***21***). However, P-cad could control the actin-SRF/MRTF signalling pathway through integrins, as knocking down *αPS2* in *P-cad* expressing wings also restored wing length (F. Janody, data not shown). Consistent with this hypothesis, in breast cancer cell lines, integrins, such as αV- and β1 have been shown to activate MRTF–SRF (Hermann, M *et. al*, 2016). In

addition, in fibroblast cell lines, integrins trigger the nuclear translocation of MRTF-A through the LINC complex (linker of nucleoskeleton and cytoskeleton) or through formins (Plessner, M, 2015).

In addition to promote bs/D-MRTF signalling activity downstream of P-cad, arpc2 and spire appear to stabilize a form of P-cad at high molecular weight (Fig. 25 andFig. ***26***). The actin cytoskeleton network controls by arpc2 and Spire could stabilize P-cad, as it was demonstrated for the cadherin/catenin cluster in another model (Indra, I *et al.*, 2020).

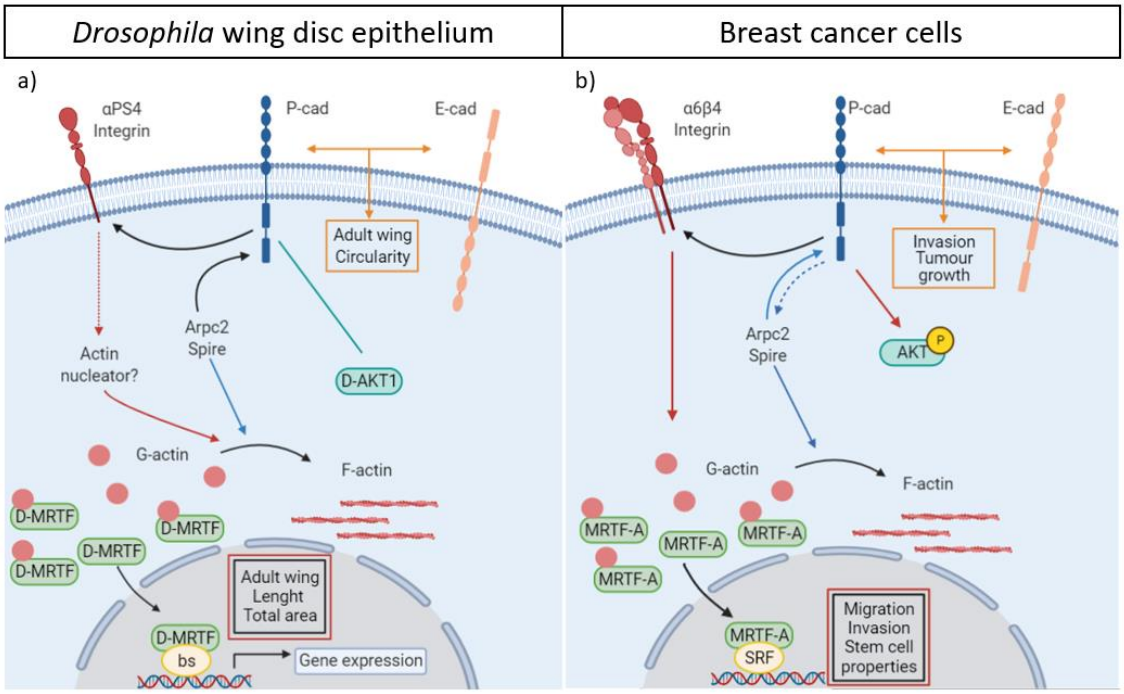


**Fig. 29- Models of P-cad overactivation of bs/MRTF pathway through promoting the conversion of actin monomers (G-actin) to actin filaments (F-actin) to a) affect the differentiation of the *Drosophila melanogaster* wing and b) promote tumorigenesis in breast cancer. a)** In *Drosophila* wing disc epithelium the actin nucleators arpc2 and spire are involved in *P-cad* stabilization. The action allows MRTF to be translocated to the nucleus binding to bs to induce gene transcription. Integrin αPS4 counteract *P-cad* effect in phenotype. *P-cad* signals trough *DE-cad* to affect wing shape, independent of the activation of bs/MRTF signalling pathway. D-Akt1 might not be involved to affect wing development downstream of P-cad. **b)** In breast cancer cells, *P-cad* promotes the conversion of G-actin to form F-actin filaments, through the action of actin binding nucleators, arpc2 and spire. The action allows MRTF to be translocated to the nucleus binding to bs or SRF to induce gene transcription. *P-cad* signals though integrin α6β4 to induce tumorigenesis. Integrin α6β4 promotes MRTF-A translocation to the nucleus. Integrin α6β4 crosstalk with *P-cad* induces AKT phosphorylation.

# Concluding remarks and future perspectives

The particular relevance of this work relies in the generated knowledge of understanding the link between P-cadherin and aggressive breast cancer. The aim was to establish a valid model in which P-cadherin functional effects in Drosophila could be reminiscent of the role of P-cadherin in mammals.

It was possible to uncover some aspects of how P-cadherin acts to affect Drosophila wing phenotype, identifying a signalling pathway and components that cooperate and cross-talk to induce a more aggressive phenotype. As well as the relevance of the contribution of each component for the mechanism. Those observations could be extrapolated and fitted into the mechanisms of how P-cadherin promotes cancer tumorigenesis.

These discoveries open the door to possible new target options for treatment of aggressive tumours.

# Annexes

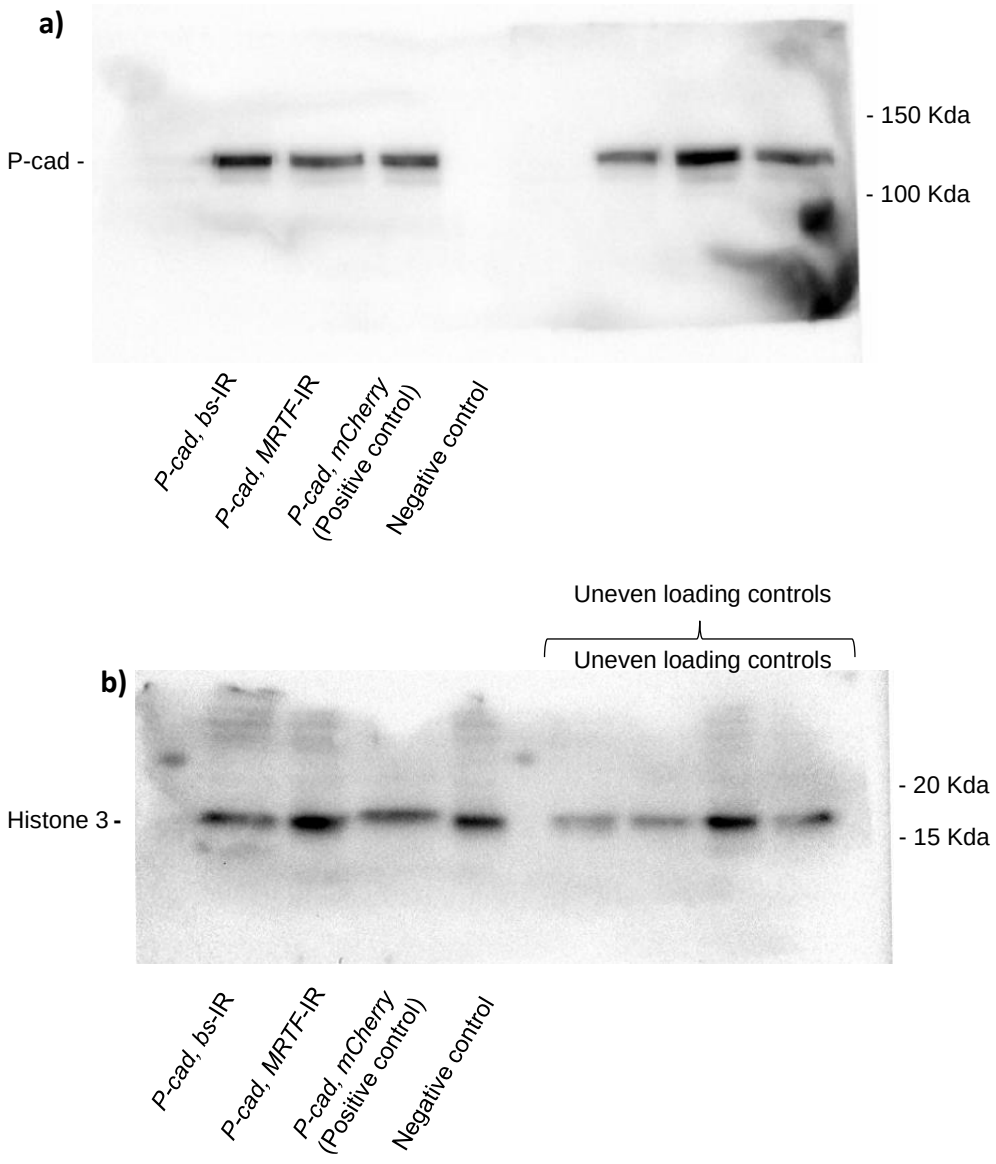
a)
P-cad -
- 150 Kda
- 100 Kda
P-cad, bs-IR
P-cad, MRTF-IR
P-cad, mCherry (Positive control)
Negative control
Uneven loading controls
Uneven loading controls
b)
Histone 3 -
- 20 Kda
- 15 Kda
P-cad, bs-IR
P-cad, MRTF-IR
P-cad, mCherry (Positive control)
Negative control

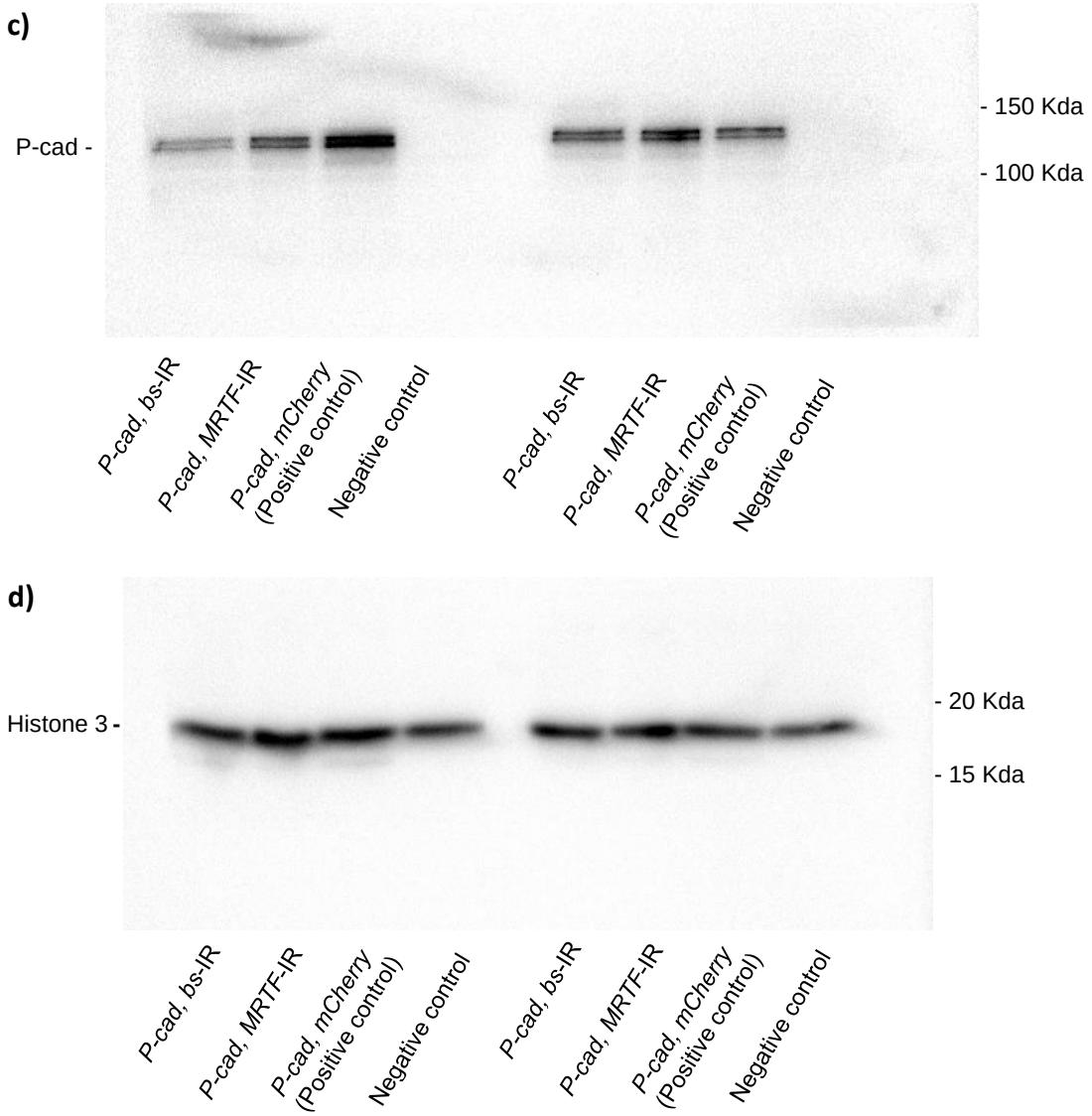


**Supplementary figure 1- Whole western blot membranes imaging in a) and c) P-cad, in b) and d) Histone 3 used for cropped data presented in Fig. 6 a) and quantification in Fig. 6 b)**

**a)**

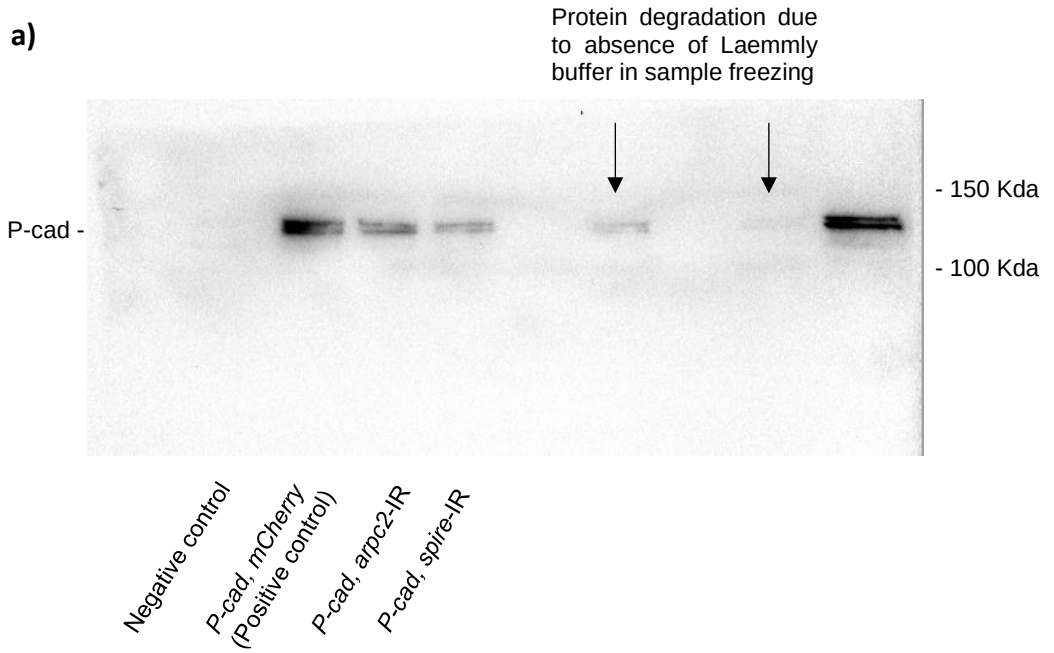
Protein degradation due to absence of Laemmly buffer in sample freezing
P-cad -
- 150 Kda
- 100 Kda
Negative control
P-cad, mCherry (Positive control)
P-cad, arpc2-IR
P-cad, spire-IR

**b)**

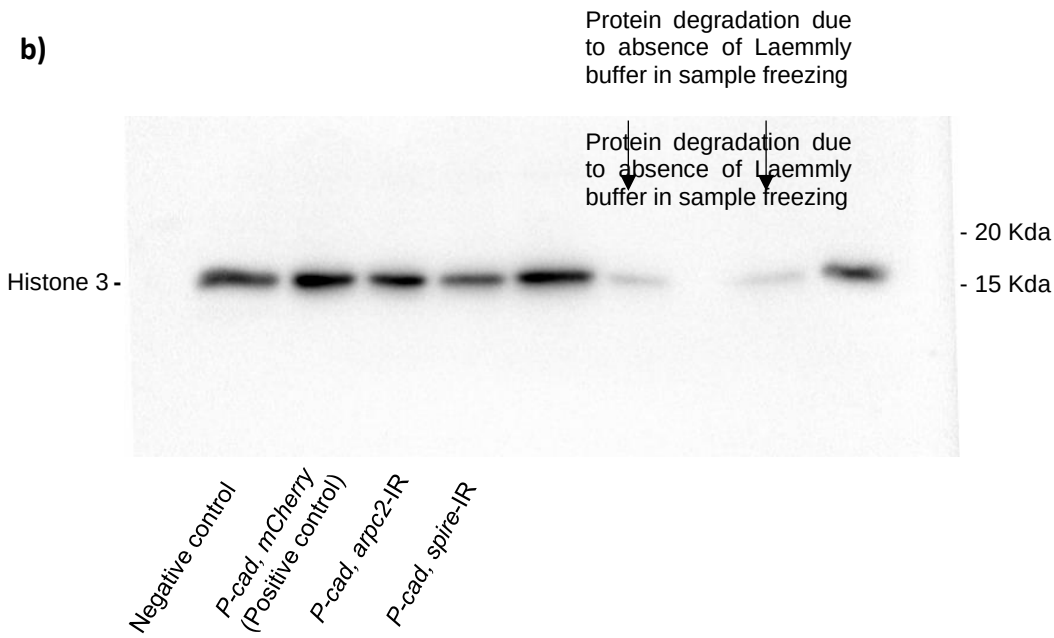
Protein degradation due to absence of Laemmly buffer in sample freezing
Protein degradation due to absence of Laemmly buffer in sample freezing
Histone 3 -
- 20 Kda
- 15 Kda
Negative control
P-cad, mCherry (Positive control)
P-cad, arpc2-IR
P-cad, spire-IR

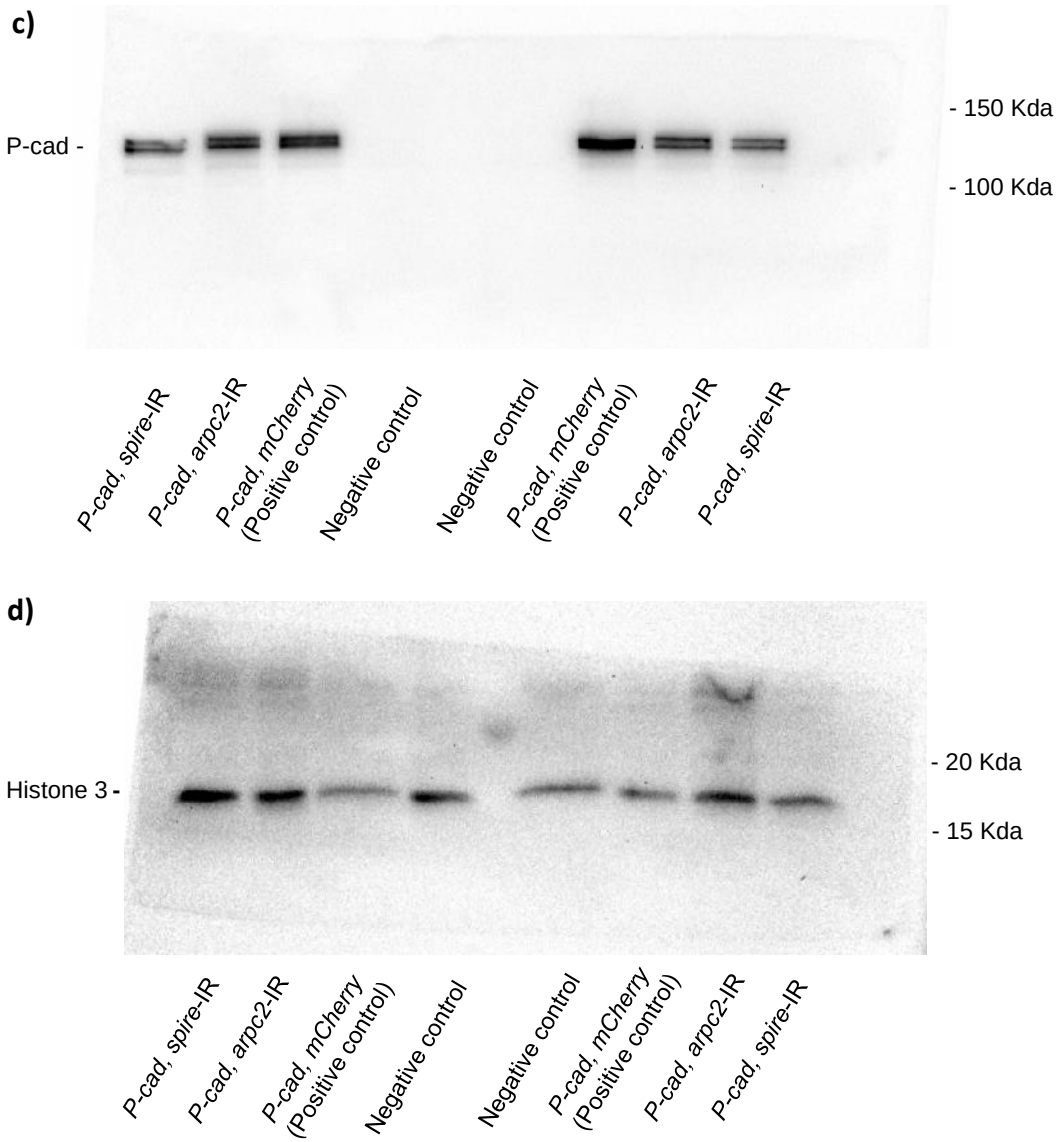


**Supplementary figure 2- Whole western blot membranes imaging in a) and c) P-cad, in b) and d) Histone 3 used for cropped data presented in Fig. 10 a) and quantification in Fig. 10 b)**

**a)**

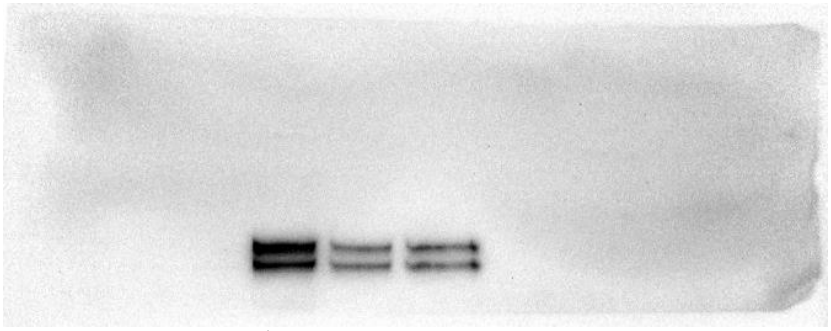


Negative control

*P-cad, mCherry* (Positive control)

*P-cad, arpc2-IR*

*P-cad, spire-IR*

**b)**

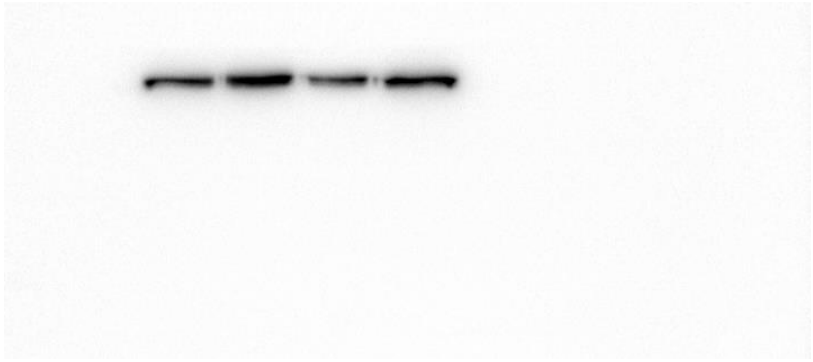


Negative control

*P-cad, mCherry* (Positive control)

*P-cad, arpc2-IR*

*P-cad, spire-IR*

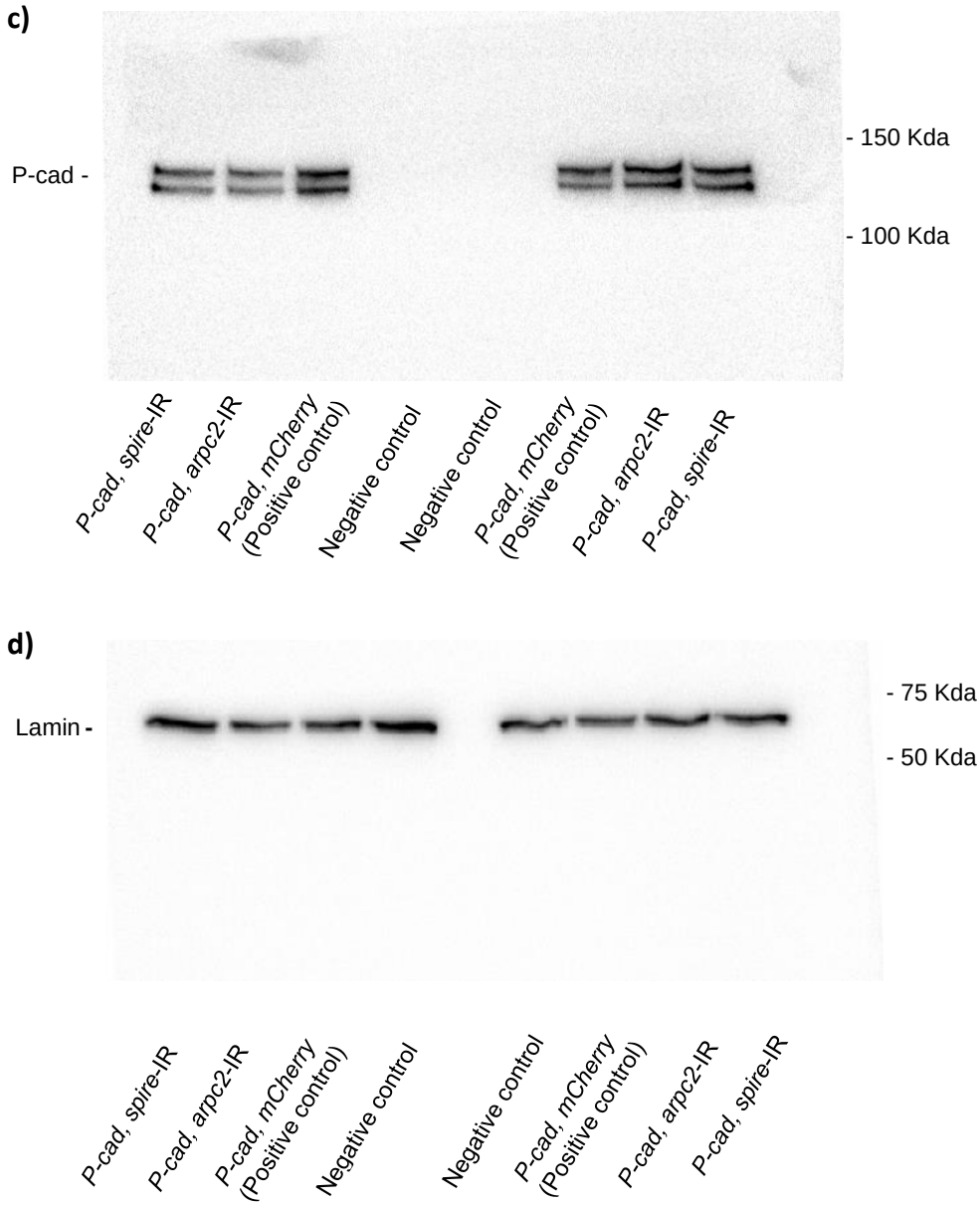


**Supplementary figure 3- Whole western blot membranes imaging in a) and c) P-cad, in b) and d) Lamin used for cropped data presented in Fig. 11 a) and quantification in Fig. 11 b)**

# References


- Abduljauwad, S. N., & Ahmed, H. ur R. (2019). Enhancing cancer cell adhesion with clay nanoparticles for countering metastasis. *Scientific Reports*, *9*(1), 1–12. https://doi.org/10.1038/s41598-019-42498-y
- Albergaria, A., Ribeiro, A. S., Vieira, A. F., Sousa, B., Nobre, A. R., Seruca, R., Schmitt, F., & Paredes, J. (2011). P-cadherin role in normal breast development and cancer. *International Journal of Developmental Biology*, *55*(7–9), 811–822. https://doi.org/10.1387/ijdb.113382aa
- Alsaleem, M., Toss, M. S., Joseph, C., Aleskandarany, M., Kurozumi, S., Alshankyty, I., Ogden, A., Rida, P. C. G., Ellis, I. O., Aneja, R., Green, A. R., Mongan, N. P., & Rakha, E. A. (2019). The molecular mechanisms underlying reduced E-cadherin expression in invasive ductal carcinoma of the breast: high throughput analysis of large cohorts. *Modern Pathology*, *32*(7), 967–976. https://doi.org/10.1038/s41379-019-0209-9
- Basel-Vanagaite, L., Pasmanik-Chor, M., Lurie, R., Yeheskel, A., & Kjaer, K. W. (2011). CDH3-related syndromes: Report on a new mutation and overview of the genotype-phenotype correlations. *Molecular Syndromology*, *1*(5), 223–230. https://doi.org/10.1159/000327156
- Bauer, R., Valletta, D., Bauer, K., Thasler, W. E., Hartmann, A., Müller, M., Reichert, T. E., & Hellerbrand, C. (2014). Downregulation of P-cadherin expression in hepatocellular carcinoma induces tumorigenicity. *International Journal of Clinical and Experimental Pathology*, *7*(9), 6125–6132. https://doi.org/10.1055/s-0032-1332048
- Bazellières, E., Conte, V., Elosegui-Artola, A., Serra-Picamal, X., Bintanel-Morcillo, M., Roca-Cusachs, P., Muñoz, J. J., Sales-Pardo, M., Guimerà, R., & Trepat, X. (2015). Control of cell-cell forces and collective cell dynamics by the intercellular adhesome. *Nature Cell Biology*, *17*(4), 409–420. https://doi.org/10.1038/ncb3135
- Borsig, L. (2019). *Europe PMC Funders Group Selectins in cancer immunity*. *28*(9), 648–655. https://doi.org/10.1093/glycob/cwx105.Selectins
- Bray, F., Ferlay, J., Soerjomataram, I., Siegel, R. L., Torre, L. A., & Jemal, A. (2018). Global Cancer Statistics 2018: GLOBOCAN Estimates of

Incidence and Mortality Worldwide for 36 Cancers in 185 Countries. *CA Cancer J Clinic*, *68*, 394–424. https://doi.org/10.3322/caac.21492

- Bussemarkers, M; Bokhoven, A; Völler, M. (1994). Bussemakers, M 1994.pdf. *Biochemical and Biophisical Research Communications*, *203*(2), 1291–1294.
- Calzado-Martín, A., Encinar, M., Tamayo, J., Calleja, M., & San Paulo, A. (2016). Effect of Actin Organization on the Stiffness of Living Breast Cancer Cells Revealed by Peak-Force Modulation Atomic Force Microscopy. *ACS Nano*, *10*(3), 3365–3374. https://doi.org/10.1021/acsnano.5b07162
- Caygill, E. E., & Brand, A. H. (2016). *Drosophila: Methods and Protocols, Methods in Molecular Biology*. *1478*(October 2017), 4–6. https://doi.org/10.1007/978-1-4939-6371-3
- Chanson, L., Brownfiel, D., Garbe, J. C., Kuhn, I., Stampfer, M. R., Bissell, M. J., & LaBarge, M. A. (2011). Self-organization is a dynamic and lineage-intrinsic property of mammary epithelial cells. *Proceedings of the National Academy of Sciences of the United States of America*, *108*(8), 3264–3269. https://doi.org/10.1073/pnas.1019556108
- Chen, M., Marrs, B., Qi, L., Knifley, T., Jarrett, S. G., Weiss, H. L., Stewart, R. L., D'Orazio, J. A., & O'Connor, K. L. (2019). *Integrin α6β4 signaling switches DNA repair from homologous recombination to non-homologous end-joining pathway to sensitize breast cancer cells to cisplatin*. https://doi.org/https://doi.org/10.1101/785873
- Cheng, Z., Wei, W., Wu, Z., Wang, J., Ding, X., Sheng, Y., Han, Y., & Wu, Q. (2019). ARPC2 promotes breast cancer proliferation and metastasis. *Oncology Reports*, *41*(6), 3189–3200. https://doi.org/10.3892/or.2019.7113
- Choi, J., Lee, Y. J., Yoon, Y. J., Kim, C. H., Park, S. J., Kim, S. Y., Doo Kim, N., Cho Han, D., & Kwon, B. M. (2019). Pimozide suppresses cancer cell migration and tumor metastasis through binding to ARPC2, a subunit of the Arp2/3 complex. *Cancer Science*, *110*(12), 3788–3801. https://doi.org/10.1111/cas.14205
- Da Cruz Paula, A., & Lopes, C. (2017). Implications of different cancer stem cell phenotypes in breast cancer. *Anticancer Research*, *37*(5), 2173–2183. https://doi.org/10.21873/anticanres.11552

- Donaldson, A. R., McCarthy, C., Goraya, S., Pederson, H. J., Sturgis, C. D., Grobmyer, S. R., & C. Calhoun, B. (2017). Breast Cancer Risk Associated With Atypical Hyperplasia and Lobular Carcinoma In Situ Initially Diagnosed on Core-Needle Biopsy. *Wiley Online Library*, *118*, 42–53. https://doi.org/10.1002/cncr.31061
- Dumont, N., Wilson, M. B., Crawford, Y. G., Reynolds, P. A., Sigaroudinia, M., & Tlsty, T. D. (2008). Sustained induction of epithelial to mesenchymal transition activates DNA methylation of genes silenced in basal-like breast cancers. *Proceedings of the National Academy of Sciences of the United States of America*, *105*(39), 14867–14872. https://doi.org/10.1073/pnas.0807146105
- Elliott DA, B. A. (2008). The GAL4 system : a versatile system for the expression of genes. In *Methods in Molecular Biology* (pp. 79–95). Humana Press. https://doi.org/oi: 10.1007/978-1-59745-583-1_5
- Epifano, C., Megias, D., & Perez-Moreno, M. (2014). P120-catenin differentially regulates cell migration by Rho-dependent intracellular and secreted signals. *EMBO Reports*, *15*(5), 592–600. https://doi.org/10.1002/embr.201337868
- Esnault, C., Stewart, A., Gualdrini, F., East, P., Horswell, S., Matthews, N., & Treisman, R. (2014). Rho-actin signaling to the MRTF coactivators dominates the immediate transcriptional response to serum in fibroblasts. *Genes and Development*, *28*(9), 943–958. https://doi.org/10.1101/gad.239327.114
- Farahani, E., Patra, H. K., Jangamreddy, J. R., Rashedi, I., Kawalec, M., Rao Pariti, R. K., Batakis, P., & Wiechec, E. (2014). Cell adhesion molecules and their relation to (cancer) cell stemness. *Carcinogenesis*, *35*(4), 747–759. https://doi.org/10.1093/carcin/bgu045
- Feng, Y., Spezia, M., Huang, S., Yuan, C., Zeng, Z., Zhang, L., Ji, X., Liu, W., Huang, B., Luo, W., Liu, B., Lei, Y., Du, S., Vuppalapati, A., Luu, H. H., Haydon, R. C., He, T. C., & Ren, G. (2018). Breast cancer development and progression: Risk factors, cancer stem cells, signaling pathways, genomics, and molecular pathogenesis. *Genes and Diseases*, *5*(2), 77–106. https://doi.org/10.1016/j.gendis.2018.05.001

- Firat-Karalar, E. N., & Welch, M. D. (2011). New mechanisms and functions of actin nucleation. *Current Opinion in Cell Biology*, *23*(1), 4–13. https://doi.org/10.1016/j.ceb.2010.10.007
- Foster, C. T., Gualdrini, F., & Treisman, R. (2017). Mutual dependence of the MRTF-SRF and YAP-TEAD pathways in cancer-associated fibroblasts is indirect and mediated by cytoskeletal dynamics. *Genes and Development*, *31*(23–24), 2361–2375. https://doi.org/10.1101/gad.304501.117
- Gau, D., & Roy, P. (2018). SRF'ing and SAP'ing - The role of MRTF proteins in cell migration. *Journal of Cell Science*, *131*(19), 1–11. https://doi.org/10.1242/jcs.218222
- Green, K. J., Getsios, S., Troyanovsky, S., & Godsel, L. M. (2010). Intercellular junction assembly, dynamics, and homeostasis. *Cold Spring Harbor Perspectives in Biology*, *2*(2), 1–22. https://doi.org/10.1101/cshperspect.a000125
- Hanahan, D., & Weinberg, R. A. (2011). Hallmarks of cancer: The next generation. *Cell*, *144*(5), 646–674. https://doi.org/10.1016/j.cell.2011.02.013
- Hermann, M. R., Jakobson, M., Colo, G. P., Rognoni, E., Jakobson, M., Kupatt, C., Posern, G., & Fässler, R. (2016). Integrins synergise to induce expression of the MRTF-A-SRF target gene ISG15 for promoting cancer cell invasion. *Journal of Cell Science*, *129*(7), 1391–1403. https://doi.org/10.1242/jcs.177592
- Hinck, L., & Näthke, I. (2014). Changes in cell and tissue organization in cancer of the breast and colon. *Current Opinion in Cell Biology*, *26*, 87–95. https://doi.org/10.1016/j.ceb.2013.11.003.Changes
- Hollestelle, A., Peeters, J. K., Smid, M., Timmermans, M., Verhoog, L. C., Westenend, P. J., Heine, A. A. J., Chan, A., Sieuwerts, A. M., Wiemer, E. A. C., Klijn, J. G. M., Van Der Spek, P. J., Foekens, J. A., Schutte, M., Den Bakker, M. A., & Martens, J. W. M. (2013). Loss of E-cadherin is not a necessity for epithelial to mesenchymal transition in human breast cancer. *Breast Cancer Research and Treatment*, *138*(1), 47–57. https://doi.org/10.1007/s10549-013-2415-3
- Horne, H. N., Oh, H., Sherman, M. E., Palakal, M., Hewitt, S. M., Schmidt,

M. K., Milne, R. L., Hardisson, D., Benitez, J., Blomqvist, C., Bolla, M. K., Brenner, H., Chang-Claude, J., Cora, R., Couch, F. J., Cuk, K., Devilee, P., Easton, D. F., Eccles, D. M., … Figueroa, J. D. (2018). E-cadherin breast tumor expression, risk factors and survival: Pooled analysis of 5,933 cases from 12 studies in the Breast Cancer Association Consortium. *Scientific Reports*, *8*(1), 1–11. https://doi.org/10.1038/s41598-018-23733-4

- Hu, J., Zhou, Y., Obayemi, J. D., Du, J., & Soboyejo, W. O. (2018). An investigation of the viscoelastic properties and the actin cytoskeletal structure of triple negative breast cancer cells. *Journal of the Mechanical Behavior of Biomedical Materials*, *86*, 1–13. https://doi.org/10.1016/j.jmbbm.2018.05.038
- Humphries, J. D., Byron, A., & Humphries, M. J. (2006). Integrin ligands at a glance. *Journal of Cell Science*, *119*(19), 3901–3903. https://doi.org/10.1242/jcs.03098
- Iliopoulos, D., Hirsch, H. A., & Struhl, K. (2009). An Epigenetic Switch Involving NF-κB, Lin28, Let-7 MicroRNA, and IL6 Links Inflammation to Cell Transformation. *Cell*, *139*(4), 693–706. https://doi.org/10.1016/j.cell.2009.10.014
- Imai, K., Hirata, S., Irie, A., Senju, S., Ikuta, Y., Yokomine, K., Harao, M., Inoue, M., Tsunoda, T., Nakatsuru, S., Nakagawa, H., Nakamura, Y., Baba, H., & Nishimura, Y. (2008). Identification of a novel tumor-associated antigen, cadherin 3/P-cadherin, as a possible target for immunotherapy of pancreatic, gastric, and colorectal cancers. *Clinical Cancer Research*, *14*(20), 6487–6495. https://doi.org/10.1158/1078-0432.CCR-08-1086
- Imai, S., Kobayashi, M., Takasaki, C., Ishibashi, H., & Okubo, K. (2018). High expression of P-cadherin is significantly associated with poor prognosis in patients with non-small-cell lung cancer. *Lung Cancer*, *118*(January), 13–19. https://doi.org/10.1016/j.lungcan.2018.01.018
- Jacobs, K., Feys, L., Vanhoecke, B., Van Marck, V., & Bracke, M. (2011). P-cadherin expression reduces melanoma growth, invasion, and responsiveness to growth factors in nude mice. *European Journal of Cancer Prevention*, *20*(3), 207–216. https://doi.org/10.1097/CEJ.0b013e3283429e8b

- Janiszewska, M., Primi, M. C., & Izard, T. (2020). Cell adhesion in cancer: Beyond the migration of single cells. *Journal of Biological Chemistry*, *295*(8), 2495–2505. https://doi.org/10.1074/jbc.REV119.007759
- Jonchère, V., Alqadri, N., Herbert, J., Dodgson, L., Mason, D., Messina, G., Falciani, F., & Bennett, D. (2017). Transcriptional responses to hyperplastic MRL signalling in Drosophila. *Open Biology*, *7*(2). https://doi.org/10.1098/rsob.160306
- Juliano, R. L. (2002). SIGNAL TRANSDUCTION BY CELL ADHESION RECEPTORS AND THE CYTOSKELETON: Functions of Integrins, Cadherins, Selectins, and Immunoglobulin-Superfamily Members. *Annu. Rev. Pharmacol. Toxicol*, *42*, 283–323. https://doi.org/10.1146/annurev.pharmtox.42.090401.151133
- Kader, T., Hill, P., Zethoven, M., Goode, D. L., Elder, K., Thio, N., Doyle, M., Semple, T., Sufyan, W., Byrne, D. J., Pang, J. M. B., Murugasu, A., Miligy, I. M., Green, A. R., Rakha, E. A., Fox, S. B., Mann, G. B., Campbell, I. G., & Gorringe, K. L. (2019). Atypical ductal hyperplasia is a multipotent precursor of breast carcinoma. *Journal of Pathology*, *248*(3), 326–338. https://doi.org/10.1002/path.5262
- Kaszak, I., Witkowska-Piłaszewicz, O., Niewiadomska, Z., Dworecka-Kaszak, B., Toka, F. N., & Jurka, P. (2020). Role of cadherins in cancer—a review. *International Journal of Molecular Sciences*, *21*(20), 1–17. https://doi.org/10.3390/ijms21207624
- Kim, M. A., Jung, E. J., Lee, H. S., Lee, H. E., Yang, H. K., Oh, D. Y., Bang, Y. J., & Kim, W. H. (2010). P-cadherin expression in gastric carcinoma: its regulation mechanism and prognostic significance. *Human Pathology*, *41*(6), 877–885. https://doi.org/10.1016/j.humpath.2009.04.031
- Kim, T., Hwang, D., Lee, D., Kim, J., Kim, S., & Lim, D. (2017). MRTF potentiates TEAD - YAP transcriptional activity causing metastasis . *The EMBO Journal*, *36*(4), 520–535. https://doi.org/10.15252/embj.201695137
- Kitayama, M., Mizutani, K., Maruoka, M., Mandai, K., Sakakibara, S., Ueda, Y., Komori, T., Shimono, Y., & Takai, Y. (2016). A novel nectin-mediated cell adhesion apparatus that is implicated in prolactin receptor signaling for mammary gland development. *Journal of Biological Chemistry*, *291*(11),

5817–5831. https://doi.org/10.1074/jbc.M115.685917

- Ko, S. Y., & Naora, H. (2014). HOXA9 promotes homotypic and heterotypic cell interactions that facilitate ovarian cancer dissemination via its induction of P-cadherin. *Molecular Cancer*, *13*(1), 1–13. https://doi.org/10.1186/1476-4598-13-170
- Kümper, S., & Ridley, A. J. (2010). P120ctn and P-cadherin but not E-cadherin regulate cell motility and invasion of DU145 prostate cancer cells. *PLoS ONE*, *5*(7). https://doi.org/10.1371/journal.pone.0011801
- Lagal, V., Abrivard, M., Gonzalez, V., Perazzi, A., Popli, S., Verzeroli, E., & Tardieux, I. (2014). Spire-1 contributes to the invadosome and its associated invasive properties. *Journal of Cell Science*, *127*(2), 328–340. https://doi.org/10.1242/jcs.130161
- Lysne, D., Johns, J., Walker, A., Ecker, R., Fowler, C., & Lawson, K. R. (2014). P-cadherin potentiates ligand-dependent EGFR and IGF-1R signaling in dysplastic and malignant oral keratinocytes. *Oncology Reports*, *32*(6), 2541–2548. https://doi.org/10.3892/or.2014.3545
- Makrilia, N., Kollias, A., Manolopoulos, L., & Syrigos, K. (2009). Cell adhesion molecules: Role and clinical significance in cancer. *Cancer Investigation*, *27*(10), 1023–1037. https://doi.org/10.3109/07357900902769749
- Medjkane, S., Perez-Sanchez, C., Gaggioli, C., Sahai, E., & Treisman, R. (2009). Myocardin-related transcription factors and SRF are required for cytoskeletal dynamics and experimental metastasis. *Nature Cell Biology*, *11*(3), 257–268. https://doi.org/10.1038/ncb1833
- Molinie, N., & Gautreau, A. (2018). The Arp2/3 regulatory system and its deregulation in cancer. *Physiological Reviews*, *98*(1), 215–238. https://doi.org/10.1152/physrev.00006.2017
- Navarro, P., Gómez, M., Pizarro, A., Gamallo, C., Quintanilla, M., & Cano, A. (1991). A role for the E-cadherin cell-cell adhesion molecule during tumor progression of mouse epidermal carcinogenesis. *Journal of Cell Biology*, *115*(2), 517–533. https://doi.org/10.1083/jcb.115.2.517
- Nisticò, P., Modugno, F. Di, Spada, S., & Bissell, M. J. (2014). β1 and β4 integrins: From breast development to clinical practice. *Breast Cancer*

*Research*, *16*(1), 1–9. https://doi.org/10.1186/s13058-014-0459-x

- Owens, M. B., Hill, A. D., & Hopkins, A. M. (2013). Ductal barriers in mammary epithelium. *Tissue Barriers*, *1*(4), e25933. https://doi.org/10.4161/tisb.25933
- Pai, S. G., Carneiro, B. A., Mota, J. M., Costa, R., Leite, C. A., Barroso-Sousa, R., Kaplan, J. B., Chae, Y. K., & Giles, F. J. (2017). Wnt/beta-catenin pathway: Modulating anticancer immune response. *Journal of Hematology and Oncology*, *10*(1), 1–12. https://doi.org/10.1186/s13045-017-0471-6
- Paredes, J., Albergaria, A., Oliveira, J. T., Jeronimo, C., Milanezi, F., & Schmitt, F. C. (2005). P-cadherin overexpression is an indicator of clinical outcome in invasive breast carcinomas and is associated with CDH3 promoter hypomethylation. *Clinical Cancer Research*, *11*(16), 5869–5877. https://doi.org/10.1158/1078-0432.CCR-05-0059
- Paredes, J., Figueiredo, J., Albergaria, A., Oliveira, P., Carvalho, J., Ribeiro, A. S., Caldeira, J., Costa, A. M., Simões-Correia, J., Oliveira, M. J., Pinheiro, H., Pinho, S. S., Mateus, R., Reis, C. A., Leite, M., Fernandes, M. S., Schmitt, F., Carneiro, F., Figueiredo, C., … Seruca, R. (2012). Epithelial E- and P-cadherins: Role and clinical significance in cancer. *Biochimica et Biophysica Acta - Reviews on Cancer*, *1826*(2), 297–311. https://doi.org/10.1016/j.bbcan.2012.05.002
- Patel, S. D., Chen, C. P., Bahna, F., Honig, B., & Shapiro, L. (2003). Cadherin-mediated cell-cell adhesion: Sticking together as a family. *Current Opinion in Structural Biology*, *13*(6), 690–698. https://doi.org/10.1016/j.sbi.2003.10.007
- Peralta Soler, A., Knudsen, K. A., Salazar, H., Han, A. C., & Keshgegian, A. A. (1999). P-cadherin expression in breast carcinoma indicates poor survival. *Cancer*, *86*(7), 1263–1272. https://doi.org/10.1002/(SICI)1097-0142(19991001)86:7<1263::AID-CNCR23>3.0.CO;2-2
- Pfaffl, M. (2001). A new mathematical model for relative quantification in real-time RT–PCR. *Nucleic Acids Research*, *29*(9), 2003–2007. https://doi.org/10.1093/nar/29.9.e45
- Pfender, S., Kuznetsov, V., Pleiser, S., Kerkhoff, E., & Schuh, M. (2011).

Spire-type actin nucleators cooperate with formin-2 to drive asymmetric oocyte division. *Current Biology*, *21*(11), 955–960. https://doi.org/10.1016/j.cub.2011.04.029

- Pizarro-Cerdá, J., Chorev, D. S., Geiger, B., & Cossart, P. (2017). The Diverse Family of Arp2/3 Complexes. *Trends in Cell Biology*, *27*(2), 93–100. https://doi.org/10.1016/j.tcb.2016.08.001
- Place, A. E., Jin Huh, S., & Polyak, K. (2011). The microenvironment in breast cancer progression: Biology and implications for treatment. *Breast Cancer Research*, *13*(6). https://doi.org/10.1186/bcr2912
- Quinlan, M. E., Heuser, J. E., Kerkhoff, E., & Mullins, R. D. (2005). Drosophila Spire is an actin nucleation factor. *Nature*, *433*(7024), 382–388. https://doi.org/10.1038/nature03241
- Radice, G. L., Ferreira-Cornwell, M. C., Robinson, S. D., Rayburn, H., Chodosh, L. A., Takeichi, M., & Hynes, R. O. (1997). Precocious mammary gland development in P-cadherin-deficient mice. *Journal of Cell Biology*, *139*(4), 1025–1032. https://doi.org/10.1083/jcb.139.4.1025
- Rauhala, H. E., Teppo, S., Niemelä, S., & Kallioniemi, A. (2013). Silencing of the arp2/3 complex disturbs pancreatic cancer cell migration. *Anticancer Research*, *33*(1), 45–52.
- Ribeiro, A. S., Albergaria, A., Sousa, B., Correia, A. L., Bracke, M., Seruca, R., Schmitt, F. C., & Paredes, J. (2010). Extracellular cleavage and shedding of P-cadherin: A mechanism underlying the invasive behaviour of breast cancer cells. *Oncogene*, *29*(3), 392–402. https://doi.org/10.1038/onc.2009.338
- Ribeiro, Ana Sofia, Sousa, B., Carreto, L., Mendes, N., Nobre, A. R., Ricardo, S., Albergaria, A., Cameselle-Teijeiro, J. F., Gerhard, R., Söderberg, O., Seruca, R., Santos, M. A., Schmitt, F., & Paredes, J. (2013). P-cadherin functional role is dependent on E-cadherin cellular context: A proof of concept using the breast cancer model. *Journal of Pathology*, *229*(5), 705–718. https://doi.org/10.1002/path.4143
- Schatten, H. (2015). The cytoskeleton in health and disease. *The Cytoskeleton in Health and Disease*, 1–391. https://doi.org/10.1007/978-1-4939-2904-7

- Seifert, A., & Posern, G. (2017). Tightly controlled MRTF-A activity regulates epithelial differentiation during formation of mammary acini. *Breast Cancer Research*, *19*(1), 1–16. https://doi.org/10.1186/s13058-017-0860-3
- Serrano-Gomez, S. J., Maziveyi, M., & Alahari, S. K. (2016). Regulation of epithelial-mesenchymal transition through epigenetic and post-translational modifications. *Molecular Cancer*, *15*(1), 1–14. https://doi.org/10.1186/s12943-016-0502-x
- Shamir, E. R., & Ewald, A. J. (2015). *Adhesion in Mammary Development*. 353–382. https://doi.org/10.1016/bs.ctdb.2014.12.001
- Shantha Kumara, H. M. C., Bellini, G. A., Caballero, O. L., Herath, S. A. C., Su, T., Ahmed, A., Njoh, L., Cekic, V., & Whelan, R. L. (2017). P-cadherin (CDH3) is overexpressed in colorectal tumors and has potential as a serum marker for colorectal cancer monitoring. *Oncoscience*, *4*(9–10), 139–147. https://doi.org/10.18632/oncoscience.370
- Sitar, T., Gallinger, J., Ducka, A. M., Ikonen, T. P., Wohlhoefler, M., Schmoller, K. M., Bausch, A. R., Joel, P., Trybus, K. M., Noegel, A. A., Schleicher, M., Huber, R., & Holak, T. A. (2011). Molecular architecture of the Spire-actin nucleus and its implication for actin filament assembly. *Proceedings of the National Academy of Sciences of the United States of America*, *108*(49), 19575–19580. https://doi.org/10.1073/pnas.1115465108
- Sousa, B., Paredes, J., Milanezi, F., Lopes, N., Martins, D., Dufloth, R., Vieira, D., Albergaria, A., Veronese, L., Carneiro, V., Carvalho, S., Costa, J. L., Zeferino, L., & Schmitt, F. (2010). P-cadherin, Vimentin and CK14 for identification of basal-like phenotype in breast carcinomas: An immunohistochemical study. *Histology and Histopathology*, *25*(8), 963–974. https://doi.org/10.14670/HH-25.963
- Turashvili, G., McKinney, S. E., Goktepe, O., Leung, S. C., Huntsman, D. G., Gelmon, K. A., Los, G., Rejto, P. A., & Aparicio, S. A. J. R. (2011). P-cadherin expression as a prognostic biomarker in a 3992 case tissue microarray series of breast cancer. *Modern Pathology*, *24*(1), 64–81. https://doi.org/10.1038/modpathol.2010.189
- Vidi, P. A., Bissell, M. J., & Lelièvre, S. A. (2013). Three-dimensional culture

of human breast epithelial cells: The how and the why. *Methods in Molecular Biology*, *945*, 193–219. https://doi.org/10.1007/978-1-62703-125-7_13

- Vieira, A. F., & Paredes, J. (2015). P-cadherin and the journey to cancer metastasis. *Molecular Cancer*, *14*(1), 1–12. https://doi.org/10.1186/s12943-015-0448-4
- Vieira, A. F., Ribeiro, A. S., Dionísio, M. R., Sousa, B., Nobre, A. R., Albergaria, A., Santiago-Gómez, A., Mendes, N., Gerhard, R., Schmitt, F., Clarke, R. B., & Paredes, J. (2014). P-cadherin signals through the laminin receptor α6β4 integrin to induce stem cell and invasive properties to basal-like breast cancer cells. *Oncotarget*, *5*(3), 679–692. https://doi.org/10.18632/oncotarget.1459
- Vieira, A. F., Ricardo, S., Ablett, M. P., Dionísio, M. R., Mendes, N., Albergaria, A., Farnie, G., Gerhard, R., Cameselle-Teijeiro, J. F., Seruca, R., Schmitt, F., Clarke, R. B., & Paredes, J. (2012). P-cadherin is coexpressed with CD44 and CD49f and mediates stem cell properties in basal-like breast cancer. *Stem Cells*, *30*(5), 854–864. https://doi.org/10.1002/stem.1075
- Wagner, A. R., Luan, Q., Liu, S. L., & Nolen, B. J. (2013). Dip1 defines a class of Arp2/3 complex activators that function without preformed actin filaments. *Current Biology*, *23*(20), 1990–1998. https://doi.org/10.1016/j.cub.2013.08.029
- Werner, S., Lützkendorf, J., Müller, T., Müller, L. P., & Posern, G. (2019). MRTF-A controls myofibroblastic differentiation of human multipotent stromal cells and their tumour-supporting function in xenograft models. *Scientific Reports*, *9*(1), 1–12. https://doi.org/10.1038/s41598-019-48142-z
- Wong, S. H. M., Fang, C. M., Chuah, L. H., Leong, C. O., & Ngai, S. C. (2018). E-cadherin: Its dysregulation in carcinogenesis and clinical implications. *Critical Reviews in Oncology/Hematology*, *121*(October 2017), 11–22. https://doi.org/10.1016/j.critrevonc.2017.11.010
- Zhang, C. C., Yan, Z., Zhang, Q., Kuszpit, K., Zasadny, K., Qiu, M., Painter, C. L., Wong, A., Kraynov, E., Arango, M. E., Mehta, P. P., Popoff, I., Casperson, G. F., Los, G., Bender, S., Anderes, K., Christensen, J. G., &

VanArsdale, T. (2010). PF-03732010: A fully human monoclonal antibody against P-cadherin with antitumor and antimetastatic activity. *Clinical Cancer Research*, *16*(21), 5177–5188. https://doi.org/10.1158/1078-0432.CCR-10-1343